Expression and Neural Correlates of Schizophrenia Risk Gene *ZNF804A*

Helena Cousijn

University College, University of Oxford

Thesis submitted for the degree of DPhil

Michaelmas term, 2013

Abstract

Genome wide association studies have provided evidence for a significant association between *ZNF804A* (zinc finger protein 804A) - specifically the intronic single nucleotide polymorphism (SNP) rs1344706 - and schizophrenia, but little is known about the function of the gene or the effects of the SNP. By studying post-mortem human brain tissue, I characterised ZNF804A immunoreactivity in adult and foetal human brain and investigated effects of diagnosis and rs1344706 genotype on ZNF804A mRNA and protein expression. Secondly, I looked in a large sample of healthy volunteers (n=922) at the effects of rs1344706 on brain structure using volumetry and voxel based morphometry (VBM). Furthermore, I recruited healthy volunteers who were either homozygous for the risk allele or homozygous for the non-risk allele (n=50). They participated in magnetoencephalography (MEG) and magnetic resonance (MR) sessions in which brain activity was measured during a working memory task, a visual processing task, and rest. Using magnetic resonance spectroscopy, also neurotransmitter levels were assessed. The experiments conducted for this thesis showed for the first time that ZNF804A immunoreactivity can be detected in both foetal and adult human brain and that it is mainly localised to layer III pyramidal cells, with a granular subcellular distribution throughout the cytoplasm. No effect of rs1344706 on mRNA and protein expression was found. In our structural MRI study, rs1344706 did not affect macroscopic brain structure as measured by volumetry and VBM, and given the large sample size, this seems a convincing negative. However, we did find that rs1344706 alters prefrontal-hippocampal connectivity, with increased connectivity being observed in risk homozygotes. Additionally, using MEG, we found an effect of *ZNF804A* genotype on hippocampal connectivity in the theta band (4-8Hz), with non-risk homozygotes displaying more connectivity. This finding provides a first clue as to the mechanisms that might underlie the previously observed effects of rs1344706 on prefrontal-hippocampal connectivity. Future studies will need to elucidate the actual function of the ZNF804A protein, in order to bridge the gap between the molecular and neuroimaging findings described in this thesis.

Acknowledgements

Many people have been actively involved in this project, and I would like to take the opportunity to thank them here. First of all, my supervisors Paul Harrison and Kia Nobre, who were willing to start on this complex project with me and provided me with the tools and advice necessary to carry it out. Furthermore, Phil Burnet, who provided hands-on supervision in the lab and generated the ZNF804A-expressing bacteria. His company has made my lab work a lot more enjoyable. Sharon Eastwood supervised my initial experiments, in particular the qPCR studies. I would like to thank Mary Walker and Tracy Lane for their help with establishing and conducting the immunohistochemistry protocol. Li Chen helped with the extraction of DNA, mRNA, and protein. The MEG data were acquired together with George Wallis. I would like to thank Steve Knight and Mark Stokes for help with the MRI data acquisition. Jamie Near kindly provided the tools to analyse the MRS data. Henry Luckhoo and Verena Heise made it possible to carry out the MEG resting state analysis. In particular, I would like to thank Saskia Haegens for collaborating with me on the MEG project. Without her, I might still be preprocessing the data. I'm grateful to Tom Hyde (Lieber Institute for Brain Development, Baltimore, USA) and Charlie Schroeder (Columbia University, New York, USA), who have kindly hosted me during my stay in the USA. I would like to thank Alejandro Arias Vasquez and Mark Rijpkema (Donders Institute, Nijmegen, The Netherlands) for providing the data analysed in chapter 4. I was also very happy to have Freya Edwards and Marc Eissing do their FHS projects with me. They analysed some of the data discussed in this thesis.

Human brain tissue used in these studies was generously provided by the Stanley Medical Research Institute (courtesy of Maree Webster), the Clinical Brain Disorders Branch at the National Institute of Mental Health and the Lieber Institute for Brain Development (courtesy of Joel Kleinman and Tom Hyde), and the Australian National Brain Bank (courtesy of Cyndi Shannon-Weickert).

This project was funded by a Wellcome Trust scholarship.

I would also like to thank my parents and Kati, whose support has been invaluable.

Table of contents

This thesis contains ~ 40.000 words.

Index of Figures and Tables

List of Abbreviations

ACC - Anterior Cingulate Cortex

ANOVA - Analysis of Variance

APOE - Apolipoprotein E

BA - Brodmann's Area

B2M - β-2-Microglobulin

BIG - Brain Imaging Database

BOLD - Blood Oxygen Level Dependent

BSA - Bovine Serum Albumin

CBF - Cerebral Blood Flow

cDNA - Complementary DNA

CNV - Copy Number Variation

COMT - Catechol-O-Methyltransferase

DAB - Diaminobenzidine

dH2O - Distilled Water

DISC1- Disrupted In Schizophrenia1

DLPFC - Dorsolateral Prefrontal Cortex

DMN - Default-Mode Network

DNA - Deoxyribonucleic Acid

DNase - Deoxyribonuclease

DSM - Diagnostic and Statistical Manual

DTI - Diffusion Tensor Imaging

ECL - Electrochemiluminescence

EEG - Electroencephalography

EPI - Echo Planar Imaging

FFT - Fast Fourier Transform

fMRI - Functional MRI

FOV - Field of View

FWE - Family Wise Error

FWHM - Full-Width Half-Maximum

GABA - Gamma-Aminobutyric Acid

gDNA - Genomic DNA

GFP - Green Fluorescent Protein

GM - Grey Matter

GUSB - Glucuronidase Beta

GWAS - Genome-Wide Association Study

HKG - Housekeeping Gene

HPI - Head-Position Indicator

HPRT1 - Hypoxanthine Guanine Phosphoribosyl Transferase1

HRF - Hemodynamic Response Function

HRP - Horseradish Peroxidase

ICA - Independent Component Analysis

ICD - International Classification of Disease

IPL - Inferior Parietal Lobule

IPSP - Inhibitory Post Synaptic Potential

kDa - Kilodaltons

LC - Linear Combination

LCMV - Linearly Constrained Minimum Variance

MAF - Minor Allele Frequency

MEG - Magnetoencephalography

MNI - Montreal Neurological Institute

MRI - Magnetic Resonance Imaging

mRNA - Messenger RNA

MRS - Magnetic Resonance Spectroscopy

MTL - Medial Temporal Lobe

NAA - N-Acetyl Aspartate

PBS - Phosphate Buffered Saline

PCC - Posterior Cingulate Cortex

PCR - Polymerase Chain Reaction

PET - Positron Emission Tomography

PMI - Post Mortem Interval

PPI - Psycho-Physiological Interaction

PVDF - Polyvinylidene Fluoride

qPCR - Quantitative PCR

RACE - Rapid Amplification of PCR Ends

RNA - Ribonucleic Acid

RNase - Ribonuclease

RIN - RNA Integrity Number

ROI - Region of Interest

RSN - Resting State Network

RT-PCR - Reverse Transcription PCR

SDS-PAGE - Sodium Dodecyl Sulphate Polyacrylamide Gel Electrophoresis

SEM - Standard Error of the Mean

sMRI - Structural MRI

SNP - Single Nucleotide Polymorphism

SPECIAL - Spin-Echo Full-Intensity Acquired Localized

SPM - Statistical Parametric Mapping

STG - Superior Temporal Gyrus

SVC - Small Volume Correction

T - Tesla

TBV - Total Brain Volume

TE - Echo Time

TFCE - Threshold-Free Cluster Enhancement

TFR - Time Frequency Representation

TFRC - Transferrin Receptor

TR - Repetition Time

VBM - Voxel Based Morphometry

WM -White Matter

ZNF804A - Zinc Finger Protein 804A

Chapter 1 - Introduction

1.1 Schizophrenia

Schizophrenia is a complex and debilitating psychotic illness which is poorly understood and only partially treatable. It results in high mortality and continues to impose a heavy burden on sufferers and carers. Usually presenting during adolescence or early adulthood, schizophrenia affects about 1% of the population (Freedman, 2003) and leads to significant direct and indirect health costs worldwide. It consists of a varied range of symptoms, which are usually divided into positive and negative symptoms (Berrios, 1985). The positive symptoms consist of thoughts and sensations not usually experienced by healthy people but which are present in schizophrenia, and include hallucinations, delusions, and disorganisation of thought and behaviour (Arango & Carpenter, 2011). The negative symptoms, including avolition, alogia, apathy, asociality, anhedonia, and blunted affect, lead to a loss of normal function; these are usually more resistant to treatment (Andreasen, 1995). Additionally, patients with schizophrenia suffer from a range of cognitive dysfunctions, with many of the negative symptoms being cognitive in nature. Impairment is particularly marked in the domains of working memory, executive function, and attention (Censits et al., 1997; Aleman et al., 1999; Bilder et al., 2000; Freedman & Brown, 2011; Barch & Ceaser, 2012). These impairments are found in medication-free first-episode patients (Saykin et al., 1994; Censits et al., 1997; Bilder et al., 2000) and may even precede disease onset (Hambrecht et al., 2002; Gschwandtner et al., 2003).

There are two widely used classification systems for the diagnosis of schizophrenia: 1) the Diagnostic and Statistical Manual, of which a new version has appeared recently (DSM-5, American Association of Psychiatry, 2013); however, the brain collections used in this thesis were still classified using the previous version (DSM-IV, American Association of Psychiatry, 1994) and 2) the International Classification of

Disease (ICD-10; World Health Organisation, 1992). Although these two classification systems are similar and both base the diagnosis on positive and negative symptoms, the DSM classification requires a longer duration of illness and deterioration of function and is therefore a narrower definition than that of the ICD-10. According to the DSM criteria, at least two of the previously discussed symptoms must be present for six months, including at least one month of active symptoms, for schizophrenia to be diagnosed.

Schizophrenia is highly heterogeneous both in terms of symptoms and course (Huber, 1997; Arango & Carpenter, 2011). Despite the development of classification systems to diagnose schizophrenia, the validity of the diagnosis is unknown and the discovery of biological markers for schizophrenia remains a research goal. Therefore, despite some new pharmacological and psychological treatments, there has been no significant improvement in therapy or outcome, and no realistic prospects for prevention. Greater understanding of the aetiology and neurobiology of schizophrenia is essential if this is to change. Identifying schizophrenia-associated genetic loci is likely to present one of the most valuable approaches for elucidating the pathogenesis of the disease, thus in the future paving the way to establishing new diagnostic markers for schizophrenia and novel therapies that target the relevant biological processes (O'Connell et al., 2011).

1.2 Neuropathology and aetiology

Several neuropathological changes have been identified in schizophrenia. These changes represent subtle differences observed between schizophrenia and control groups, rather than overt diagnostic pathology. Main findings at a macroscopic level for schizophrenia to date include: enlarged lateral and third ventricles of the brain, decreased brain size, decreased brain weight, decreased cortical volume, and decreased grey matter volume (Lawrie & Pantelis, 2011). The reduction in brain volume is particularly marked in

the hippocampus, amygdala, parahippocampus, superior temporal gyrus, frontal cortex, and thalamus (Nelson et al., 1998; Wright et al., 1999; Wright et al., 2000; Halliday, 2001). These structural changes at the macroscopic level indicate that there must be histological and molecular alterations in schizophrenia.

At the microscopic level many findings remain unconfirmed, but some more robust changes have been reported for the hippocampal formation and dorsolateral prefrontal cortex (Harrison et al., 2011). There is now reasonably good evidence for smaller neurons, a decrease in pyramidal neuron dendritic spines, a decrease in cortical and hippocampal synaptic markers, abnormal gene expression in GABA interneurons, fewer oligodendrocytes, and abnormalities of white matter (Harrison, 1999; Harrison & Weinberger, 2005). Reports have varied as to whether these pathological changes are progressive (Weinberger & McClure, 2002), but imaging studies indicate that abnormalities are present at the onset of the disease, and post-mortem findings do not seem to correlate with duration of illness. Furthermore, post-mortem studies of the brains of schizophrenia patients do not typically show the signs of a neurodegenerative disorder such as neurofibrillary tangles, amyloid plaques, or Lewy bodies, and there is no evidence of gliosis, which would indicate inflammation or injury in the brain (Weinberger & McClure, 2002; Harrison, 2005). The absence of such pathology provides support for the theory that schizophrenia is a developmental disorder (Harrison & Weinberger, 2005).

The contemporary view of schizophrenia as a neurodevelopmental disorder was developed in the mid-1980s (Murray & Lewis, 1987; Weinberger, 1987). The hypothesis postulates that a form of early developmental pathology interacts with normal brain maturation processes, occurring much later, to cause schizophrenia (Weinberger, 1987). This hypothesis has a strong supportive body of evidence. Neuropathological markers present in schizophrenia suggest abnormal development, whereas changes that would

suggest neurodegenerative processes are absent (Harrison, 1999). Furthermore, obstetric complications (Geddes et al., 1999; Cannon et al., 2002), pre- and perinatal viral infections (Tsuang, 2000), winter birth (Davies et al., 2003), and prenatal malnutrition (Susser et al., 1998) have been associated with schizophrenia. Genes important for neurodevelopment have also been found to be associated with schizophrenia (Harrison & Owen, 2003; Rapoport et al., 2005; Owen et al., 2009). Given that it is now widely accepted that developmental processes are at least partially responsible for causing schizophrenia (Lewis & Levitt, 2002), it is important that schizophrenia-associated genetic loci are also investigated in terms of their effects on and during development.

1.3 Genetics of schizophrenia

One of the few indisputable facts about the aetiology of schizophrenia is that it is highly heritable – about 80% (Cardno et al., 1999; Sullivan et al., 2003). This 80% heritability has been estimated based on the level of concordance in the occurrence of schizophrenia in monozygotic twins compared to dizygotic twins, as both sets of twins will share the same environment and so the difference in concordance between them should be predominantly due to genetic factors. Early studies (Kallmann, 1946; Slater & Shields, 1953) comparing monozygotic twins and dizygotic twins brought up in the same family found significantly higher rates of concordance amongst monozygotic compared to dizygotic twins. Based on all European studies carried out between 1921 and 1987, it was reported that the identical twin of a patient with schizophrenia has a 48% chance of having schizophrenia, whereas the non-identical twin of a schizophrenia patient has a 17% chance of also suffering from schizophrenia (Gottesman, 1991). This indicates that there is a strong genetic component to the disorder, but that genes are not the only causative factor.

Additionally, adoption studies of schizophrenia have helped to establish and

confirm the significant role of genetic factors in the aetiology of the disorder (Ingraham & Kety, 2000). These studies have shown that the adopted children of parents with schizophrenia are more vulnerable to develop such disorders themselves than adopted children from unaffected parents, with adopted children from healthy parents not being more likely to develop schizophrenia than the general population (Heston, 1966; Rosenthal et al., 1971; Wender et al., 1974; Tienari, 1991). However, it should be noted that in the heritability estimates based on twin and adoption studies, prenatal and perinatal factors may also be contributing, since these cannot be distinguished from genetic factors.

Despite the strong genetic component, no locus has been unequivocally associated with schizophrenia. Various strategies have been adopted to try and find the genes that confer susceptibility to schizophrenia. A relatively straightforward strategy is to take advantage of rare examples in which there is a highly penetrant genetic form of the disease. An example of this is a Scottish family in which a translocation between chromosomes 1 and 11 was found to be the cause of psychiatric disorders. Examination of the region of the genome affected by this translocation led to the identification of the schizophrenia susceptibility gene Disrupted In Schizophrenia 1 (DISC1) (Millar et al., 2000), which is thought to be a multifunctional protein which is particularly involved in regulation of the cytoskeleton (Ross et al., 2006; Chubb et al., 2008). Examining cases such as these can prove useful as the highly penetrant nature of the disease in these cases simplifies the identification of the genetic basis of the disease. However, this is only true for a small minority of cases, and little is known about the involvement of these factors in schizophrenia susceptibility in the general population. In the case of DISC1, subsequent linkage and association studies have provided support for a role of the affected region of chromosome 1 and of the DISC1 gene in the general population (Chubb et al., 2008).

A more common approach to finding genes for disorders is to use linkage studies, in which DNA from members of families with a history of schizophrenia is used to determine which regions of the genome are common to affected individuals but not shared by their unaffected relatives. The literature is complex and results inconsistent (partly because the method was designed for Mendelian disorders, partly because the genetic architecture of schizophrenia is complex), but an extensive meta-analysis of linkage studies indicates that regions of chromosomes 1, 2q, 3q, 4q, 5q, 8p, and 10q are likely to be linked with schizophrenia (Ng et al., 2009). A linkage finding can then be used as the start of a fine mapping and genetic association study within the region to identify the genes and variants responsible for the linkage signal. This was the strategy used, for example, for the discovery of Neuregulin 1 as a schizophrenia risk gene (Stefansson et al., 2002). However, linkage studies have poor power for detecting common alleles that have low penetrance (Hirschhorn & Daly, 2005).

Genetic association studies investigate whether a genetic variant is more common in cases than controls. Until recently, such studies were limited to a few genes at a time, and this choice was made either on the basis of linkage or because there was reason to suspect that a gene might be involved in the disorder, the so-called candidate-gene approach. Therefore, little progress was made in identifying the genes, or the genetic architecture, underlying this heritability. However, developments in the field of genetics have made it possible to study hundreds of thousands of single nucleotide polymorphisms (SNPs) across the genome at once, in genome-wide association studies (GWAS). These studies use similar methods to older association studies, but have no prior hypothesis of the possible location of the susceptibility genes and examine a large number of SNPs throughout the genome. GWAS studies are a relatively novel method, and the first

significant genome-wide association was reported in 2008 by O'Donovan et al. (2008). This study will be discussed in more detail in section 1.5.

Another genetic factor implicated in susceptibility to schizophrenia is the copy number variation (CNV) (Potash et al., 2008; Walsh et al., 2008). CNVs occur when a section of the genome is deleted or duplicated, resulting in an abnormal number of copies of a section of the DNA. CNVs seem to be present in everyone's genome, but several recent studies have shown that CNVs anywhere in the genome can increase risk of schizophrenia. These can be either inherited or de novo mutations (Walsh et al., 2008). There are high levels of negative selection operating against schizophrenia associated CNVs, but the rate of de novo CNV mutation is increased in cases when compared with controls (Rees et al., 2012). The CNV field is developing rapidly, with estimates suggesting that 2% of schizophrenia cases may be attributable to CNVs at 1q21.1, 15q13.3, and 22q11 alone, but this is a very provisional figure (Bassett et al., 2010).

One thing that is clear is that the genetic risk is not inherited in a Mendelian manner, with the risk of schizophrenia in most people being conferred by the combination of the effects of several genes. The current view on risk genes for schizophrenia can be seen in Figure 1.1. As discussed, there are some CNVs of high penetrance, but these are very rare. In the majority of cases, the risk is conferred by many SNPs of very small effect (Rodriguez-Murillo et al., 2012), making identification of risk polymorphisms a challenging endeavour.

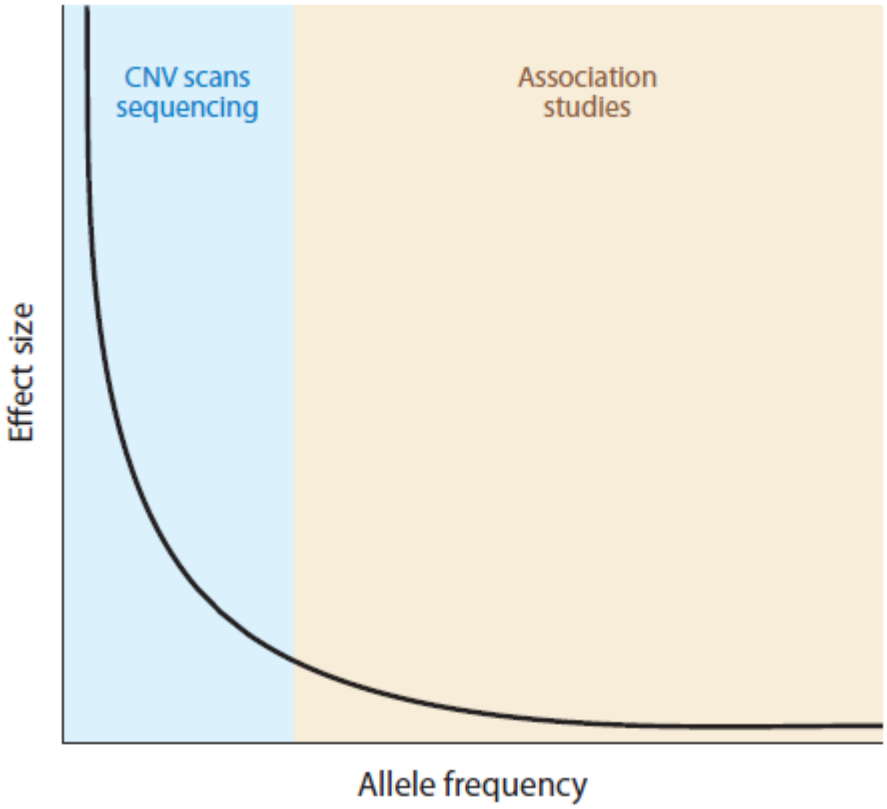

Figure 1.1: The graph represents the relationship between allele frequency and effect size. Rare CNVs generally have large effects and substantially increase the risk of schizophrenia. However, in the majority of cases, common SNPs of small effect increase the risk of schizophrenia. Taken from Rodriguez-Murillo et al., 2011.

1.4 Intermediate phenotypes

Despite advances in genetics research, links between polymorphisms and disorders have remained weak (Gottesmann & Shields, 1972; Malhotra & Goldman, 1999). This is perhaps not surprising, given the polygenic nature of the disorder as well as the complexity of the phenotype. To address these issues, researchers started to focus on intermediate phenotypes or endophenotypes. The term endophenotype was used by Gottesman and Shields (1973) to describe a trait that is thought to be intermediate on the chain of causality from gene to disease. Endophenotypes were seen as internal phenotypes that provide a means of identifying the downstream facets of clinical phenotypes as well as the upstream consequences of genes (therefore also called intermediate phenotypes). Endophenotypes were thought to represent simpler clues to genetic underpinnings than the disease itself,

enabling the psychiatric diagnoses to be decomposed or deconstructed, which can result in more straightforward genetic analysis. These endophenotypes could be neurophysiological, biochemical, endocrinological, neuroanatomical, cognitive, or neuropsychological in nature (Gottesman & Gould, 2003). Nowadays, this approach is not only used to establish the link between gene and disease. Because hypothesis-free GWAS studies show associations with genes we know very little about, it provides a way of elucidating and understanding the neurobiological pathways in which these genes are involved.

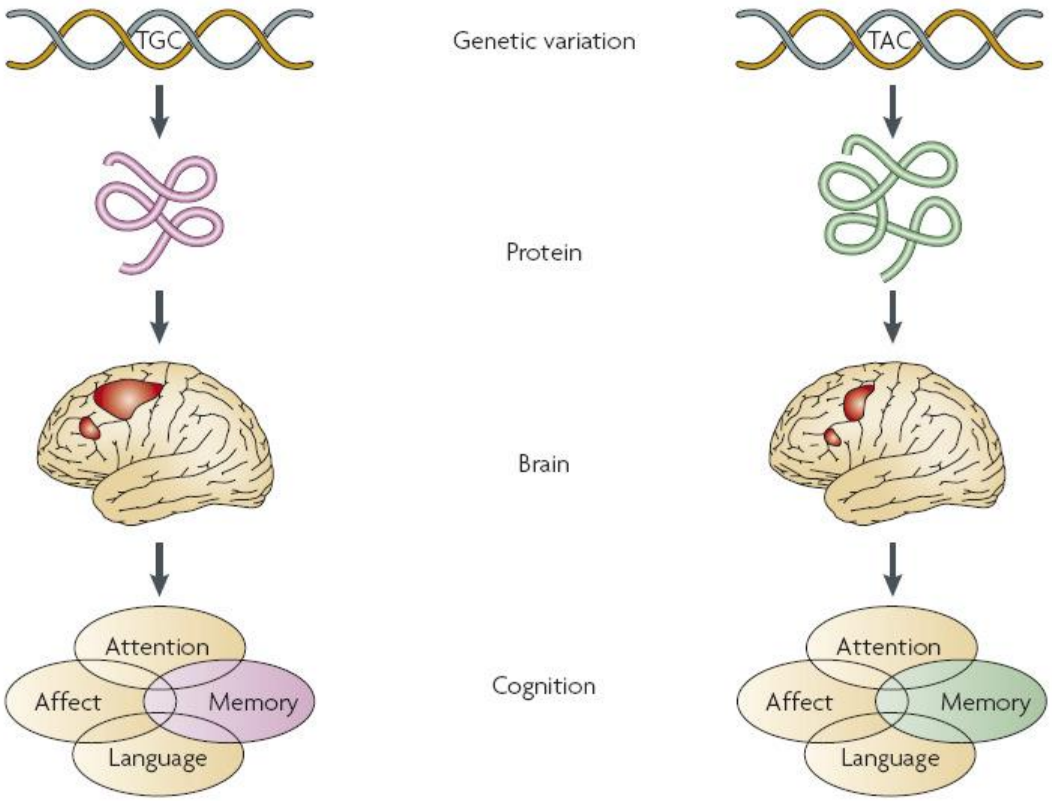

Figure 1.2: Depicts the pathway between gene and disease. Genetic variation can lead to the translation of different proteins, which can cause differences in brain structure or function, which may lead to differences in cognitive functioning. These alterations could underlie psychopathology. Brain measures lie on the pathway between gene and disease, and can therefore be studied as intermediate phenotypes. Taken from Green et al., 2008.

The principle of studying intermediate phenotypes is depicted in Figure 1.2. There are many steps in between genes and disorders, some of which depicted here (Green et al.,

2008). First, the genes will be transcribed and translated, with some polymorphisms leading to changes in gene transcription and translation. Different proteins might in turn lead to differences in brain structure or brain function. These changes could lead to differences in cognitive function and, in more extreme cases, lead to psychopathology. All these intermediate steps could theoretically be linked to the risk gene and need to be studied in order to fully understand the pathway between gene and disease. An integrated systems approach, using intermediate phenotypes from several biological levels, is needed to provide convergent evidence implicating specific pathophysiological mechanisms.

For this intermediate phenotype approach to work, plausible intermediate phenotypes need to be identified and studied. Gottesman and Gould (2003) based on Gershon and Goldin (1986) proposed several criteria: 1) the endophenotype is associated with the illness in the population; 2) the endophenotype is heritable; 3) the endophenotype is primarily state-independent (i.e. manifests itself whether or not illness is active); 4) within families, endophenotype and illness co-segregate; and 5) the endophenotype found in affected family members is found in non-affected family members at a higher rate than in the general population. In the next section, I will discuss two intermediate phenotype approaches that are relevant to this thesis.

1.5 Genetic neuroimaging and genetic neuropathology

The field where the intermediate phenotype approach has been most successful is neuroimaging, where it has even led to the development of a new field known as imaging genetics (Hariri & Weinberger, 2003) or genetic neuroimaging (de Geus et al., 2008). It has been said that the use of neuroimaging has led to a conceptual change in the way biological endophenotypes are viewed and has given access to a previously inaccessible level of biological characterization and validation of genetic effects (Meyer-Lindenberg &

Weinberger, 2006). Brain activity and structure lie on the pathway in between genes and behaviour and are considered key intermediates in bridging the gap between the two (Green et al., 2008). Imaging measures are seen as being closer to the gene than behaviour, and are hypothesised to depend on fewer genes than behaviour itself. Therefore, it should be easier to detect the effects of genes on brain measures than on behaviour. The greater penetrance of the gene at the level of the brain is also thought to make it possible to see effects in smaller sample sizes and it has been shown that current methods for data analysis with their correction procedures control well for the chance of false discoveries (Meyer-Lindenberg et al., 2008). Behavioural differences are not necessary to detect the effect of the gene and brain activity is less affected by strategy than, for example, behaviour. This makes it a more objective measure of the gene effect (Hariri & Weinberger, 2003). Many genetic neuroimaging studies have been carried out in the last decade and even though several findings have not been replicated, meta-analyses have shown robust associations between variation in COMT and prefrontal function (Mier et al., 2010) and between a 5-HTTLPR polymorphism and amygdala activation (Munafo et al., 2008), demonstrating the validity of the approach. In the future, this approach could have the potential to improve predictive testing of schizophrenia in the at-risk population and may offer early intervention and novel targets for therapeutic interventions (Redpath et al., 2013).

Another important method for elucidating the effects of putative risk genes is the study of their expression in post-mortem human tissue. In the past, case-control studies in post-mortem human brains using molecular methods have led to insight in several neuropathological changes that occur in schizophrenia (Weinberger et al., 1983; Kleinman et al., 1988; Harrison, 1999). Nowadays, similar molecular methods can be used to provide clues to possible mechanisms through which schizophrenia susceptibility genes and polymorphisms might operate (Harrison, 1996; Harrison & Weinberger, 2005). This

approach focuses on how allelic variation in risk-associated genes affects expression and function of mRNA and proteins (Kleinman et al., 2011). Using mRNA and protein expression as intermediate phenotypes provides a phenotype that is as close to the gene of interest as possible. The studies can be carried out in healthy brains, overcoming to some extent the confounding effects of studying brains from subjects with schizophrenia. Given the developmental nature of schizophrenia, the effects of genes can and should also be assessed in foetal human tissue (Colantuoni et al., 2011). Additionally, the expression of risk genes can be studied in both cases and controls. Many variants associated with schizophrenia to date, including the variant that will be discussed in this thesis, are non-coding SNPs, making it likely that the disease association arises because the SNP affects some facet of gene expression. Testing this hypothesis in human brain tissue is crucial, because the critical events may not occur in other tissues or species (Kleinman et al., 2011).

For this thesis, both genetic neuroimaging and genetic neuropathology methods were used in an attempt to elucidate the neurobiological pathway between risk gene *ZNF804A* and schizophrenia.

1.6 *ZNF804A*

As mentioned in section 1.3, developments in the field of genetics have made it possible to carry out hypothesis-free GWAS studies, where hundred-thousands of SNPs can be tested for association with schizophrenia. In 2008, these finally provided strong (genome-wide significant) evidence for genetic association to several loci. The case was statistically most compelling for a gene called *ZNF804A* (zinc finger protein 804A), at 2q32.1 ($p = 1.61 \times 10^{-7}$). A schematic of the gene can be seen in Figure 1.3. Association was originally reported in 2008 by O'Donovan et al. in a sample of 479 cases and 2973

controls and significant loci were tested in 16726 additional subjects. This association was replicated and extended by the International Schizophrenia Consortium (2009), Riley et al. (2010), Steinberg et al. (2011), and Zhang et al. (2011b). Williams et al. (2011) conducted a meta-analysis of >21,000 cases and 38,000 controls and reported an odds ratio (OR) of 1.10 [1.07-1.14], $p=2.5x10^{-11}$ for schizophrenia, and OR 1.11, $p=4x10^{-13}$ for schizophrenia and bipolar disorder combined. No differential association on the basis of family history or sex was reported (Riley et al., 2010). Importantly, the associations remained significant genome-wide after exclusion of the discovery sample.

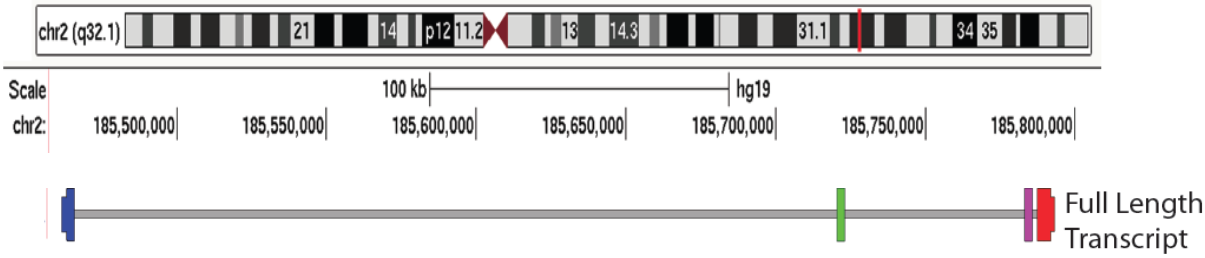

Figure 1.3: Schematic of *ZNF804A* locus, gene, and full-length transcript. Exons are coloured (E1: blue, E2: green, E3: purple, E4: red), introns in grey.

Not only was rs1344706 in *ZNF804A* the first SNP to show genome-wide significant association with schizophrenia, the *ZNF804A* findings are notable for three other reasons. First, there is little ambiguity as to the gene concerned. Second, the genetic signal appears to come almost entirely from a single, intragenic SNP, rs1344706, or possibly a haplotype including it (Riley et al., 2010), since fine mapping and sequencing has effectively excluded the presence of any other common (MAF>0.1) or coding variants (Williams et al., 2011). Furthermore, Dwyer et al. (2010) have shown that there are no rare (frequency ~0.001%) coding variants in *ZNF804A* associated with schizophrenia. Third, all the studies find the same directionality of effect, with the adenosine (A) substitution of the cytosine (C) being the risk variant. While I will always refer to A and C in this thesis, some studies determined the genotype based on the other DNA strand and refer to T as the

risk allele and G as the non-risk allele. The risk allele is the more common variant in the population (MAF = ~0.4). These three considerations meant that it could be reasonably assumed that there is genuine association of *ZNF804A* with schizophrenia, and that the risk arises primarily from rs1344706. This made the biology of *ZNF804A*, and the functionality of rs1344706, critical issues.

1.7 *ZNF804A* biology

When I started my DPhil project, very little was known about the neurobiological pathways in which *ZNF804A* might be involved or what the effect of variation at rs1344706 could be. In this section, I will discuss what was known at the time to explain what information my research questions and hypotheses were based on. I will discuss more recent findings (from 2010 onward) in the relevant chapters.

Given the gene's zinc finger protein domain, it was thought that the *ZNF804A* gene would encode a transcription factor of the classical C2H2 type (Brayer & Segal, 2008; Tadepally et al., 2008). It may therefore have a role as a regulator of gene expression, although such proteins may also be involved in recognition of mRNAs and proteins (Gamsjaeger et al., 2007). However, there are no close homologues reported in the genome or proteome, and only one other C2H2 zinc finger protein gene that has a single zinc binding domain, hindering attempts to predict *ZNF804A* function. Chung et al. (2010) found that the mouse homologue of *ZNF804A* is a downstream target of Hoxc8, which has a role in development, suggesting possible effects of *ZNF804A* during development. There was a lack of data as to the expression of *ZNF804A*, with no reports of its mRNA or encoding protein distribution in human brain.

SNP rs1344706 is intronic (in intron 2), and thus non-coding. This means that the most likely mechanism for this SNP to have an effect would be via alteration of some

parameter of transcription or translation, which would affect the amount or distribution of the protein. The limited available data did not show a clear effect of rs1344706 on ZNF804A mRNA expression in adult brain (Riley et al., 2010; Williams et al., 2011), with Riley et al. reporting increased expression for the risk allele, but Williams et al. not replicating this finding. No studies had yet attempted to detect ZNF804A protein in human brain, which is predicted to consist of 1209 amino acids with a molecular weight of 137 kDa.

1.8 *ZNF804A* neuroimaging and behaviour

As discussed in section 1.4, genetic neuroimaging methods are often used to increase understanding of an association between a gene and a disorder. The first study assessing the effects of *ZNF804A* genotype on human brain function used an N-back working memory task to probe dorsolateral prefrontal cortex (DLPFC) function as well as functional connectivity (Esslinger et al., 2009). The authors reported increased functional connectivity between the DLPFC and hippocampus and decreased interhemispheric prefrontal coupling in healthy subjects carrying the risk allele. No effect of *ZNF804A* genotype on activity in the DLPFC was found. These findings have since been replicated, as will be discussed in chapter 6. A second genetic neuroimaging study investigating the effects of *ZNF804A* genotype employed a theory-of-mind task, and found aberrant connectivity between frontal and temporo-parietal regions (Walter et al., 2011). Together, these first results from studies looking at the effects of rs1344706 on brain activity indicate network dysfunctions caused by altered connectivity. This is in line with studies reporting altered connectivity in schizophrenia patients (Meyer-Lindenberg et al., 2001; Meyer-Lindenberg et al., 2005; Repovs & Barch, 2012). Another study used structural magnetic resonance imaging (sMRI) to examine whether rs1344706 impacts upon brain structure.

Lencz et al. (2010) showed in 39 healthy volunteers that carriers of the risk allele (A) of rs1344706 had significantly larger total white matter but reduced grey matter volumes in several regions comprising the 'default mode network', suggesting possible effects of *ZNF804A* genotype on structural connectivity.

Several studies looked at associations between *ZNF804A* genotype and behaviour. The study by Lencz et al. (2010), which found effects on brain structure, also reported that risk allele carriers were impaired on a visuomotor task. Walters et al. (2010) found the risk allele to generally affect cognitive performance in patients with schizophrenia, but not in control subjects. Interestingly, in the two independent samples they studied, the risk allele actually led to improved performance in patients. Hashimoto et al. (2010) also found no effect of *ZNF804A* genotype in healthy controls, but reported that the risk allele was associated with decreased performance on a visual memory task in patients with schizophrenia. One study assessed the relationship between *ZNF804A* and clinical symptomatology and showed a modest association between the risk allele and clinical symptoms, particularly the number and severity of lifetime manic episodes (Cummings et al., 2010). These studies provided initial clues about the effects of *ZNF804A* genotype on cognition and symptomatology, but more studies are needed to strengthen the results and resolve inconsistent findings.

1.9 Research questions

ZNF804A was the first gene to show genome-wide significant association with schizophrenia and the first genetic neuroimaging study of *ZNF804A* showed that rs1344706 affects functional connectivity in human brain. This makes *ZNF804A* an important candidate gene, but more research was and is required to understand the association with schizophrenia. The main goal of this thesis was to investigate the

neurobiological pathways in human brain that *ZNF804A* is involved in and to look at the effects of risk SNP rs1344706 on these, in order to elucidate the association between *ZNF804A* and schizophrenia. To this end, I used both a genetic neuropathology and a genetic neuroimaging approach.

The first part of my thesis attempts to **characterise ZNF804A expression in human brain and establish how this is affected by diagnosis and by genotype**. In chapter 2, I show for the first time that ZNF804A immunoreactivity can be detected in both adult and foetal human brain and begin to characterise the regional and cellular expression of ZNF804A in human brain. We studied ZNF804A immunoreactivity with western blots and immunohistochemistry, using a commercially available antibody. Part of this chapter discusses validation of this antibody for use in human brain. In chapter 3, I compare ZNF804A mRNA and protein expression in schizophrenia with expression in healthy controls, and between risk and non-risk allele carriers at rs1344706.

The second question I address is whether ***ZNF804A* genotype affects brain structure in a large sample of 922 healthy young adults using both volumetry and voxel-based morphometry.** In collaboration with the Donders institute (Nijmegen, the Netherlands) we investigated a large structural MRI dataset of 922 volunteers to assess effects of *ZNF804A* genotype on macroscopic brain structure. These results are discussed in chapter 4.

In the third part of my thesis, I **assess the functional correlates of rs1344706 genotype in the living human brain using MEG and MR methods**. The basic design was to recruit and scan healthy volunteers who are homozygous at rs1344706 (n=25 vs. n=25) and compare them, using various imaging techniques. The purpose of the multimodal scanning experiments was twofold: first, and primarily, to provide convergent and multifaceted evidence about the impact of *ZNF804A* genotype on brain structure and

function. Secondly, to show the extent to which these different indices correlate within subjects, which is of broad relevance to multimodal neuroimaging. In chapter 5, I describe the imaging modalities and discuss the methods we developed to link the results from our magnetoencephalography (MEG), functional magnetic resonance imaging (fMRI), and magnetic resonance spectroscopy (MRS) experiments based on activity in occipital regions. In chapter 6, I then apply these methods to measure prefrontal function and to assess the effect of risk SNP rs1344706 on prefrontal function as measured by MEG, fMRI, and MRS. In chapter 7, I apply recently developed resting state analysis methods for MEG based on independent component analysis (ICA) to study the effects of *ZNF804A* genotype on resting state networks in healthy volunteers. Finally, in chapter 8, I discuss the findings of this thesis and their implications.

Chapter 2 - Expression of ZNF804A protein in human brain

2.1 Introduction

2.1.1 ZNF804A expression

As discussed in chapter 1, *ZNF804A* was the first gene to show genome wide significant association with schizophrenia, but very little is known about the neurobiological pathways *ZNF804A* is involved in. It is of importance to understand its biology, given that the link between a risk gene and a disease can only be understood by studying the mechanisms by which the risk is conferred. As mentioned in section 1.4, mRNA and protein expression are the intermediate phenotypes closest to the gene, and studying this in human brain is crucial, given that expression in other species or systems might differ. Furthermore, studying the pathways that putative schizophrenia risk genes are involved in might aid to the understanding of the molecular mechanisms that lead to schizophrenia.

Therefore, a key first step in understanding the neurobiology of *ZNF804A* is to establish its expression in the brain, but so far only mRNA expression has been studied. It has been shown that the gene is transcribed in human brain and mRNA can be detected in the DLPFC (Riley et al., 2010) and in frontal, temporal, and parietal regions (Williams et al., 2011), but to date there are no reports of ZNF804A protein expression and distribution in human brain. Although there is no reason to expect that *ZNF804A* would not be translated, positive evidence should be acquired. This is of importance, because it is the protein that would actually impact on neurobiological processes involved in schizophrenia. Additionally, providing evidence for ZNF804A immunoreactivity would allow the study of protein expression, distribution, and eventually function, in human brain. Documenting the neuroanatomical distribution of ZNF804A will reveal whether it is expressed in brain regions affected in schizophrenia, and the potential pathways it may influence.

2.1.2 ZNF804A protein

Based on the sequence of *ZNF804A*, the ZNF804A protein is predicted to contain zinc ion and DNA binding domains (O'Donovan et al., 2008). It contains no other strong sequence motifs and there seem to be no close homologues to other proteins. Based on its zinc finger domain, the gene was called zinc finger protein 804A. A zinc finger is a small peptide domain with a special secondary structure stabilized by a zinc ion bound to the Cys and His residues of the finger. Differential use of the two residues gives rise to several types of zinc fingers, with the ZNF804A finger being a C2H2 arrangement (Iuchi, 2001). C2H2-type domains were originally identified as DNA binding molecules with a role in transcription, but proteins with this zinc-finger domain are now known to interact with many other types of molecules (Gamsjaeger et al., 2007). Therefore, ZNF804A might function as a transcription factor, or might have other roles interacting with mRNA or protein. Only one other C2H2 zinc finger protein gene with a single zinc binding domain has been reported, GAGA factor, which does bind to DNA (Pedone et al., 1996). This lack of information on single zinc fingers makes it difficult to predict the function of ZNF804A. Should it be true that ZNF804A functions as a transcription factor, then it is likely that ZNF804A protein would be localised to the nucleus (Vaquerizas et al., 2009), although examples have been described where transcription factors are located in the cytoplasm and relocate to the nucleus in response to the appropriate signal (Whiteside & Goodbourn, 1993).

In this chapter, I describe and discuss the measurement of ZNF804A immunoreactivity in human brain. We purchased a commercially available antibody, but given that no reports on this antibody were available in the literature, it was first necessary to validate it using bacterial and mammalian cells expressing ZNF804A. Having done so, I then used western blotting to demonstrate the presence of ZNF804A immunoreactivity in

adult human brain, foetal human brain, and lymphoblast cells. Finally, immunohistochemistry was used to study the cell types expressing ZNF804A and its sub-cellular distribution.

2.2 Methods

2.2.1 Human tissue

Human tissue was provided by several different research institutes and brain banks. Human anterior cingulate cortex tissue and human inferior parietal lobule tissue were obtained from the Stanley Medical Research Institute Inferior Parietal Lobule brain collection in the USA. Human superior temporal gyrus separated into grey and white matter was provided by the Australian Brain Donor Programs NSW Tissue Resource Centre. More details about these collections will be given in chapter 3 (3.2.1). Sections from several human brain regions, both adult and infant, came from the National Institute of Mental Health, Bethesda, USA and from the Oxford brain bank at the John Radcliffe Hospital. Foetal tissue was provided by the Lieber Institute for Brain Development, Baltimore, USA. Lymphoblast cell lines came from the National Institute of Mental Health. These were collected and transformed as described previously (Sei et al., 2007). Ethical approval for this work was provided by Oxfordshire NHS REC B (O02.040).

2.2.2 Antibody validation

For characterization of the protein, an anti-ZNF804A antibody was obtained from Santa Cruz (D14, sc-241170). This is a goat polyclonal antibody raised against a peptide mapping within an internal region of ZNF804A of human origin. To validate the antibody, a commercially available plasmid construct of *ZNF804A* with a green fluorescent protein (GFP) tag (Origene, USA) was cloned in competent bacteria (KRX cells, Promega UK)

according to the manufacturer's recommendations. The ZNF804A-GFP bacteria were grown overnight in the appropriate growth media (10ml), and the basal expression of the ZNF804-GFP recombinant protein in cells was confirmed by fluorescent microscopy the following day. Further synthesis of ZNF804A-GFP protein in cells was achieved by adding 0.1% rhamnose to the bacterial culture (manufacturer's recommendations), and leaving the cells for 16 hours at room temperature. Cloning was carried out by Dr. Phil Burnet.

A sample of cultured bacteria (1ml) was pelleted in a microfuge tube, and rinsed once with PBS. The pellet was resuspended (1:5, w:v) in RIPA buffer containing protease inhibitor and frozen on dry ice for 2min. The sample was thawed and placed in the bead homogeniser to extract protein. The cells were centrifuged for 2min and replaced on the dry ice. This freeze-thaw extraction procedure was repeated five times. Protein concentration was measured with a Bradford assay, described as part of the western blot procedure.

Additionally, we obtained human embryonic kidney (HEK293) cells which had been transfected with a *ZNF804A* construct from Dr B. Maher, Lieber Institute for Brain Development. The cells had been transfected as described in Girgenti et al. (2012) and protein was extracted as above.

2.2.3 Western blotting

Western blotting can be used to determine the presence of immunoreactivity of an antibody in a particular sample. With this method, the proteins are first separated by size using gel electrophoresis, because smaller proteins are able to move faster through the gel towards the anode. The proteins are then transferred to a membrane and incubated with an

antibody specific to the protein of interest, so that the binding of this antibody can be visualised.

Protein was extracted using RIPA buffer (Thermo-Fisher), with protease inhibitor (Roche, Welwyn Garden City, UK) to reduce protein degradation. Approximately 1ml of buffer containing protease inhibitor was added for every 0.1g of tissue and extractions were done with a bead homogenizer. Protein concentration of extracts was determined by Bradford assay. Bradford reagent changes colour in the presence of protein, and the optical density can be quantified to determine the amount of protein in each sample. Nine bovine serum albumin (BSA) protein standards ranging from 0.9µg/µl to 0µg/µl were used to determine the concentration of the samples. Extracts and standards were diluted 1:19 in 1M NaOH. 5µl of each sample was loaded into a 96–well plate in duplicate along with 250µl Bradford Reagent (Sigma-Aldrich) in each well and incubated at room temperature for 5 minutes. Absorbance was read at 595nm and 450nm using a SpectraMax 190 plate reader and Softmax Pro 4.0 software (both Molecular Devices, Wokingham, UK). The protein content of each sample was determined in relation to the protein standards.

Protein was separated by size using sodium dodecyl sulphate polyacrylamide gel electrophoresis (SDS-PAGE) using pre-cast gels. Before gel electrophoresis, 3µl of loading buffer was added to each sample. Approximately 100 volts was passed through the gels until the samples had travelled sufficient distance to separate the proteins, which took typically around 90 minutes. The gels used were any kD pre-cast gels (Bio-Rad Mini-Protein TGX Gels) containing either 10 or 15 wells. To estimate the size of the protein, a Kaleidoscope Precision Plus Protein Standard (Bio-Rad) ladder was used in each gel. Protein samples were transblotted onto polyvinylidene fluoride (PVDF) membranes (Immobilon-P, Millipore, Watford, UK) overnight at 25 volts.

The PVDF membranes were dried for 15 minutes and then soaked in blocking buffer (2% milk in PBS with 0.1% Tween20) for 1 hour at room temperature. The gels were probed with the primary antibody, diluted to 1:250 or 1:500 in blocking buffer, for 1 hour at room temperature. Following three 15 minute washes in PBS containing 0.1% Tween20 (PBS-Tw), the membranes were incubated for 30 minutes with donkey anti-goat secondary antibody horseradish peroxidase (HRP) conjugate diluted to 1/15000 in blocking buffer, followed by a further three 15 minute washes in PBS-Tw. Antibody binding was visualised by electrochemiluminescence (ECL), which produces light in a reaction catalysed by the HRP on the secondary antibody, using an ECL Plus Western Blotting Detection System and Hyperfilm ECL (both GE Healthcare).

As further controls to show specificity, we repeated this protocol with a second ZNF804A antibody (Santa Cruz, P13, sc-241173) using a concentration of 1:200 in blocking buffer. Additionally, we used a commercially available blocking peptide (D14p, sc-241170P) to ensure that blocking the primary antibody would abolish the signal.

2.2.4 Immunohistochemistry

Immunohistochemistry uses antibodies to detect and visualise the location of a protein antigen in tissue sections. Frozen, paraffin-embedded formalin-fixed, and formalin-fixed free-floating sections were all pre-treated in the appropriate manner. The free-floating sections were washed in phosphate-buffered saline (PBS) and heated at 90°C in a waterbath while in citrate-based Vector Antigen Unmaking Solution (Vector laboratories) for 30 minutes and cooled for 20 minutes. These sections will be discussed in more detail in chapter 3. Slide-mounted paraffin-embedded sections were pretreated by overnight incubation in xylene followed by rehydration in alcohol (100%, 95%; 70%, 1 minute each) followed by a minute in dH2O, before being heated at 90°C in a waterbath while in citrate-

based Vector Antigen Unmaking Solution (Vector laboratories) for 30 minutes and cooled for 20 minutes. Frozen sections were fixed in 4% paraformaldehyde in PBS for 5 minutes before being washed in dH2O for 5 minutes. Tissue sections were dehydrated in increasing concentrations of alcohol (70%, 95%, and 100%, 1 minute each). The slides were placed in solution of 3% hydrogen peroxide (VWR) in methanol for 30 minutes. The slides were then rehydrated by placing them in decreasing concentrations of alcohol (100%, 95%, and 70%, 1 minute each) followed by a 1 minute in dH2O and 2x5min washes in PBS.

For all types of sections, non-specific binding sites were blocked by incubation with 5% normal rabbit serum in PBS with 0.3% Triton X-100 (PBS-T) for 1 hour at room temperature. The sections were then rinsed in PBS and incubated at 4°C for 72 hours with the primary antibody (D14, Santa Cruz) diluted to 1/1000 for the free-floating sections and overnight with the primary antibody diluted to 1/100 for the slide-mounted fixed and frozen sections in solution of 1% normal rabbit serum and PBS-T. The sections were then washed in PBS (3x10min) and bound antibody was visualised using the Vectastain elite ABC kit (Vector Laboratories). The ABC kit detects binding of the primary antibody using an avidin and biotinylated HRP macromolecular complex which produces a coloured product localised to the biotinylated secondary antibody. The sections were incubated in a solution of PBS-T with 1% rabbit anti-goat secondary antibody and 1% normal rabbit serum for one hour at room temperature and washed in PBS (3x10 minutes). The sections were then incubated in a solution made up of 1% of each of reagents A and B in PBS-T for 1 hour at room temperature, washed in PBS (3x10 minutes), and developed by immersion in a filtered solution of 0.025% diaminobenzidine (DAB) and 0.00018% hydrogen peroxide in PBS for ten minutes. DAB acts as the substrate for the colour-change reaction. For Nissl staining, sections were stained with 0.75% cresyl violet and dehydrated through

increasing concentrations of alcohol. Coverslips were placed over the slides, fixed in place with DPX.

2.3 Results

2.3.1 Antibody validation

Basal expression of the ZNF804-GFP recombinant protein in cells was confirmed by fluorescent microscopy. Figure 2.1 shows a microscopic image of bacteria containing ZNF804A tagged with GFP (left). Synthesis of ZNF804A-GFP protein in cells was achieved by adding 0.1% rhamnose to the bacterial culture (Figure 2.1, right).

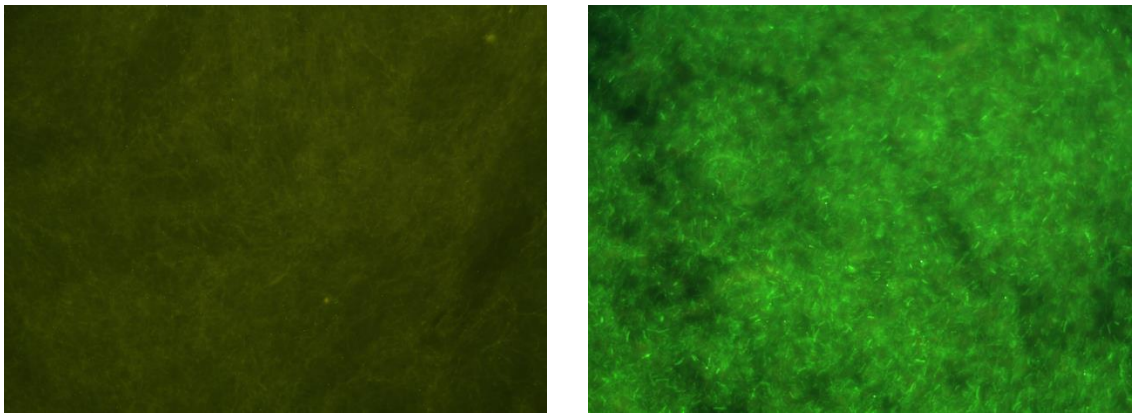

Figure 2.1: Images obtained with fluorescent microscopy showing bacteria expressing ZNF804A tagged with GFP. The left image shows the bacteria that have not been induced, while the right image shows bacteria induced with 0.1% rhamnose.

Figure 2.2 shows immunoreactivity in extract from bacteria and cells expressing ZNF804A. The upper part of the image shows that the antibody detects immunoreactivity in bacteria expressing ZNF804A (lane 1), while it does not detect immunoreactivity in bacteria expressing GFP only (lane 2). The middle image shows an increase in signal when more protein is added (from left to right: 3µg/6µg/12µg) and shows bands of greater intensity when expression of ZNF804A is induced (+ vs -). The lower image shows that there is immunoreactivity in the extract from the HEK cells transfected with the ZNF804A construct (lane 1), but not in the extract from HEK cells expressing GFP only (lane 2). The

bands can be detected between 100 kDa and 150 kDa, which is in line with the predicted weight of the ZNF804A protein (136 kDa). These western blots together indicate that the antibody specifically detects ZNF804A immunoreactivity.

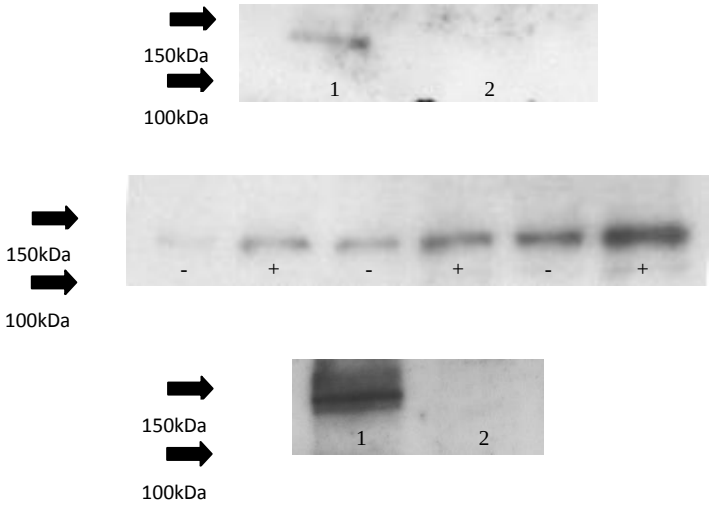

Figure 2.2: The upper part of the image shows that the antibody detects immunoreactivity in extract from bacteria expressing ZNF804A (left band), while it does not detect immunoreactivity in extract from bacteria expressing GFP only. The middle image shows an increase in signal when more protein is added (from left to right: 3µg/6µg/12µg) and shows bands of greater intensity when expression of ZNF804A is induced (+ vs -). The lower part of the image shows that there is immunoreactivity with extract from the HEK cells transfected with the *ZNF804A* construct, but not with extract from HEK cells expressing GFP only. Arrows show the molecular weight as indicated by the ladder.

2.3.2 Western blotting

After the validation steps described above, which showed immunoreactivity in extract from both bacteria and HEK cells transfected with ZNF804A, we carried out several western blot experiments in human tissue. Figure 2.3 shows a small western blot containing protein extracted from HEK cells transfected with ZNF804A (lane 1), HEK cells transfected with only GFP (lane 2), foetal human brain tissue (lane 3) and adult human ACC tissue (lane 4). The HEK cell lanes again confirm the validity of the antibody, because HEK cells transfected with ZNF804A give a clear band of around 140 kDa, whereas no band appeared for control cells transfected with GFP. Importantly, on this same blot, immunoreactive bands of a similar size appeared for foetal and adult human

brain tissue, demonstrating that ZNF804A immunoreactivity is present in both foetal brain and adult brain and has the molecular weight predicted for ZNF804A.

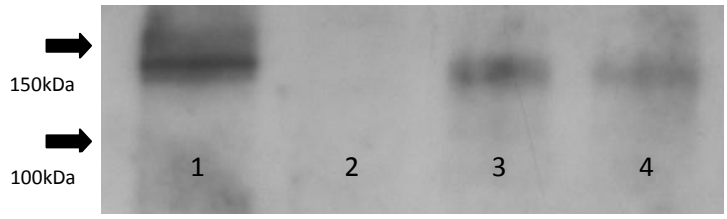

Figure 2.3: Western blot, containing protein from HEK cells transfected with ZNF804A (lane 1), HEK cells transfected with GFP (lane 2), foetal human tissue (lane 3), and adult human ACC (lane 4), probed with ZNF804A antibody (D14). Arrows indicate the sizes (kDa) provided by a Kaleidoscope Precision Plus Protein Standard ladder. A band was observed around the expected molecular weight of ~136 kDa.

A larger blot, depicted in Figure 2.4, containing protein extracted from the HEK cells transfected with ZNF804A (lane 1), foetal brain tissue (lanes 2/3/4), adult human STG tissue (lanes 5/6) and adult human ACC tissue (lanes 7/8) shows a similar pattern, confirming the presence of a similar size immunoreactive band in both adult and foetal brain. On this blot a smaller second band became visible for some cases (lanes 7 and 8), which was not detected on the blot displayed in Figure 2.3.

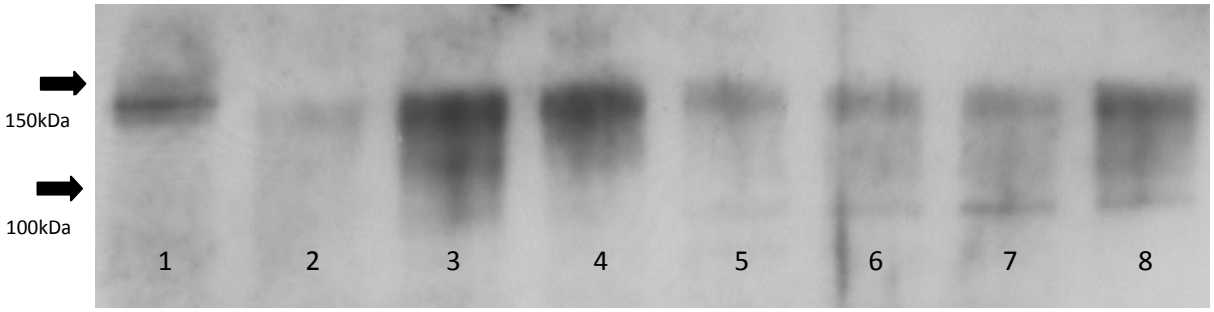

Figure 2.4: Western blot, containing protein from HEK cells transfected with ZNF804A (lane 1), foetal brain tissue (lanes 2/3/4), adult human STG (lanes 5/6), and adult human ACC (lanes 7/8), probed with ZNF804A antibody (D14). Arrows indicate the sizes (kDa) provided by a Kaleidoscope Precision Plus Protein Standard ladder.

An additional blot was carried out to confirm these observations and characterise tissues in which ZNF804A immunoreactivity could be detected. This blot contained protein from human STG grey matter (lanes 1/2/3), human STG white matter (lanes 4/5/6),

human ACC (lanes 7/8), and lymphoblast cells (lane 9), shown in Figure 2.5. For all these types of tissue it was possible to detect ZNF804A immunoreactivity. On this blot, two immunoreactive bands were seen in human ACC and STG extracts, which were observed just below 150 kDa and just below 100 kDa. For the lymphoblasts, one immunoreactive band was visible (lane 9) between the two bands observed in human brain tissue.

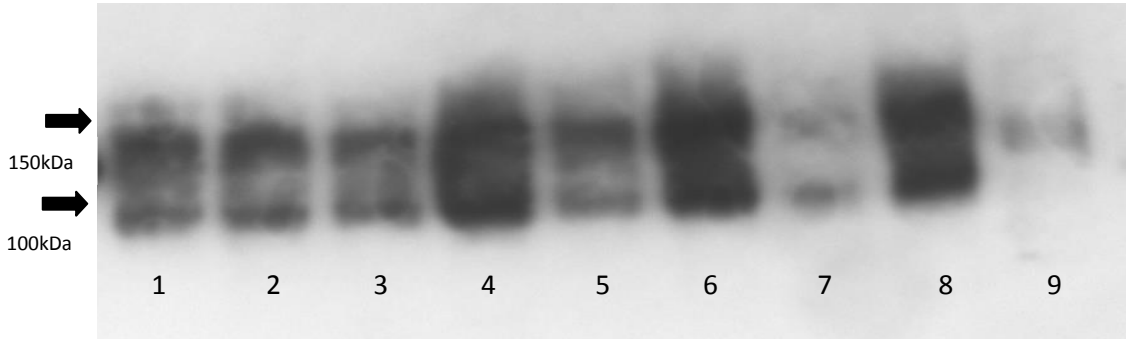

Figure 2.5: Western blot, containing protein from STG grey matter (lanes 1/2/3), STG white matter (lanes 4/5/6), adult human ACC (lanes 7/8), and human lymphoblast cells (lane 9), probed with ZNF804A antibody (D14). Arrows indicate the sizes (kDa) provided by a Kaleidoscope Precision Plus Protein Standard ladder.

When we pre-incubated the primary antibody with its blocking peptide, no signal was observed on the western blots. Additionally, we loaded a gel with the exact same samples as the gel depicted in Figure 2.5, but probed it with another ZNF804A antibody (Santa Cruz, P13) which is directed against the c-terminal of the protein. In this case similar but fainter bands appeared (data not shown), again confirming that ZNF804A immunoreactivity can be detected in human brain and human lymphoblast cells.

2.3.3 Immunohistochemistry

Immunohistochemistry experiments with the same antibody as used for the western blot study (Santa Cruz, D14) were carried out on frozen, paraffin-embedded formalin-fixed, and formalin-fixed free-floating tissue sections from different regions of the human brain. The pattern of staining was very consistent, with mainly pyramidal neurons in layer III providing evidence for the presence of ZNF804A. The first row of Figure 2.6 shows

that ZNF804A immunoreactivity could be detected in all three types of tissue. Staining of paraffin-embedded and free-floating sections looked very similar (2.6A and 2.6B), while the quality of the tissue and staining was not as good for frozen tissue (2.6C). Therefore, frozen tissue was only used when staining hippocampal sections, because no other hippocampal tissue was available.

The first and second rows of Figure 2.6 together show that ZNF804A immunoreactivity can be detected throughout the cortical areas studied. Image 2.6A depicts a section taken from the superior temporal gyrus of an adult human brain, indicating the presence of ZNF804A in the temporal lobe. Image 2.6B shows an inferior parietal lobule section, showing the presence of ZNF804A in the parietal lobe. In the second row, image 2.6D shows a cell in the hippocampus stained with the ZNF804A antibody and counterstained with a Nissl stain at a high magnification. Image 2.6E shows staining of neurons in the frontal lobe, whereas image 2.6F depicts staining (at a lower magnification) in occipital regions.

The third row of Figure 2.6 shows the laminar localization of the cells that were stained by the ZNF804A antibody. Staining was consistently found in pyramidal cells, which are mainly localised to layer III and layer V of the cortex. Some staining of pyramidal neurons in layer V was found, but the majority of cells that contained ZNF804A immunoreactivity were found in layer III of the cortex. Image 2.6G shows a counterstained section at low magnification, where ZNF804A staining (in brown) is mainly seen in layer III. Also images 2.6H and 2.6I show a clear band of stained pyramidal cells, here on sections probed with the ZNF804A antibody only.

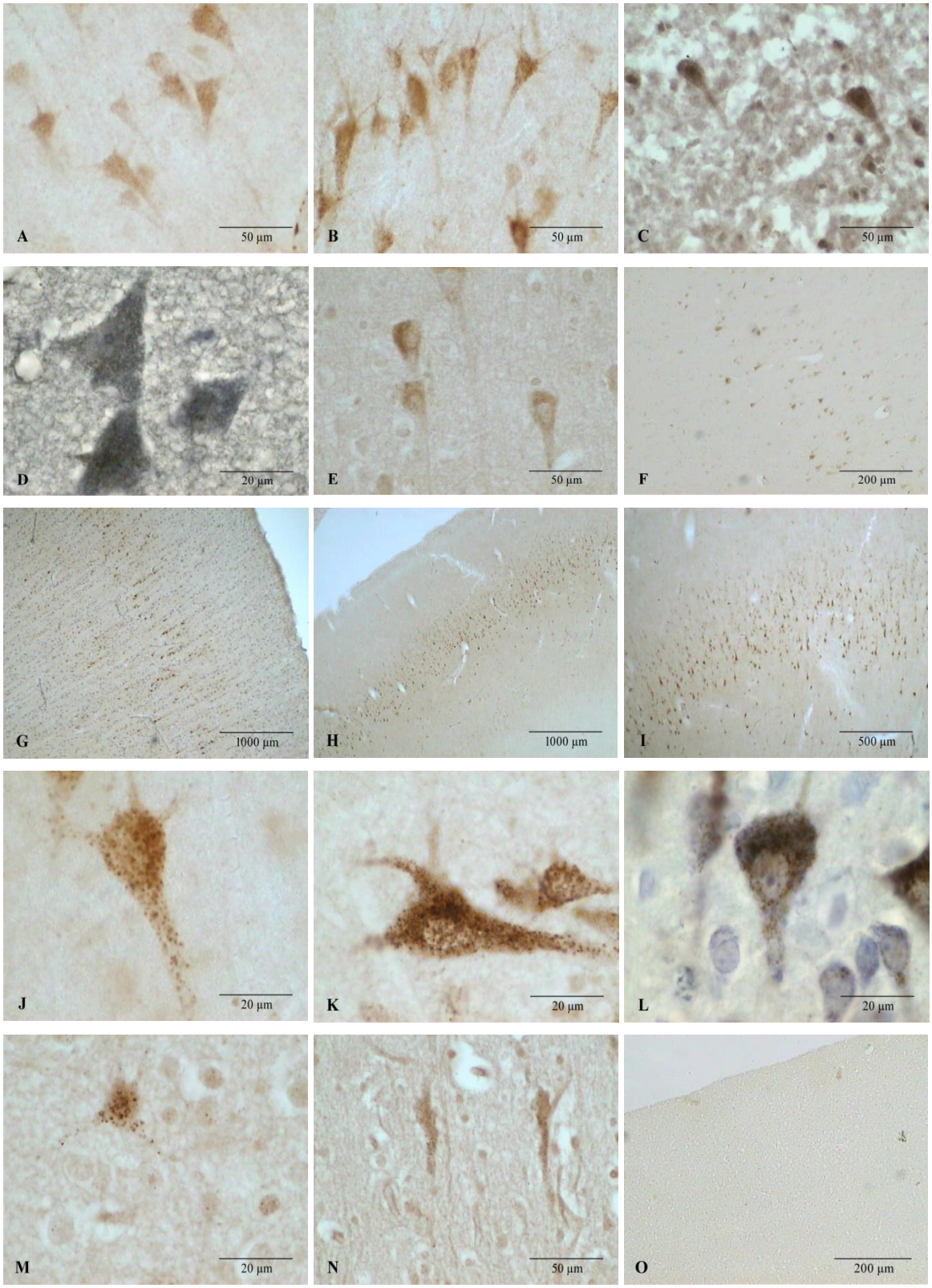

Figure 2.6: Microscopic immunohistochemistry images of human brain sections showing staining of pyramidal cells in layer III. A) paraffin-embedded STG section B) free-floating IPL section C) frozen STG section D) frozen hippocampal section with counterstain E) paraffin-embedded prefrontal section F) paraffin-embedded occipital section G) paraffin-embedded STG section with counterstain H) free-floating IPL section I) free-floating IPL section J) free-floating IPL section K) paraffin-embedded STG section L) paraffin-embedded STG section with counterstain M) paraffin-embedded frontal section from infant N) paraffin-embedded frontal section from infant O) paraffin-embedded control section. Scales have been indicated in the lower right corner.

Row four (Figure 2.6J-K) shows the pattern of ZNF804A immunoreactivity in three individual pyramidal neurons at a high magnification. These images again underline the clear staining of pyramidal neurons, but also allow a closer look at the pattern of staining within the cell. Staining can be seen throughout the cytoplasm, and has a slightly granular structure, as can be observed in pictures 2.6J and 2.6K. Interestingly, if anything, there seems to be less staining in the nucleus of the cells than throughout the cytoplasm. This is particularly clear in image 2.6L, which shows a pyramidal cell stained with the ZNF804A antibody and counterstained with a Nissl stain.

The last row (Figure 2.6) shows immunoreactivity in infant tissue. The tissue was taken from the frontal lobe of an infant who died 3 hours after birth. Also in this case, staining can be seen in pyramidal neurons (2.6M), some of which were not yet fully developed (2.6N). ZNF804A already seems to be present throughout the cell, with a similar pattern of granular staining throughout the cytoplasm. Finally, image 2.6O shows a control section that underwent the same immunohistochemistry procedure as described in section 2.2.4, but without incubation with the primary antibody.

2.4 Discussion

Based on the western blot studies, it can be concluded that 1) an antibody is available which specifically detects ZNF804A in human cells and transfected bacteria. 2) ZNF804A immunoreactivity can be detected in adult grey and white matter, foetal brain tissue, and lymphoblast cells. 3) There are either one or two bands detected.

The immunohistochemistry results show that: 4) ZNF804A immunoreactivity can be detected with this antibody in frozen, paraffin-embedded formalin-fixed, and formalin-fixed free-floating tissue. 5) ZNF804A is mainly localised to layer III pyramidal cells. 6) In cerebral cortex, ZNF804A is present throughout the cytoplasm of these cells, and if

anything, staining is less prominent in the cell nucleus. 7) This pattern is true in all brain regions studied, and in adult as well as infant brain.

Two results require further clarification. First of all, whereas some western blots provided evidence for the presence of only one band, other blots clearly showed two bands, indicating there might be one or two isoforms of the ZNF804A protein. In both cases, the exact same experimental protocol was used, making it difficult to pinpoint why this difference might arise. A possible explanation is that some property of the reagents that were used had changed. Given that the western blots experiments were carried out at different time points, new gels and a new aliquot of the ZNF804A antibody had been obtained. Even though the antibody supposedly came from the same batch, it is not impossible that it did not react with the ZNF804A protein in the same way. In Figure 2.4 there is a hint of a second band, but this band is somewhat lower than the second band in Figure 2.5, making it hard to predict the real weight of this second band. Further experiments, possibly with a different ZNF804A antibody, will have to resolve this. However, most importantly, we did detect an immunoreactive band at 136 kDa, and provided convincing evidence that this band represents ZNF804A immunoreactivity. In chapter 8 of this thesis, I will discuss the possibility of there being two bands and the implications of this in more detail.

Secondly, the immunohistochemistry experiments showed a very clear and consistent pattern of staining that was mainly limited to pyramidal cells. However, on the western blots, it was equally clear that ZNF804A immunoreactivity can be detected in white matter (Figure 2.5). The possibility that our white matter samples did contain grey matter including pyramidal cells should be considered, but in the next chapter I will study ZNF804A mRNA and also detect mRNA in white matter. This means that it is likely that ZNF804A protein is present in white matter, possibly in the axons of pyramidal cells or

outside of pyramidal neurons. Future studies will have to clarify where in white matter ZNF804A protein can be found, and why our initial immunohistochemistry studies were unable to detect it. For instance, it is possible that the epitope recognised by the antibody is not accessible in the white matter, and more stringent immunohistochemical methods might be required to retrieve it.

Since the completion of the present analyses, two other studies have used the same Santa Cruz D14 antibody to detect ZNF804A immunoreactivity. Umeda-Yano et al. (2013) carried out a western blot on HEK cells overexpressing exogenous ZNF804A. As in our experiment, they were able to detect ZNF804A and showed one clear band with a fainter band underneath, leaving the discussion about the number of isoforms open. Girgenti et al. (2012) subcloned human *ZNF804A* into rat neural progenitor cells. Using ZNF804A protein obtained from these cells, they carried out a western blot experiment showing one clear band at 136 kDa. Using the D14 anti-ZNF804A antibody, they carried out immunohistochemistry experiments on these cells as well as on rat cortical progenitor cells in vivo. They found that ZNF804A immunoreactivity is localised to the nucleus of neural progenitor cells in culture and in vivo. There could be several reasons why their immunohistochemistry findings are not in line with ours. First of all, they studied a different species, having taken progenitor cells from rat embryos. Secondly, they looked at prenatal tissue, whereas our experiments were carried out on adult or postnatal infant tissue. We did try to address these issues by carrying out immunohistochemistry experiments with tissue at the earliest developmental stage we could obtain (3 hours postnatal), but these experiments showed the same pattern of staining as the adult brains. We also carried out some immunohistochemistry on mouse tissue (data not shown) and still found staining throughout the cytoplasm. Therefore, it might be a combination of

species and developmental stage that leads to these different findings. Alternatively, ZNF804A might only be localised to the nucleus during very early development.

The staining observed throughout the cytoplasm appeared granular (Figure 2.6J-K). A similar kind of granular structure can be observed in immunohistochemistry studies staining the ribosome, which led us to hypothesise that ZNF804A might be associated with the ribosome. Therefore, we attempted double-labelling studies with an anti-ribosomal antibody, and saw a comparable pattern of granular staining, but no clear overlap of the staining patterns (data not shown). Hence, we were unable to identify the organelles that ZNF804A is associated with. However, the spread of ZNF804A throughout the cytoplasm suggests roles beyond those of a transcription factor. Given its zinc finger domain, it could for example bind to mRNA and have a role in alternative splicing (Ladomery & Dellaire, 2002; Plambeck et al., 2003).

Furthermore, it is of particular interest that ZNF804A immunoreactivity was primarily detected in layer III pyramidal cells. Pyramidal neurons in layer III are responsible for sending axonal projections to other parts of the cortex and are suspected to be of particular relevance to the pathophysiology of schizophrenia, given their long-range cortico-cortical projections (Lewis et al., 2003). Some morphological abnormalities have been reported in brains of schizophrenia patients, with both Garey et al. (1998) and Glantz and Lewis (2000) showing decreased dendritic spine density in layer III pyramidal neurons in the DLPFC. In line with this, studies have reported decreases in synaptophysin, a marker of axon terminals, in several brain regions (Eastwood et al., 1995; Glantz & Lewis, 1997), as well as decreased neuropil space (Selemon & Goldman-Rakic, 1999). Other neuropathological studies of schizophrenia have shown that the size of layer III pyramidal cells decreases in schizophrenia, both in the DLPFC (Rajkowska et al., 1998; Pierri et al., 2001) and in the STG (Sweet et al., 2003). Another study has reported elevated neuronal

density in prefrontal area 46 in brains from schizophrenia patients (Selemon et al., 1998). What should be noted is the important role of layer III pyramidal cells in connectivity. Esslinger et al. (2009) reported in a first neuroimaging study of *ZNF804A* that rs1344706 affects functional connectivity between the DLPFC and several other brain regions. The finding that ZNF804A is found in the cells responsible for long-range connectivity provides a first clue as to the neurobiological pathway via which *ZNF804A* might affect functional connectivity in the brain.

Chapter 3 - Genotype and diagnosis effects on expression of ZNF804A mRNA and protein

3.1 Introduction

3.1.1 Effect of rs1344706 on ZNF804A expression

In the previous chapter, it was shown that ZNF804A immunoreactivity can be detected in both adult and foetal human brain and that it is mainly localised to layer III pyramidal neurons. The next important question is whether variation at rs1344706 affects mRNA and protein expression in human brain. Genetic variation can affect disease susceptibility in several ways. If the variation is in a coding region, it can change the structure of the encoded protein by causing an amino-acid substitution or frame-shift mutation. Alternatively, genetic variation can alter the expression of the gene by altering some parameter of transcription or translation and thereby the amount or distribution of the protein (Harrison & Weinberger, 2005). Whereas the effect of an intronic SNP such as rs1344706 cannot occur via the former mechanism, it can affect expression of the gene.

Given the absence of a known coding variant in linkage disequilibrium with rs1344706, rs1344706 might affect expression of ZNF804A directly. Two studies already investigated whether the rs1344706 allele affects mRNA expression in human brain. Findings were inconsistent, because whereas Riley et al. (2010) reported that the risk allele is associated with an increase in mRNA in the DLPFC, the findings of Williams et al. (2011) suggested that effects on expression might occur through additional regulatory variants at the *ZNF804A* locus. Riley et al. (2010) also carried out a bioinformatics analysis, which indicated that the alleles lead to differential prediction of the presence of binding sites for two different brain-expressed transcription factors, thereby providing a possible explanation as to how an allelic difference in mRNA expression might arise. Given the lack of conclusive evidence, this chapter investigates the effect of rs1344706 on mRNA expression levels, and for the first time, on protein expression in human brain.

3.1.2 Effect of diagnosis on ZNF804A expression

Additionally, it is of interest to investigate whether ZNF804A mRNA and protein expression levels are associated with a diagnosis of schizophrenia. If ZNF804A expression levels would be found to be altered in the brains of schizophrenia patients, this would demonstrate possible involvement in the pathophysiology of the disease independent of the risk allele. Several studies investigating the effects of schizophrenia risk genes have studied whether expression differed between cases and controls (Law et al., 2006; Sartorius et al., 2008; Bristow et al., 2009). So far, only the study by Riley et al. (2010) has compared ZNF804A mRNA expression levels in schizophrenia patients and controls, and found somewhat increased expression levels in the brains of schizophrenia patients, but this difference did not reach statistical significance. Therefore, this question remains to be answered.

Studying ZNF804A expression in brain tissue obtained from both schizophrenia patients and healthy controls also allows the study of genotype x diagnosis interactions. However, should we find an effect of rs1344706 in one group only, this would not necessarily be easy to interpret. On the one hand, it may indicate an epistatic or gene–environment interaction that is present in the schizophrenia group more than in control subjects (or more in the control than schizophrenia group) and thus is worthy of further study. On the other hand, if a genetic effect on expression is seen in patients only, it may cast doubt on the robustness of the result, because one might expect a true genetic effect on gene expression to be seen in the healthy brain as well. An effect only in patients may reflect a genetic effect not on risk per se, but on something that is an illness-related epiphenomena, such as for example medication effects (Kleinman et al., 2011). Therefore, further experiments would be required to assess possible explanations.

3.1.3 Experiments to investigate effects of rs1344706 and diagnosis

In this chapter, I will first describe three quantitative polymerase chain reaction (qPCR) studies that were carried out to further investigate the effect of rs1344706, as well as diagnosis, on ZNF804A mRNA expression. The first of these was carried out on lymphoblast cell lines. Lymphoblast cell lines provide a useful model for investigating genetic or diagnostic differences in gene expression, as they reflect the genetic makeup of the individual from which the cell line was derived, but the influence of external factors such as anti-psychotic medication, substance abuse, and smoking will be removed as all cell lines will be grown under the same conditions. This means that any differences observed between groups should be due to genetic factors. Previous studies investigating schizophrenia risk genes have identified changes in expression in lymphoblast cell lines associated with genotype and diagnosis (Liu et al., 2007; Sei et al., 2007; Slonimsky et al., 2010).

Two other qPCR studies were carried out on superior temporal gyrus (STG) tissue. The STG, which contains the auditory cortex, is one of the structures that is most consistently reported by neuroimaging studies to be altered in schizophrenia (Shapleske et al., 1999; Shenton et al., 2001). Also post-mortem studies have reported a decrease in volume of the STG, as well as disruption of the normal asymmetry (Heckers, 1997), with both grey and white matter volume in the STG being significantly reduced (Highley et al., 1999). Two recent studies of the planum temporale of the superior temporal gyrus in schizophrenia have revealed reduced cortical thickness that was especially prominent in the upper layers, and was not accompanied by obvious changes in neuron density or size (Smiley et al., 2009; 2011). The Australian brain collection from which we obtained STG samples contains tissue separated into grey and white matter, and other studies looking at the expression of schizophrenia risk genes have shown that changes might be limited to or

more prominent in grey or white matter (Ghose et al., 2008; Mitkus et al., 2008; Habl et al., 2009; Morris et al., 2009; Habl et al., 2012). Given that not much is known about the expression of ZNF804A and inconsistent results have been reported by studies not distinguishing between grey and white matter, we decided to carry out our RT-qPCR experiments in grey and white matter separately. The tissue used in this study has been shown to be suitable for use in qPCR experiments (Weickert et al., 2010).

In addition to the ZNF804A transcript analysis, this chapter will assess the effects of rs1344706 and diagnosis on ZNF804A protein by using immunohistochemistry to estimate the densities and morphologies of cells containing ZNF804A immunoreactivity. This approach was chosen because limited frozen material was available and the signal in the western blotting experiments was variable, making it difficult to carry out quantitative comparisons. Instead, we carried out an immunohistochemistry study on free-floating inferior parietal lobule sections, which had shown very clear staining patterns in pilot studies (see chapter 2). In schizophrenia, neuroimaging experiments have found that the IPL has reduced cortical thickness (Narr et al., 2005; Schultz et al., 2010; Venkatasubramanian et al., 2011), and altered functional activation (Spence et al., 1997; Franck et al., 2002; Schnell et al., 2008) mainly during tasks assessing sensory integration, body image, concept of self, and executive function (Torrey, 2007). Several schizophrenia risk genes have also been found to be associated with altered activation of the IPL (Chakirova et al., 2011; Thimm et al., 2011). Very few post-mortem studies have looked at the effect of a schizophrenia diagnosis on the parietal lobe (Pakkenberg, 1993; Ongur et al., 1998). However, a recent study using tissue from the same brain collection (Smiley et al., 2012) did assess thickness and volume of the upper and lower cortical layers as well as neuron density and size in inferior parietal lobule sections and found no differences between schizophrenia patients and controls.

3.2 Methods

3.2.1 Human tissue

Several of the brain series mentioned in section 2.2.1 were used for the experiments described in this chapter. One RT-qPCR experiment was carried out using the lymphoblast cell lines obtained from the National Institute of Health, Bethesda, USA. Lymphoblast cell lines were available from 22 schizophrenia patients (13 male, 9 female) and 39 control subjects (18 male, 21 female). All subjects were Caucasian. Lymphocytes collected from subjects were transformed by infection with Epstein-Barr virus to produce the lymphoblast cell lines. The lymphocytes were collected and transformed as described previously (Sei et al., 2007). Two more RT-qPCR experiments were carried out on grey matter and white matter taken from adult human STG, obtained from the Australian Brain Donor Programs NSW Tissue Resource Centre (Weickert et al., 2010). Demographics of this series can be found in Table 3.1. The second brain series, used for immunohistochemistry, came from the Stanley Medical Research Institute, who provided free-floating sections of inferior parietal lobe tissue from men with schizophrenia and male controls (www.stanleyresearch.org/dnn/Default.aspx?tabid=199; Table 3.2). For this series, after brief formalin fixation of the cerebral hemisphere, 3-5 cm coronal slabs were cut, formalin-fixed for 3-15 weeks, and stored in buffered 30% sucrose. All blocks containing inferior parietal lobe were serially cryostat-sectioned at 60μm. Pilot studies showed no differences in ZNF804A immunoreactivity rostro-caudally across the inferior parietal lobule, and the studies were carried out on sections (three per subject, blind to group) randomly taken from the most rostral block.

Table 3.1: Demographics for schizophrenia and control group from the Australian brain collection, mean (SEM).

	Control	**Schizophrenia**
Sex M:F	30:7	24:13
Age (y)	51.1 (2.3)	51.3 (2.4)
Brain pH	6.52 (0.05)	6.44 (0.04)
RIN	7.3 (0.09)	7.3 (0.1)
Post-mortem interval (h)	24.8 (1.8)	28.9 (2.3)
Storage time (months)	69.6 (7.0)	79.9 (6.1)
Brain weight (gr)	1446 (21)	1394 (27)
Genotype (CC,CA,AA)	6, 14, 17	6, 21, 10

Table 3.2: Demographics for schizophrenia and control group from the Stanley inferior parietal lobule series, mean (SEM). All subjects were males.

	Control	**Schizophrenia**
Number	23	24
Age (y)	44.3 (2.0)	39.8 (2.2)
Brain pH	6.67 (0.04)	6.53 (0.05)
Post-mortem interval (h)	24.7 (2.3)	29.1 (2.4)
Hemisphere (L,R)	13,10	14,10
Storage time (months)	119 (5)	117 (5)
Brain weight (gr)	1479 (12)	1469 (11)
Genotype (AA, C carriers)	6, 17	10, 14

3.2.2 RT-qPCR

Quantitative reverse transcription polymerase chain reaction (RT-qPCR) allows investigation of the presence and quantity of expression of mRNA. The mRNA is first reverse transcribed to create cDNA, after which specific cDNA sequences of interest are detected by complementary primers and can be amplified using thermal cycling. More of the target cDNA will be produced with each cycle, resulting in exponential amplification of the target sequence which can be visualised through the detection of a fluorescent

reporter using RT-qPCR. The number of cycles it takes to reach a certain threshold allows quantitative comparison of the amount of mRNA present in the samples.

For the experiments reported here, tissue was homogenised in Tri-reagent (Sigma-Aldrich), with approximately a 1:10 ratio of tissue to Tri-reagent. 200µl of chloroform was then added for every 1ml of Tri reagent, and samples were vortexed and left at room temperature for 10 minutes before being spun at 14,000rpm in a bench-top centrifuge for 15 minutes. The top phase of the solution containing the RNA was collected and placed into a fresh tube along with an equal volume of isopropanol to precipitate the RNA. After an overnight incubation at -20°C, the solution was centrifuged at 14,000rpm for 10 minutes to form a pellet of the precipitated RNA. The supernatant was discarded and the pellet washed twice in 70% ethanol. The pellet was then left to dry at room temperature for ten minutes before being re-suspended in nuclease free water. The final concentration of RNA was measured using a NanoDrop ND-1000 Spectrophotometer and NanoDrop 3.0.1 software (NanoDrop Technologies, Delaware, USA).

For the next step, the samples underwent reverse transcription into cDNA, which was carried out as follows: 2µg RNA was DNase treated by heating at 37°C for 30 minutes followed by 10 minutes at 70°C with 1 unit RNase-free DNase and 24 units ribonuclease inhibitor (both Promega) added to each sample. The DNase treatment was used to remove genomic DNA to ensure that cDNA rather than genomic DNA was amplified in the subsequent qPCR studies. The resulting DNase free RNA was then reverse transcribed by heating at 42°C for 1 hour followed by 10 minutes at 70°C with 30ng oligo dT (20xTTP), 200 units M-MLV reverse transcriptase, 24 units ribonuclease inhibitor, and 0.5mM of each dNTP (ATP, CTP, GTP, and TTP) added to each sample.

In the final qPCR step, it is measured how many PCR cycles it takes for the level of fluorescence in each reaction well to reach a threshold, so that the amount of the target

cDNA present can be estimated by comparing the threshold cycle (Ct) of each well to a standard curve made up of known cDNA quantities. TaqMan probes, which were used for these experiments, are complementary to a sequence within the target cDNA and located between the target sequences of the primers used for amplification. The probe consists of a fluorescent tag and a non-fluorescent quencher which prevents the fluorescence being released while the probe is intact. During the amplification phase the probe will bind to the target sequence and will be broken down by the exonuclease activity of the Taq polymerase enzyme as the cDNA is amplified. The breakdown of the probe causes the fluorescent tag to be released into the solution, which allows this fluorescence to be detected.

The quantity of mRNA was measured by qPCR in human lymphoblast cells (n=61) and in grey and white matter taken from human STG tissue (n=74). ZNF804A and two Housekeeping genes (B2M and TFRC) were quantified using TaqMan Universal PCR Master Mix and specific Taqman probes for these genes (Applied Biosystems, ZNF804A: assay Hs00290118_s1; β-2-microglobulin (B2M): assay Hs99999907_m1; transferrin receptor (TFRC): assay Hs00951094_m1). For the lymphoblast cells, we additionally used Housekeeping genes hypoxanthine phosphoribosyltransferase 1 (HPRT1, assay Hs02800695_m1) and glucuronidase beta (GUSB, assay Hs00939627_m1). Each reaction contained 60ng of cDNA, which was found in pilot studies to be the optimal concentration of cDNA. Each plate included a standard curve ranging from 400 to 3ng cDNA which was made up of a pool of cDNA samples from the tissue being measured. Each sample was loaded in triplicate on all plates. The qPCR conditions were: initial denaturing step of 10 minutes at 95°C, followed by 40 cycles of 15 seconds denaturing at 95°C and 60 seconds of primer annealing/extension at 60°C. Samples were quantified using a standard curve and SDS v2.2.2 software with a 7900HT qPCR system (Applied Biosystems).

3.2.3 Immunostaining and quantification methods

This quantitative immunohistochemistry experiment was carried out together with a medical student, whose FHS (final honours school) project I supervised. For staining of the IPL sections, we used the same methods as described in section 2.2.4. In brief, the sections were pre-treated by being heated in a waterbath at 90°C while immersed in Vector Antigen Unmaking Solution. Non-specific binding sites were blocked by incubation with 5% normal rabbit serum in PBS with 0.3% Triton X-100 (PBS-T) for 1 hour at room temperature. Sections were incubated at 4°C for 72 hours with the primary antibody diluted to 1/1000 in a solution of 1% normal rabbit serum and PBS-T. Bound antibody was visualised using the Vectastain elite ABC kit (Vector Laboratories). The sections were incubated in a solution of PBS-T with 1% secondary antibody and 1% normal rabbit serum for 1 hour at room temperature and washed in PBS (3x10 minutes). Lastly, they were incubated in a solution made up of 1% of each of reagents A and B in PBS-T for 1 hour at room temperature, washed in PBS (3x10 minutes), and developed by immersion in a filtered solution of 0.025% diaminobenzidine (DAB) and 0.00018% hydrogen peroxide in PBS for ten minutes.

Given our finding, discussed in chapter 2, that staining was most prominent in layer III, we focused our quantitative analyses on layer III pyramidal neurons. Adjacent Nissl stained sections were available to aid identification of the layers. To estimate the density of ZNF804A immunoreactive neurons, an Olympus Prior BX50 optical imaging microscope was used with the CAST grid system. A counting frame of ~35,000μm² was generated and placed over a representative part of the section, always containing layer 3 only. At x40 magnification, a field sampler systematically moved across the box to allow systematic counting of the cells within the counting frame. Criteria for counting a cell were: 1) that it could be brought into focus, 2) that there was clear immunostaining, 3) that

the cell was pyramidal-shaped, 4) that the cell resided within layer III (Law and Harrison, 2003). Cells were included when they touched the left or upper border of the frame, but not if they were in contact with the right or lower border. The shape, size, and staining intensity of ZNF804A-immunoreactive lamina III pyramidal neurons were measured using a Nikon Eclipse E600 microscope linked to an MCID Elite 7.0 image analysis system, by manually tracing around the perimeter of the pyramidal neuron soma (n=50 neurons per case). Shape was quantified by way of the 'fcircle' function. Increasing 'fcircle' values indicate objects that are increasingly circular in shape. This same method for measuring shape, size, and staining intensity has also been reported in Gittins and Harrison (2004) and Gittins and Harrison (2011). Inter-rater reliability was r>0.9 for all parameters. We also measured the depth of the grey matter and depth of lamina III, and the final section thickness (Z-axis); none of these indices differed between diagnostic or genotype groups (data not shown). Because of the small sample size, C carriers were grouped together and compared to AA homozygotes for the immunohistochemical analyses.

3.2.4 Genotyping of samples

The human STG samples used for the qPCR study had been genotyped by the Australian brain bank. In order to genotype the cases from which IPL sections were taken, we obtained additional cerebellar tissue. DNA was extracted using a similar procedure as described for the RNA extraction in section 3.2.2. All samples were then treated with RNase prior to genotyping. Genotyping for each sample was undertaken using a 'Taqman©' genotyping assay (C___2834835_10) and the 7900HT qPCR system (Applied Biosystems). Samples were loaded in duplicate. The Taqman© probe was complementary to the part of the sequence that contains rs1344706, and the assay contained both forward and reverse primers spanning the site of the rs1344706 SNP. Two fluorescent labelled

probes were present, each specific to one of the alleles of the rs1344706 SNP. The probe targeting the A allele was labelled with VIC fluorescence, while the probe targeting the C allele was labelled with FAM fluorescence, each of which emitted fluorescence at distinct wavelengths. As a result of the different fluorescence emitted by each probe, the genotype of each sample could be determined by measuring the wavelength of fluorescence released. If only VIC was detected then the case was homozygous for the A allele, if FAM was detected the case was homozygous for the C allele, and if both FAM and VIC were detected the case was heterozygous.

3.2.5 Statistical analysis

All statistical analyses were carried out by Prof Paul Harrison, because I remained blind to genotype and diagnosis throughout the experiments. All statistical analyses were carried out using SPSS 20. All data were normally distributed and therefore parametric tests were used (ANOVA and post-hoc t-tests). Possible effects of age of onset, duration of illness, brain pH, freezer storage time, and post-mortem interval (PMI) were investigated using Pearson's coefficient. A p-value $\leq .05$ was considered to be significant.

3.3 Results

3.3.1 RT-qPCR

Our qPCR studies demonstrated that ZNF804A mRNA is detectable in lymphoblast cells, grey matter, and white matter. Figure 3.1 shows the amplification graphs for the STG grey matter and STG white matter. The plots show that STG grey matter mRNA reaches the amplification threshold at around 30 cycles, while amplification of white matter mRNA on average reaches the threshold around 32 cycles, indicating that ZNF804A mRNA is slightly more abundant in grey matter.

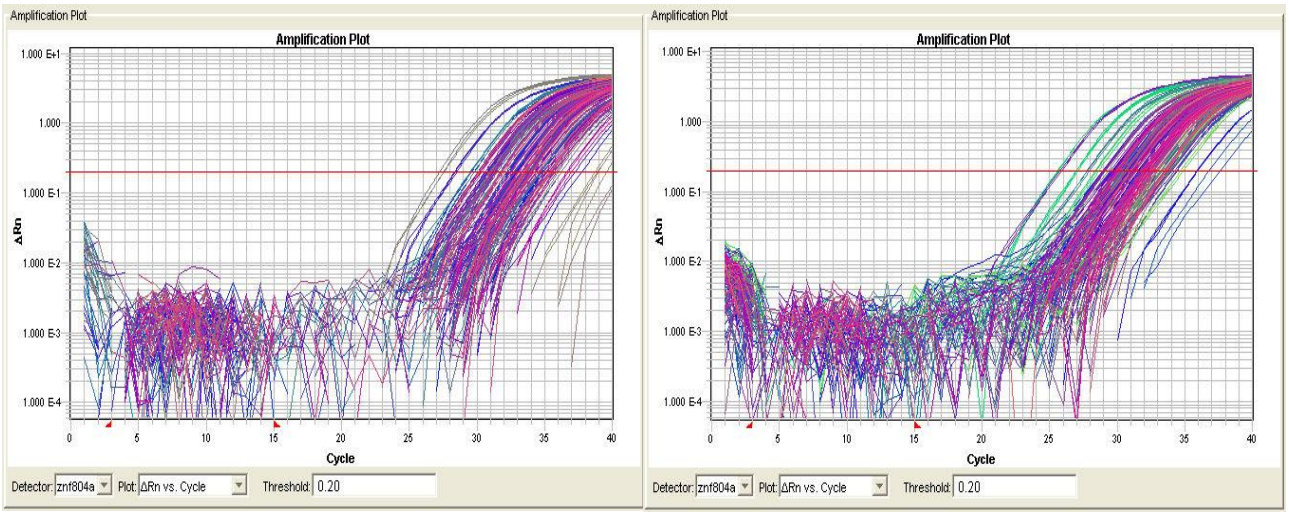

Figure 3.1: qPCR amplification plots showing amplification of STG grey matter mRNA (right) reaching the threshold around 30 cycles, while amplification of white matter mRNA (left) was more variable and on average reached the threshold around 32 cycles, indicating that ZNF804A mRNA is more abundant in grey matter.

Grey matter data were normalised to Housekeeping genes B2M and TFRC (see methods), while for white matter there was a difference between diagnostic groups in B2M mRNA abundance and therefore we only normalised to TFRC. This seemed an acceptable solution because there is no conclusive evidence that the use of multiple reference transcripts results in better normalization than one reference gene (Tunbridge et al., 2011). Furthermore, limited mRNA was available for these experiments. The lymphoblast data were normalised to the geometric mean of Housekeeping genes TFRC, HPRT1, and GUSB.

The results of these experiments can be seen in Table 3.3. None of the qPCR experiments showed an effect of rs1344706 genotype or diagnosis, indicating that there are no differences in ZNF804A mRNA between schizophrenia patients and healthy controls, nor between risk and non-risk carriers. (Lymphoblast cells: effect of diagnosis p=.73, effect of genotype p=.28, genotype x diagnosis interaction p=.59; Grey matter: effect of diagnosis p=.53, effect of genotype p=.35, genotype x diagnosis interaction p=.37; White matter: effect of diagnosis p=.54, effect of genotype p=.82, genotype x diagnosis interaction p=.49).

Table 3.3: mRNA results showing no differences between diagnostic groups or between the three genotype groups, mean (SEM).

	Schizophrenia	**Control**	**CC**	**CA**	**AA**
	N=37	N=37	N=12	N=35	N=27
Grey matter ZNF/ (HKG mean)	0.53 (0.09)	0.59 (0.03)	0.53 (0.09)	0.56 (0.03)	0.56 (0.04)
White matter ZNF/ TFRC	1.50 (0.19)	1.31 (0.16)	1.49 (0.40)	1.58 (0.22)	1.12 (0.13)
	N= 22	N=39	N=14	N=28	N=19
Lymphoblasts ZNF/ (HKG mean)	.680 (.106)	.634 (.077)	.649 (.132)	.745 (.102)	.513 (.362)

3.3.2 Immunohistochemistry

We did not observe associations between any of the measured parameters (Table 3.4) and age, PMI, pH, or brainweight. Similarly, in the schizophrenia group, potential confounding factors such as duration of illness, age of onset, and cumulative medication exposure did not correlate with any of the parameters of interest. Therefore, no confounding factors were taken into account in the remaining analyses.

Comparisons between schizophrenia patients and healthy controls revealed no difference in mean neuronal size (p=.525), mean neuronal shape (p=.946), neuronal density (p=.579) or staining intensity (p=.618) of ZNF804A immunoreactive cells in layer III. Likewise, the risk allele had no effect on the mean neuronal size (p=.271), mean neuronal shape (p=.489), neuronal density (p=.642), or staining intensity (p=.896) . There were also no interactions between diagnosis and genotype: mean neuronal size (p=.899), mean neuronal shape (p=.263), neuronal density (p=.178), or staining intensity (p=.093).

Table 3.4: ZNF804A immunoreactivity in layer III pyramidal neurons of the inferior parietal lobe. There are no main effects of diagnosis, genotype, nor interactions between them, on any of the parameters, mean (SEM).

	Controls	**Schizophrenia**	**AA**	**C-carriers**
	N=23	N=24	N=16	N=31
Neural density ($mm^{2)}$	46.5 (2.6)	42.0 (3.0)	42.9 (3.7)	44.9 (2.3)
Neuronal size ($\mu m^{2)}$	249 (9)	242 (7)	254 (11)	241.1 (6)
Neuronal shape (a.u.)	.676 (.017)	.673 (.015)	.684 (.023)	.670 (.012)
Staining intensity (a.u.)	0.25 (0.01)	0.26 (0.01)	0.26 (0.02)	0.25 (0.01)

3.4 Discussion

The results from the RT-qPCR studies described in this chapter indicate that the variation at rs1344706 does not impact on ZNF804A mRNA expression, at least in lymphoblast cell lines and grey and white matter of the superior temporal gyrus. In line with this, also our immunohistochemistry study carried out on IPL sections did not show any effects of rs1344706 on neuronal shape, size, neural density, or staining intensity. Additionally, we did not detect any differences between schizophrenia patients and controls, nor any interactions between genotype and diagnosis, in both the RT-qPCR studies and in the immunohistochemistry study.

The studies reported here are relatively small, leaving open the possibility that we did not have the power to detect any effects rs1344706 might have. Alternatively, rs1344706 might affect expression in other brain regions. However, no studies to date have provided clear evidence that rs1344706 exerts its effects by altering expression of ZNF804A in adult brain. As mentioned previously, the initial finding by Riley et al. (2010) of increased mRNA being associated with the risk allele were not replicated by Williams et al. (2011). Williams et al. did not use RT-qPCR but investigated effects on expression by studying differences in allelic expression in rs1344706 heterozygotes. Both they and Buonocore et al. (2010) found an allelic effect on expression, but in both studies the allelic

expression imbalance was observed in homozygotes as well, indicating that the differences in expression were most likely due to regulatory variants other than rs1344706. Hill and Bray (2011) used this same technique and showed allelic differences in nuclear protein binding for the two alleles, but the identity of the proteins that bind to the sequence containing rs1344706 remained unknown. Another SNP in *ZNF804A*, rs7597593, has been associated with mRNA levels in females (Zhang et al., 2011a).

Recent studies investigating *ZNF804A* do imply that the gene is likely to be functional. To investigate the role of *ZNF804A*, Hill et al. (2012) knocked down *ZNF804A* in human neural progenitor cells and found that it altered the expression of genes involved in cell adhesion, suggesting a role for *ZNF804A* in processes such as neural migration, neurite outgrowth, and synapse formation. Girgenti et al. (2012) demonstrated that overexpression of *ZNF804A* results in a significant increase in transcript levels of PRSS16 and COMT, and a statistically significant decrease in transcript levels of PDE4B and DRD2. Furthermore they showed, using chromatin immunoprecipitation assays, that both epitope-tagged and endogenous ZNF804A directly interacts with the promoter regions of PRSS16 and COMT, suggesting a direct upregulation of their transcription by ZNF804A. Another study looking at the effects of ZNF804A overexpression reported upregulation of ANKRD1, INHBE, PIK3AP1, and DDIT3, as well as downregulation of CLIC2, MGAM, and BIRC3. Several of these genes are related to transforming growth factor-β signaling, which plays an important role in cell growth and differentiation (Umeda-Yano et al., 2013). ZNF804A has also been shown to be a target for another major schizophrenia risk gene, miR-137 (Kim et al., 2012).

Furthermore, several studies looking at *ZNF804A* have now indicated that the gene and SNP might have effects during development. Pedrosa et al. (2011), studying induced pluripotent stem cells derived from schizophrenia patients, found that early differentiating

neurons express ZNF804A mRNA, while Lin et al. (2011) demonstrated a change in expression of ZNF804A during the transition from pluripotent stem cell to differentiating neuron. One of most informative studies about *ZNF804A* and its importance during development was carried out by Hill and Bray (2012). They studied the effect of rs1344706 on ZNF804A mRNA expression in adult DLPFC, hippocampus and substantia nigra tissue, as well as foetal human tissue from the first and second trimester of gestation. They found no effects in any of the adult brain regions, but did report an effect during the second trimester of gestation, with the risk allele being associated with lower mRNA expression.

Several explanations for the lack of effect of rs1344706 on expression remain open: 1) the SNP might have its effect during development and therefore the effects cannot be detected in adult brain. This would be in line with the findings of Hill and Bray (2012). 2) there is another, as yet unknown, isoform of ZNF804A and rs1344706 has its effects on this isoform. This has been shown to be true for other schizophrenia risk genes (Kleinman et al., 2011). A novel mRNA variant of ZNF804A has already been described (Okada et al., 2012), but it was more common in lymphoblast cells than brain, could not be detected in all cases, and no difference between cases and controls was found. 3) There is no effect of rs1344706 on expression, and any functional effect occurs via another, yet unknown, polymorphism which is in fact responsible for the association of *ZNF804A* with schizophrenia. I will discuss these possibilities in more detail in chapter 8.

Chapter 4 - The effect of *ZNF804A* genotype on macroscopic brain structure

4.1 Introduction

4.1.1 Schizophrenia and brain structure

Whereas the two previous chapters described experiments investigating *ZNF804A* at the microscopic level, this chapter will investigate whether *ZNF804A* genotype affects macroscopic brain structure, using structural MRI. Macroscopic brain structure is a phenotype that has been shown to be heritable (Thompson et al., 2001), with brain structure being increasingly similar in subjects with increasing genetic affinity. Unaffected relatives of schizophrenics do show some of the structural changes associated with the disorder, albeit to a lesser extent, suggesting that a proportion of the structural neuropathology associated with schizophrenia is a result of genetic liability (Sharma et al., 1998). However, investigation of monozygotic twins discordant for schizophrenia has revealed that in almost all cases the affected twin shows greater structural abnormalities than their sibling (Suddath et al., 1990). These findings suggest that the structural changes in schizophrenia exist even after the effect of genetic background is controlled for and that they are associated with the expression of the disease phenotype and not just the underlying genetic background (Harrison, 1999). The fact that this phenotype is heritable, co-segregates with the disease, but is present in unaffected family members at a higher rate than in the general population, makes it a possible intermediate phenotype in the study of schizophrenia risk genes (Gottesman & Gould, 2003).

Although case-control differences will not be assessed in this chapter, previously observed differences between cases and controls do provide clues about the brain regions where effects of schizophrenia risk genes might be observed. In this regard, there are several macroscopic brain changes in schizophrenia which have been replicated and confirmed by meta-analysis. Schizophrenia is associated with an enlargement of the lateral

and third ventricles and a reduction in total brain volume of around 3% (Ward et al., 1996; Wright et al., 2000), which reflects a decrease in brain weight (Harrison et al., 2003). The best replicated findings are brain volume reductions of around 5% in prefrontal and temporal regions (Lawrie & Abukmeil, 1998). Whole brain grey matter volume is reduced by approximately 3-4% compared to white matter in structural magnetic resonance imaging studies, with generally the anterior cingulate cortex, superior temporal gyrus, and medial temporal regions including the hippocampus and amygdala showing substantial reductions (Gaser et al., 1999; Job et al., 2002; Fornito et al., 2009). Additionally, there may be a reduction in the normal asymmetry of the cerebral hemispheres in schizophrenia (reviewed in Harrison, 1999).

4.1.2 *ZNF804A* and brain structure

At the start of this study, three other studies had been published assessing the effects of variation in schizophrenia risk gene *ZNF804A* genotype on brain structure. The first of these studies was carried out by Lencz et al. (2010), who looked at the effect of rs1344706 on brain structure in 39 healthy volunteers. Structural MRI scans were acquired using a 1.5T scanner and differences in total brain volume, grey matter (GM), and white matter (WM) volume were assessed based on segmentation, whereas voxel-wise comparisons were carried out to detect differences in specific brain regions. They found that double risk carriers had larger WM volumes, with no effect on GM or total brain volume being detected. Additionally, the voxel-wise analysis revealed that regions including the angular gyrus, parahippocampal gyrus, posterior cingulate, inferior frontal gyrus, inferior temporal gyrus, and cerebellum were significantly smaller in subjects homozygous for the risk allele, which was interpreted as showing possible alterations of default-mode network structures.

The second study was published by Donohoe et al. (2011), who looked at the effect of *ZNF804A* genotype in a sample of 70 schizophrenia patients and 38 healthy volunteers. They compared subjects homozygous for the risk allele with C carriers using voxel based morphometry (VBM) looking at whole brain volumes and specifically at the DLPFC, hippocampus, and amygdala. No effect of the risk SNP was found in the healthy participants, but in patients with schizophrenia they reported that double risk carriers had larger grey matter volumes, which was particularly pronounced in the hippocampus. These findings were seen as supporting the theory that *ZNF804A* delineates a schizophrenia subtype characterised by relatively intact grey matter volume. The third study (Voineskos et al., 2011) also looked at the effect of the risk SNP in healthy volunteers (n=62), but measured cortical thickness and white matter tract integrity using sMRI and diffusion tensor imaging (DTI) scans. Comparing subjects homozygous for the A allele with C carriers, they found no effects of variation in *ZNF804A* on white matter integrity. They did report an effect on cortical thickness, with this parameter showing a reduction in the STG, ACC, and PCC of double risk carriers compared to carriers of the C allele. Together, these studies provide mixed evidence about the effects of rs1344706 on brain structure. Given the small sample sizes of the studies, all findings remain to be replicated.

4.1.3 Methods for assessing brain structure

Traditionally, differences in brain structure had to be assessed by manually tracing around the volume of interest based on anatomical landmarks, which was usually done by several experienced raters. Nevertheless, there was still the risk of measurement error and subjectivity (Lawrie & Pantelis, 2011). Nowadays, many automated ways exist to estimate the volume of a structure of interest and provide quantification of its size. For this study, automated volumetry as implemented in the FIRST module (version 1.2) of FSL (version

4.1) (http://www.fmrib.ox.ac.uk/fsl/first/) was used (Smith et al., 2004). It uses a Bayesian model constructed from manually segmented images to segment subcortical brain structures (Patenaude et al., 2011). A second method that was used to assess possible differences in brain structure is voxel based morphometry. The method was developed by Ashburner and Friston (2000) and rather than comparing whole volumes, brains are compared at the voxel level. In short, structural scans are transformed into a common space, then segmented into grey and white matter, and the average images for the different groups are compared on a voxel by voxel basis. Studies and reviews comparing volumetry with a VBM approach have shown that these generally lead to comparable results (McIntosh & Lawrie, 2004).

Data used for this study came from the Brain Imaging Genetics (BIG) database from the Donders Institute for Brain, Cognition and Behaviour of the Radboud University Nijmegen, The Netherlands (Franke et al., 2010). This database contains a large number of subjects for whom both a structural MRI scan and extensive genetic information are available. The scans have been acquired on both 1.5T and 3T scanners, which has led to the availability of two large (>400 subjects) independent cohorts. These two large independent cohorts allow investigation of the question of interest within one cohort, with the second group functioning as replication cohort (Bralten et al., 2011a). Volumetric measurements of several subcortical structures are available as part of the database, which have allowed several studies to detect effects of risk genes of brain structure (Bralten et al., 2011a; van der Heijden et al., 2013). Other studies have used VBM on the available scans to detect effects of their genes of interest (Bralten et al., 2011b; Gerritsen et al., 2011). For this study, we looked at both cohorts and used the volumetry measurements as well as VBM analyses to investigate the effects of *ZNF804A* genotype on macroscopic brain structure. Given that structural scans, genetic information, and volumetric measurements

were available, sections 4.2.1 to 4.2.4 describe procedures that had been carried out before I started this project. The results described in this chapter have been published (Cousijn et al., 2012), but are not exactly identical to the results described in the paper. In this chapter, I describe a somewhat larger sample (922 vs. 892 participants) and only analyses that were carried out for rs1344706, whereas the paper assesses 266 SNPs in *ZNF804A*.

4.2 Methods

4.2.1 Sample description

Structural MRI data were collected from 922 healthy, highly educated adults of Caucasian origin between 18 and 35 years of age (mean age 22.8, all right-handed, 58.4% female), with no self-reported neurological or psychiatric history. The study was approved by the regional medical ethics committee (CMO Arnhem-Nijmegen) and all participants gave written informed consent.

4.2.2 Genotyping

Genetic analyses were performed at the Department of Human Genetics of the Radboud University Nijmegen Medical Centre. DNA was isolated from saliva using Oragene containers (DNA Genotek, Ottawa, Ontario, Canada) according to the protocol supplied by the manufacturer. Affymetrix GeneChip SNP 6.0 arrays (Affymetrix Inc., Santa Clara, CA, USA) were used for genome-wide genotyping of SNPs as described before (Franke et al., 2010). The call rate threshold was set at 90% for the arrays. Participants were excluded from the analysis if the call rate per participant was lower than 95%.

4.2.3 Neuroimaging procedures

MRI data were acquired at the Donders Centre for Cognitive Neuroimaging. Images were acquired at 1.5 Tesla Siemens Sonata and Avanto scanners (Siemens, Erlangen, Germany) for 437 participants, using small variations to a standard T1-weighted 3D MPRAGE sequence (TR 2300ms, TI 1100ms, TE 3.03ms, 192 sagittal slices, field of view 256mm). These variations included a TR/TI/TE/slices of 2730/1000/2.95/176, 2250/850/2.95/176, 2250/850/3.93/176, 2250/850/3.68/176, and the use of GRAPPA parallel imaging with an acceleration factor of 2. For a group of 485 participants images were acquired at 3 Tesla Siemens Trio and TrioTim scanners (Siemens, Erlangen, Germany), using small variations to a standard T1-weighted 3D MPRAGE sequence (TR 2300ms, TI 1100ms, TE 3.93ms, 192 sagittal slices, field of view 256mm. These variations included a TR/TI/TE/slices of 2300/1100/3.03/192, 2300/1100/2.92/192, 2300/1100/2.96/192, 2300/1100/2.99/192, 1940/1100/3.93/176, 1960/1100/4.58/176, and the use of GRAPPA parallel imaging with an acceleration factor of 2. Slight variations in these imaging parameters have been shown not to affect the reliability of morphometric results (Jovicich et al., 2009).

4.2.4 Brain segmentation

All T1-weighted structural MRI data covered the entire brain and had a voxel size of 1x1x1mm3. Automated volumetry as implemented in the FIRST module (version 1.2) of FSL (version 4.1) (http://www.fmrib.ox.ac.uk/fsl/first/) was applied to segment bilateral subcortical volumes. To correct for total brain volume (TBV), raw DICOM MR imaging data were converted to NIFTI format using the conversion as implemented in SPM5 (www.fil.ion.ucl.ac.uk/spm/software/spm5/). Normalizing, bias-correcting, and segmenting into GM and WM was performed using the VBM 5.1 toolbox version 1.19

(http://dbm.neuro.uni-jena.de/vbm/) in SPM using default settings. This method uses an optimised VBM protocol (Ashburner & Friston, 2000; Good et al., 2001) as well as a model based on Hidden Markov Random Fields (HMRF) developed to increase signal-to-noise ratio (Cuadra et al., 2005). Total volume of GM and WM was calculated by adding the resulting tissue probabilities. Total Brain Volume was defined as the sum of GM and WM volumes.

Whole-brain VBM was performed in SPM5, separately for data acquired at 1.5T and 3T. Data were analysed using the grey and white matter images in two separate analyses. Diffeomorphic image registration was performed using DARTEL (Jovicich et al., 2009) followed by calculation of Jacobian-scaled images and transformation to Montreal Neurological Institute (MNI) space using affine transformation. Finally, all data were smoothed with an 8mm FWHM Gaussian smoothing kernel.

4.2.5 Analysis

We looked at the effect of rs1344706 on several subcortical brain volumes in two separate cohorts, one scanned at 1.5T and one scanned at 3T, using volumetric measurements. Given that not much is known about the effects of *ZNF804A* genotype on brain volume, we analysed all available subcortical volumes, which included the hippocampus, amygdala, thalamus, accumbens, caudate, globus pallidus, putamen, and brain stem. Statistical analysis on the automated volumetry measures was performed using SPSS18. ANCOVAs were carried out for all brain regions of interest with rs1344706 as factor of interest and using sex, age, and TBV as covariates. The analysis of WM was adjusted by GM volume and vice versa. Results were considered significant at $p \leq .05$.

For the VBM data, a full-factorial ANCOVA was applied using genotype (rs1344706) as factor with participants' age, gender, total brain volume, and scan protocol

added to the model as covariates. Statistics were corrected for non-stationarity and were applied at p(whole brain uncorrected) < .001 and subsequent cluster statistics at p(FWE) < .05. We specifically defined the DLPFC, amygdala, hippocampus, posterior cingulate, and anterior cingulate as regions of interest (ROIs) because of the results from previous studies assessing the relation between rs1344706 and brain volume (Lencz et al., 2010; Donohoe et al., 2011; Voineskos et al., 2011) and/or because these regions have been implicated in schizophrenia (Goldstein et al., 1999; Job et al., 2002; Fornito et al., 2009). The ROIs were based on the WFU pickatlas (Tzourio-Mazoyer et al., 2002) with the DLPFC being defined as BA9 and BA46.

4.3 Results

4.3.1 Volumetry

We studied the effect of rs1344706 on macroscopic brain structure using volumetric measurements in two separate cohorts. The results are shown in Table 4.1, and were negative for total brain volume, total white matter, total grey matter, and each of the grey matter regions analysed. This was true for both cohorts.

Table 4.1: Brain volumes according to rs1344706 genotype and the effect of rs1344706 on the studied brain volumes in the volumetry analysis, mean (s.d.).

	1.5 Tesla				**3 Tesla**			
Brain structure	*AA* (N=146)	*CA* (N=210)	*CC* (N=81)	Sign.	*AA* (N=162)	*CA* (N=241)	*CC* (N=82)	Sign.
Left hippocampus	3.99 (0.45)	4.00 (0.43)	4.08 (0.43)	p=.145	4.01 (0.41)	4.08 (0.45)	3.95 (0.49)	p=.289
Right hippocampus	3.98 (0.42)	3.93 (0.41)	3.96 (0.42)	p=.496	3.96 (0.42)	4.03 (0.39)	3.94 (0.42)	p=.588
Left amygdala	1.71 (0.25)	1.71 (0.22)	1.73 (0.24)	p=.581	1.57 (0.24)	1.57 (0.24)	1.57 (0.24)	p=.588
Right amygdala	1.75 (0.23)	1.73 (0.22)	1.75 (0.23)	p=.967	1.59 (0.23)	1.62 (0.24)	1.60 (0.26)	p=.675
Left thalamus	8.30 (0.71)	8.37 (0.68)	8.39 (0.79)	p=.138	8.09 (0.71)	8.15 (0.73)	7.94 (0.72)	p=.398
Right thalamus	8.54 (0.73)	8.58 (0.72)	8.62 (0.80)	p=.159	8.38 (0.74)	8.44 (0.69)	8.29 (0.76)	p=.968
Left accumbens	0.60 (0.15)	0.60 (0.15)	0.60 (0.15)	p=.841	0.57 (0.11)	0.59 (0.12)	0.58 (0.11)	p=.219
Right accumbens	0.63 (0.14)	0.65 (0.13)	0.63 (0.15)	p=.308	0.60 (0.12)	0.62 (0.11)	0.61 (0.11)	p=.207
Left caudate	3.67 (0.51)	3.65 (0.50)	3.69 (0.52)	p=.898	3.79 (0.42)	3.79 (0.44)	3.73 (0.44)	p=.763
Right caudate	3.82 (0.41)	3.81 (0.44)	3.83 (0.48)	p=.941	3.90 (0.43)	3.91 (0.43)	3.83 (0.43)	p=.725
Left globus pallidus	1.89 (0.17)	1.88 (0.18)	1.89 (0.18)	p=.849	1.88 (0.18)	1.87 (0.17)	1.84 (0.18)	p=.211
Right globus pallidus	1.86 (0.17)	1.85 (0.18)	1.85 (0.17)	p=.865	1.84 (0.17)	1.83 (0.18)	1.81 (0.18)	p=.149
Left putamen	5.42 (0.53)	5.41 (0.51)	5.42 (0.49)	p=.906	5.26 (0.51)	5.31 (0.48)	5.22 (0.50)	p=.987
Right putamen	5.44 (0.50)	5.38 (0.52)	5.41 (0.53)	p=.808	5.34 (0.52)	5.38 (0.50)	5.31 (0.50)	p=.943
Brainstem	22.30 (2.33)	22.37 (2.41)	22.50 (2.44)	p=.380	21.88 (2.48)	22.00 (2.51)	21.67 (2.44)	p=.786
White matter	487.26 (51.41)	485.09 (52.53)	485.40 (58.14)	p=.957	466.95 (51.16)	473.94 (49.22)	463.08 (53.32)	p=.433
Grey matter	837.57 (76.14)	833.02 (70.06)	837.25 (87.20)	p=.555	835.99 (79.54)	842.63 (71.33)	822.11 (71.70)	p=.582
Total brain volume	1324.84 (116.70)	1318.11 (113.70)	1322.65 (138.20)	p=.461	1302.94 (123.04)	1316.57 (111.83)	1285.19 (118.13)	p=.119

4.3.2 VBM

Additionally, we carried out a VBM analysis looking at grey and white matter separately. Both whole-brain analyses revealed no significant differences between the different genotype groups studied. Region of interest analyses were carried out on

prespecified brain structures, but none of these revealed any significant differences based on rs1344706 genotype. The results are shown in Table 4.2.

Table 4.2: Effect of SNP rs1344706 on the studied brain volumes in the region of interest VBM analysis.

Brain Volume	1.5 Tesla p-value	3 Tesla p-value
Amygdala	0.92	0.66
ACC	0.92	0.95
DLPFC	0.60	0.65
Hippocampus	0.99	0.86
PCC	0.71	0.73

ACC = anterior cingulate cortex, DLPFC = dorsolateral prefrontal cortex, PCC = posterior cingulate cortex

4.4 Discussion

In this study, we found no effect of rs1344706 genotype on macroscopic brain structure in two independent cohorts. Given the size of the cohorts and the use of two separate analysis methods, it seems reasonable to conclude that this reflects a true negative. However, this study only looked at healthy volunteers and not patients, so rs1344706 might affect brain structure in patients, as previously reported by Donohoe et al. (2011). Furthermore, we only looked at structural MRI scans to assess possible changes in grey and white matter. Effects on white matter and structural connectivity are better assessed using DTI scans, so large future studies using DTI scans might still show effects of *ZNF804A* genotype. Also different analysis methods, for example studying cortical thickness (Voineskos et al., 2011), might reveal effects of the gene.

Six more studies have now been published addressing the question whether rs1344706 affects macroscopic brain structure, one of which used methods similar to those described in this chapter. Wassink et al. (2012) studied a large sample of 335 subjects with schizophrenia, as well as 198 healthy controls. Looking at white matter volumes of the whole brain and at the 4 lobes separately, they found an overall effect of genotype on total, frontal, and parietal lobe WM volumes. In the schizophrenia group, the effect was present

for total and frontal WM volumes, while in the healthy control group there was a specific effect of rs1344706 on total WM volume. This finding is not in line with the findings from the study described in this chapter, but is in line with the findings of Lencz et al. (2010). However, our study included two independent cohorts each of which was more than twice the size of the healthy cohort studied by Wassink et al. (2012) and more than ten times the size of the group studied by Lencz et al. (2010), which underlines the importance of studying large cohorts to reliably measure effects of putative risk genes.

Three other recent studies have also reported no evidence for an association between rs1344706 and brain structure, albeit using different methods. Sprooten et al. (2012) looked at DTI scans of 133 healthy volunteers and 84 unaffected relatives of bipolar patients. Both voxel-based analysis and tract-based analysis did not reveal any difference in white matter structure between double risk carriers and C carriers. This was true for both healthy volunteers and unaffected relatives. Also Wei et al. (2013) assessed the possible association of *ZNF804A* genotype with white matter integrity, studying 100 patients with schizophrenia and 69 healthy volunteers. Differences in fractional anisotropy were found between schizophrenia patients and controls, but no differences between genotype groups or any interactions between diagnosis and genotype were reported. However, one of these groups did report an effect on white matter density in a study looking at structural MRI scans (Wei et al., 2012). Structural scans of 80 schizophrenics and 69 healthy controls were obtained, and an interaction between diagnosis and genotype was found in the left prefrontal lobe. Risk carriers in the schizophrenia group were reported to have higher WM density in left prefrontal regions, whereas healthy risk carriers had lower WM density in these regions. In both groups, the risk allele was associated with increased WM density in bilateral hippocampus. Also Kuswanto et al. (2012) used DTI to assess the impact of *ZNF804A* genotype on WM as measured by DTI. They included 89

schizophrenic patients and 64 controls, and next to effects of diagnosis found several diagnosis by genotype interactions. These showed that double risk carriers with schizophrenia had less white matter integrity in parietal and temporal regions than healthy double risk carriers. Together, these studies do not provide convincing evidence for the association between *ZNF804A* and schizophrenia being mediated by structural integrity differences in large, long-range white matter fibre connections. Lastly, a study by Bergmann et al. (2013) looked at 63 SNPs in *ZNF804A* in 365 psychosis patients and healthy volunteers to assess their effect on cortical thickness. None of these SNPs, including rs1344706, was found to affect cortical thickness in the schizophrenia, bipolar disorder, and healthy control groups.

The evidence that structural changes in patients with schizophrenia are trait measures related to genetic risk is variable, with some studies providing evidence that they are state factors related to the experience of illness. Despite reasonably robust brain morphological differences between patients and healthy volunteers, studies exploring samples of patients, siblings, and normal controls did not always detect differences in structural measurements between siblings and healthy volunteers, despite relevant sample sizes (n = 600) and different analysis methods (VBM, Honea et al., 2008; cortical thickness, Goldman et al., 2009; automated subcortical segmentation technique, Goldman et al., 2008). This suggests that structural measures might not be the most robust intermediate phenotype, even though several studies have detected effects of schizophrenia risk genes on brain structure (Callicott et al., 2005; Buckholtz et al., 2007; Crespo-Facorro et al., 2007; McIntosh et al., 2008).

Together, the results strongly suggest that rs1344706 does not impact upon regional brain volumes as measured by sMRI in young adults. Our study was the largest study to date and found no effects, with other smaller studies reporting mixed findings.

While we cannot rule out such effects occurring at earlier developmental stages, in clinical populations, or on other parameters of macroscopic brain structure not measured here, it seems more likely that any pathophysiological correlates of rs1344706 in *ZNF804A* occur via modulation of brain function or connectivity. In chapters 6 and 7, I will discuss brain function and connectivity as intermediate phenotypes to study the effects of *ZNF804A* genotype.

Chapter 5 - Methods for multimodal imaging

5.1 Introduction

5.1.1 Multimodal imaging

The main goal of the neuroimaging experiments carried out for this thesis is to assess the effects of *ZNF804A* genotype on brain activity. At the same time, this also gives us the opportunity to link and compare magnetoencephalography, functional magnetic resonance imaging, and magnetic resonance spectroscopy datasets of a large number of healthy volunteers. Although there are some studies that have addressed multimodal imaging questions, there are no established ways of linking these datasets. Furthermore, the methods we use for the analysis of the MEG and MRS data are relatively novel. Therefore, we decided to add a simple gratings task, known to activate areas involved in visual processing, to our experiment. Because it is well-established that the gratings lead to gamma oscillations and a blood-oxygen-level dependent (BOLD) response in occipital regions, this gives us a clear read-out and the opportunity to work out the best methods to analyse our multimodal datasets. Additionally, a recent study has linked resting GABA concentrations to visual gamma oscillations and visual fMRI BOLD responses (Muthukumaraswamy et al., 2009), which makes the visual system a suitable model for developing multimodal analysis tools and linking results from the different modalities. In this chapter, I will not discuss effects of *ZNF804A* genotype on brain activity, but will explain the methods we used to analyse the different datasets and our findings with regard to correlations between GABA, gamma, and BOLD responses in occipital regions. In chapter 6, these same methods will then be applied to assess the effect of *ZNF804A* genotype on prefrontal function.

5.1.2 BOLD fMRI and gamma oscillations

The relationship between hemodynamic responses as measured with BOLD fMRI and underlying neuronal activity has been an important topic of investigation (Logothetis, 2008). Recordings in both anesthetized and awake monkeys have shown that hemodynamic responses are preferentially sensitive to local field potentials as opposed to action potentials (Logothetis et al., 2001; Goense & Logothetis, 2008). In addition, recordings from anesthetized cat visual cortex have revealed a strong positive correlation between BOLD and neuronal synchronization in the gamma frequency range (>30Hz) together with a negative correlation of BOLD with lower frequency bands (Niessing et al., 2005). Most studies in humans using simultaneous EEG and fMRI have reported negative correlations with BOLD in the low-frequency ranges (Goldman et al., 2002; Laufs et al., 2003; Scheeringa et al., 2008; 2009; Yuan et al., 2010). For higher frequencies, Scheeringa et al. (2011) demonstrated that trial-by-trial BOLD fluctuations correlate positively with simultaneously recorded trial-by-trial fluctuations in narrow-band high frequency (60–80 Hz) EEG gamma power. Using fMRI and MEG, Zumer et al. (2010) reported that the higher gamma frequencies were positively correlated with BOLD. Zaehle et al. (2009) showed that visual stimuli that evoked high gamma responses in occipital regions in subjects also elicited strong BOLD responses, with inter-individual variations of BOLD responses to visual stimuli correlating with the gamma power of the subjects.

In contrast, in two experiments by Muthukumaraswamy and Singh (2008; 2009) which also addressed the question of the relationship between the BOLD signal and gamma oscillations measured by MEG, it was found that the gamma signal was sensitive to changing stimulus properties, but the BOLD signal was not. They interpreted this functional decoupling as a demonstration that increased amplitude of gamma band oscillations as measured with MEG is not sufficient to drive the subsequent BOLD

response. In another study, however, they showed that individual differences in gamma oscillations are negatively correlated with peak gamma frequency in occipital cortex (Muthukumaraswamy et al., 2009). This finding was not replicated in a later study (Swettenham et al., 2013), in which it is concluded that at least in human primary visual cortex, BOLD responses are independent from gamma oscillations.

5.1.3 GABA and gamma oscillations

A finding from the same study by Muthukumaraswamy et al. (2009) that has received a lot of attention is that peak gamma frequency is correlated with resting GABA levels. Animal studies and modelling studies have clearly shown the importance of GABA for the generation of gamma oscillations (Traub et al., 1996; Wang & Buzsaki, 1996; Bartos et al., 2007), but the relationship between GABA and gamma is not easily assessed in the human brain. Muthukumaraswamy et al. (2009) attempted this by correlating resting GABA concentrations as measured by Magnetic Resonance Spectroscopy (MRS) with visual gamma oscillations as measured by MEG. MRS provides a non-invasive method to quantify metabolite concentrations in discrete regions of the human brain; however, it can only detect the total concentration of a neurochemical and cannot distinguish between separate functional pools of GABA (Stagg et al., 2011a). In their study, Muthukumaraswamy et al. (2009) found a correlation between resting GABA levels and visual gamma peak frequency in 12 participants. GABA levels in individuals correlated with the frequency level displaying the greatest power within the gamma band (gamma peak frequency). The correlation was speculated to reflect a dependence of gamma oscillations on GABA concentrations as measured by MRS, with these GABA concentrations providing a window into pyramidal-interneuron network properties. If true, such correlation would make the gamma peak frequency a useful surrogate marker of

cortical excitability for studies investigating clinical populations and/or the effects of pharmacological agents. Gamma oscillations would also be a useful intermediate phenotype in studies, such as ours, looking at effects of putative risk genes for psychiatric disorders. The same group later reported a similar correlation in a sample of 13 participants, 7 of whom participated in both studies (Edden et al., 2009). Gaetz et al. (2011) observed the correlation between GABA and gamma frequency in the motor cortex of 9 healthy adults. However, the correlation between gamma peak frequency and MRS GABA was recently also assessed in a study by Shaw et al. (2013). They studied GABA and gamma oscillations in participants with remitted depression (n=19) and healthy controls (n=18), but found no correlation.

Subsequent pharmacological MEG studies have addressed the relationship between GABA and gamma oscillations in the human brain. Hall et al. (2010) found that diazepam increases only gamma power and not frequency in the occipital cortex, while a similar study by Hall et al. (2011b) using diazepam but focusing on motor areas showed no modulation of gamma oscillations. Muthukumaraswamy et al. (2012b) found that elevation of GABA by tiagebine does not modulate gamma oscillations in the motor cortex. In the visual cortex, Muthukumaraswamy et al. (2013) found that increasing GABA with tiagebine also does not modify the amplitude or frequency of gamma oscillations. Saxena et al. (2013), using GABA-A agonist propofol, observed an increase in stimulus-induced gamma amplitude only. Taken together, these studies have not convincingly elucidated the relationship between GABA levels and visual gamma frequency in the human brain.

5.1.4 GABA and BOLD fMRI

The study by Muthukumaraswamy et al. (2009) also showed a negative correlation between GABA as measured by MRS and BOLD fMRI in occipital regions, meaning that

increased inhibition is associated with a reduced BOLD response. Two possible mechanisms that could explain this finding were proposed: GABAergic interneurons might directly affect local circulation by releasing vasoactive modulators; alternatively, GABA might affect BOLD via pyramidal cells and the metabolic demands associated with glutamate cycling with increased GABA activity creating less glutamatergic activity. Furthermore, this finding was said to have important implications for the interpretation of fMRI experiments, because differences in the BOLD response might actually be explained by differences in GABA concentrations, independent of the paradigm used.

Two other studies to date have assessed the relationship between resting GABA concentrations and the BOLD response in occipital cortex. A study by the same group (Muthukumaraswamy et al., 2012a) investigated the relationship between resting GABA and BOLD response amplitude, cerebral blood flow (CBF), the shape of the hemodynamic response function (HRF), and tissue content of the MRS voxel in 15 participants. Resting GABA concentrations were found to correlate negatively with the magnitude of the BOLD response, and positively with the width of the HRF. No correlations were found between GABA and CBF or GABA and tissue contents. The changes in HRF shape in individuals with higher GABA indicate that vascular response characteristics might partly underlie observed correlations between GABA and BOLD. A second study by Donahue et al. (2010) sought to disentangle the different components of the BOLD signal and investigate which of these components correlates with GABA in 12 participants. Negative correlations were found between GABA and BOLD magnitude, and between GABA and cerebral blood volume. A positive correlation was observed between GABA and cerebral blood flow.

The earliest study investigating whether GABA as measured by MRS underlies the BOLD signal looked at the anterior cingulate cortex (ACC). They found that the higher the

total concentration of GABA in the ACC, the stronger the negative BOLD responses that were induced by emotional processing in the same region (Northoff et al., 2007). Two other studies have linked the BOLD response in the ACC to resting glutamate concentrations (Duncan et al., 2011; Falkenberg et al., 2012). No correlations were found between the BOLD signal in the hippocampus and MRS measures of NAA and glutamate (Hutcheson et al., 2012).

5.1.5 Research questions

The study by Muthukumaraswamy et al. (2009) has generated a lot of interest and has led to many studies based on the assumption that GABA, gamma oscillations, and BOLD fMRI correlate. It is important that high impact studies are replicated (Brembs et al., 2013), to ensure that subsequent studies are based on valid assumptions. The larger dataset we had because of our genetic neuroimaging study allowed us to do so in a much larger sample. At the same time, it allowed us to develop the best analysis methods for all three imaging datasets and find parameters we could use to assess correlations between the datasets, which we can then apply to the datasets we acquired to assess activity in the DLPFC (chapter 6). In this chapter, I will explain the methods we used and address the question whether resting GABA and glutamate concentrations as measured by MRS correlate with the peak frequency and amplitude of gamma oscillations and the BOLD response in the occipital cortex. Not many studies to date have specifically looked at glutamate, because older MRS sequences could not distinguish between glutamate and glutamine (Near et al., 2013). In 50 healthy volunteers, we measured concentrations of endogenous resting GABA and glutamate from a voxel in the occipital cortex using MRS, stimulus-induced gamma oscillations using MEG, and BOLD response in the occipital cortex using fMRI.

5.2 Methods

5.2.1 Participants

Healthy right-handed participants between 18 and 35 were recruited for this study. Participants were not included if they reported a history of psychiatric or neurological illness, the use of any form of medication that might affect brain activity, or had a form of metal in or on their body that they could not remove. If they fulfilled the inclusion criteria, they provided two cheek swabs and were genotyped for *ZNF804A* rs1344706. Participants who were homozygous for either the risk allele or the non-risk allele were invited to take part in the imaging study. In total, 50 subjects were included, 23 men and 27 women. The average age of the participants was 24, ranging from 19 to 34. Five participants reported that they were regular smokers, whereas no participants reported regular drug use. Genotyping methods and additional information about these participants will be described in chapter 6. Ethical approval for this study was obtained from the research ethics committee, NHS South central, Berkshire (11/SC/0053).

5.2.2 Task

In the visual task, stimuli consisting of vertical, stationary, maximum-contrast, 3-cycles per degree gratings of 4 degrees of visual angle were presented on a mean luminance, grey background. Gratings were presented for 2s followed by 2s of fixation at a peripheral location within the lower left or right visual field (centred over 2.5 degree eccentricity). Blocks of left or right visual field stimulation contained five stimuli, followed by 20s fixation during which the subjects were allowed to blink. Overall, ninety stimuli were presented. Participants were instructed to maintain fixation on a dot in the middle of the screen for the duration of the experiment.

5.2.3 Magnetic resonance spectroscopy

For MR data acquisition, a 3T Siemens scanner with a 32-channel head coil was used. Sagittal and axial T1 scout images were acquired and used to place a 2 x 2 x 2cm voxel of interest manually in the occipital cortex. The placement of the voxel is shown in Figure 5.1.

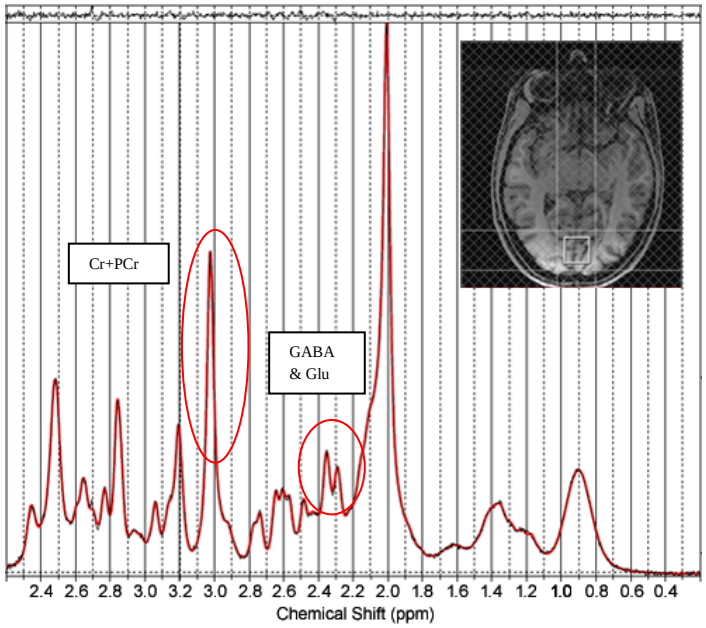

Figure 5.1: A typical spectrum acquired with the SPECIAL sequence from the voxel in occipital cortex (placement shown). Data were analysed with LCModel and the quality of the fit is represented by the small residual remaining after the fitting, shown as the little black line at the top of the figure. Peaks for GABA and glutamate as well as creatine (Cr+PCr) are indicated. Two more GABA peaks, at 3ppm and 1.9ppm, are present in the spectrum, but these are hidden by the larger peaks of other metabolites.

The SPECIAL (spin-echo full-intensity acquired localized) sequence, originally developed by Mlynarik et al. (2006) and adapted for humans by Mekle et al. (2009), localised single-voxel spectroscopy measurements in the occipital lobe. This sequence employs a very short echo-time acquisition, thereby minimizing signal loss due to T2 decay and scalar coupling. While conventional short TE MRS is typically performed using a stimulated-echo approach, the SPECIAL sequence uses a spin-echo approach, which yields a factor two improvement in signal-to-noise ratio. Volumes were acquired using the following scan parameters: VOI = 2 x 2 x 2cm, TR/TE= 3000ms, 8.5ms, spectral width = 2

kHz, number of averages = 192, vector size = 2048. Water suppression was achieved using the VAPOR method, which uses frequency selective pulses to suppress the water signal prior to excitation. A water unsuppressed scan was also acquired (averages = 8) to provide a measurement of the water signal for referencing purposes. Data acquisition could not be completed for one participant due to peripheral nerve stimulation.

Before the MRS acquisition, a high-resolution T1-weighted anatomical image was acquired for each subject. The parameters were: 224 slices (1mm thick), distance factor = 50%, fov(read) = 256mm, fov(phase) = 68.8%, matrix = 174x192, TR = 3000ms, TE = 4.8ms, TI = 1100ms, flip angle = 8°, 1 concatenation, bandwidth = 220Hz, echo spacing = 9.6ms.

For the MRS data analysis, prior to spectral analysis, eddy-current correction was applied to each water-suppressed spectrum, using the corresponding water-unsuppressed spectrum as an eddy-current reference. The spectra were then quantitatively analysed using Linear Combination (LC) Model. This analyses the *in vivo* spectrum as a linear combination of a basis set of simulated metabolite spectra (Provencher, 1993). This way, we obtained a quantitative estimate for the concentration of each metabolite in arbitrary units, as well as its estimated uncertainty (Cramer-Rao lower bound). Given our interest in GABA and glutamate, we extracted the estimated concentrations for these neurotransmitters. Furthermore, we extracted absolute levels of Creatine (Cr+PCr), which is a measure of cellular integrity and the standard reference resonance (Stagg et al., 2009). We then normalised our GABA and glutamate values by dividing them by Creatine levels.

5.2.4 Magnetoencephalography

Whole-head MEG recordings were acquired using the Elekta NeuroMag MEG System. Data from the 204 gradiometers were analysed. The signal was digitised at a

sampling rate of 1000Hz, with a high-pass filter of 0.03Hz and a low-pass filter of 330Hz. A magnetic digitizer (Polhemus FastTrach 3D) was used to measure the relative positions of four head-position indicator (HPI) coils and three anatomical landmarks (nasion, left and right auricular points). These coordinates were used for coregistration of the sensor montage to the participant's structural MRI scan.

The data were analysed using the Matlab-based Fieldtrip toolbox (Oostenveld et al., 2011; http://www.ru.nl/neuroimaging/fieldtrip). Offline, data were low-pass filtered at 200Hz and high-pass filtered at 0.5Hz. Data were downsampled to 500Hz. Bad channels and trials were rejected upon visual inspection. We used independent component analysis (Jung et al., 2000) to identify eye artefacts, which were then projected out of the data. Line noise was removed using a band stop filter from 49.5-50.5Hz.

To assess the effects of the presentation of the gratings on gamma (40-80Hz) and alpha power (8-12Hz) in sensor space, a time-frequency analysis was performed using a fast Fourier transform (FFT) approach with sliding time windows. For lower frequencies (4–30Hz) we used an adaptive time window of four cycles length and applied a Hanning taper ($\Delta t = 4/f$); for higher frequencies (35–90Hz) we applied a fixed time window of 0.5s and four orthogonal Slepian tapers resulting in +/- 5Hz smoothing (Percival and Walden, 1993). Average spectral power was then computed as the average across trials and tapers (time window between 0.5 and 2s), and presented relative to baseline (between -1 and -.5s). Statistical analysis was performed both at sensor and source level (see below), using the same cluster-based randomization procedure (Maris & Oostenveld, 2007). By clustering neighbouring sensors (or grid points in the source analysis) that show the same effect, this test deals with the multiple-comparisons problem and at the same time takes into account the dependency of the data.

We applied a linearly constrained minimum variance (LCMV) beamformer technique to extract source-reconstructed gamma peak frequency and amplitude from the occipital lobe. Using the individual anatomical MRI, we constructed a realistically shaped single-shell description of the brain for each subject. The brain volume was divided into a grid with a 1cm resolution and normalised toward the template Montreal Neurological Institute brain using SPM8 (www.fil.ion.ucl.ac.uk/spm). Lead fields were calculated for all grid points (Nolte, 2003). We calculated the covariance-matrix between all sensor pairs of the averaged band-passed (40-80Hz) single trials and computed spatial filters for each subject, which were applied to reconstruct the raw time series as a virtual channel for the region of interest. Fourier spectra for the gamma range (40-80Hz) were obtained with an FFT using 9 Slepian multitapers (+/- 5Hz spectral smoothing) applied to 1s data segments for the baseline time window (between -1.0 and 0s) and the time window of interest (0.5 to 2.0s after stimulus presentation, divided into 0.5-1.5 and 1.0-2.0s). Spectra were plotted relative to baseline and peak frequency and amplitude information extracted. We also fitted a Gaussian curve to the peaks to establish the existence of clear peaks. For 7 subjects no clear peak could be fitted, and therefore these were excluded from further analyses.

Regions of interest were generated in two ways. To directly assess the relationship of GABA and glutamate with gamma in the same location in the brain, we took the MNI coordinates of the MRS voxel of each individual subject and used these as a spatial mask to extract gamma amplitude and frequency data. Furthermore, we determined the spatial distribution of power within the gamma band (40-80Hz) in occipital cortex. A sphere of 17.5mm radius was drawn around the peak of the activation and used as a spatial mask to extract frequency and amplitude. Because a previous study reporting a correlation between gamma peak frequency and GABA only presented gratings in the left visual field

(Muthukumaraswamy et al., 2009), we also specifically analysed activity generated by the left gratings only. Amplitude was expressed as percentage change from baseline.

5.2.5 Functional magnetic resonance imaging

During the gratings task, whole-brain T2*-weighted BOLD fMRI data were acquired using echo planar imaging (EPI) and an interleaved slice acquisition sequence [34 axial slices, volume repetition time (TR) = 2s, echo time (TE) = 28ms, flip angle = 76°, slice matrix size = 64 × 64, slice thickness = 3.0mm, field of view (FOV) = 192mm]. Three hundred and ten images were acquired during the gratings task.

Image processing and statistical analyses were conducted using statistical parametric mapping software (SPM8, http://www. fil.ion.ucl.ac.uk/spm/software/spm8/). The first five EPI volumes were discarded to allow for T1 equilibration. Remaining functional images were realigned with rigid body transformation and coregistered to the anatomical T1-weighted MR image. Subsequently, images were transformed into a common stereotactic space (MNI152 T1-template) and resampled into 2 × 2 × 2mm3 isotropic voxels. Spatial smoothing was performed with an isotropic 3D Gaussian kernel of 8mm full-width at half-maximum. Statistical analysis was performed within the framework of the general linear model. The presentation of the gratings was modelled as boxcar regressor and convolved with the canonical hemodynamic response function of SPM8. Additionally, realignment parameters were included to model potential movement artefacts. Contrast parameter images generated at the single subject level (gratings vs. fixation) were submitted to second-level group analysis.

Given our interest in interindividual variation and possible correlations with other imaging measures, we extracted percent signal change for each individual using MarsBar (Brett et al., 2002). MarsBar allows you to generate a region of interest for each individual

subject and obtain a β-estimate for this region or voxel of interest. Based on this β-estimate, MarsBar can also calculate percent signal change. In this study, we generated ROIs for the voxel with strongest activity within occipital regions. Additionally, we generated a ROI that contained all voxels that had been activated by the presentations of the gratings at a threshold of p=.001 uncorrected. In line with the study by Muthukumaraswamy et al. (2009) we then also extracted percent signal change from the voxel that displayed peak activation in response to presentation of left gratings only. We also attempted the use of structural masks either based on the WFU pickatlas (Tzourio-Mazoyer et al., 2002) or on the anatomical location of the MRS voxel. However, we found that this approach was not feasible for the extraction of BOLD fMRI data, because the area of the mask was much larger than the area of activation, leading to negative values. Therefore, these values were not used in further analyses. Four subjects showed no clear BOLD response, so percent signal change could not be extracted.

5.2.6 Correlating data from different imaging modalities

Given our interest in linking data from different imaging modalities, we obtained measurements reflecting activity in the occipital lobe from three modalities. We used the same task in fMRI and MEG sessions and measured from the same location with MRS and MEG. To assess possible correlations between the tree imaging modalities, Pearson's correlation coefficient was calculated using SPSS 21. $P \leq .05$ was considered significant.

5.3 Results

5.3.1 Magnetic resonance spectroscopy

Spectra as shown in Figure 5.1 were obtained for all participants. The doublet containing GABA and glutamate is indicated, as is the peak representing Cr+PCr. For all

subjects the Cramer-Rao bounds were below 20% for both GABA and glutamate, indicating that the estimates are reliable. Line width was <10Hz for all participants.

5.3.2 Magnetoencephalography

Sensor space analyses showed a clear increase in visual gamma power (40-80Hz) and a decrease in alpha power (8-12Hz) in posterior regions in response to the gratings (cluster-based randomization test $p<.05$; Figure 5.2 upper part). These were sustained for the duration of the stimulus (Figure 5.2 lower part).

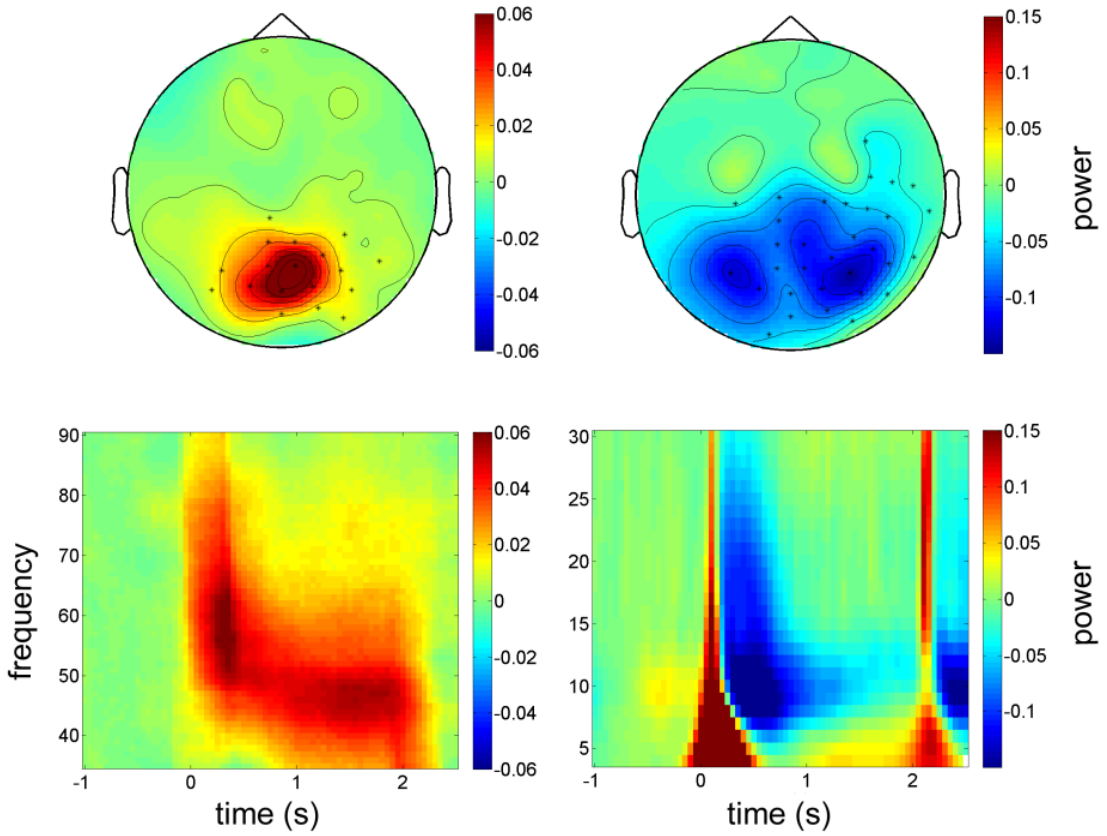

Figure 5.2: Sensor space analysis showed a clear increase in visual gamma power (upper left) and a decrease in alpha power (upper right) in posterior regions in response to gratings. Black dots in the topoplots indicate the sensors where a significant effect was observed. Time frequency representations show that the increase in gamma was sustained for the duration of the stimulus presentation (lower left), as was the decrease in alpha (lower right).

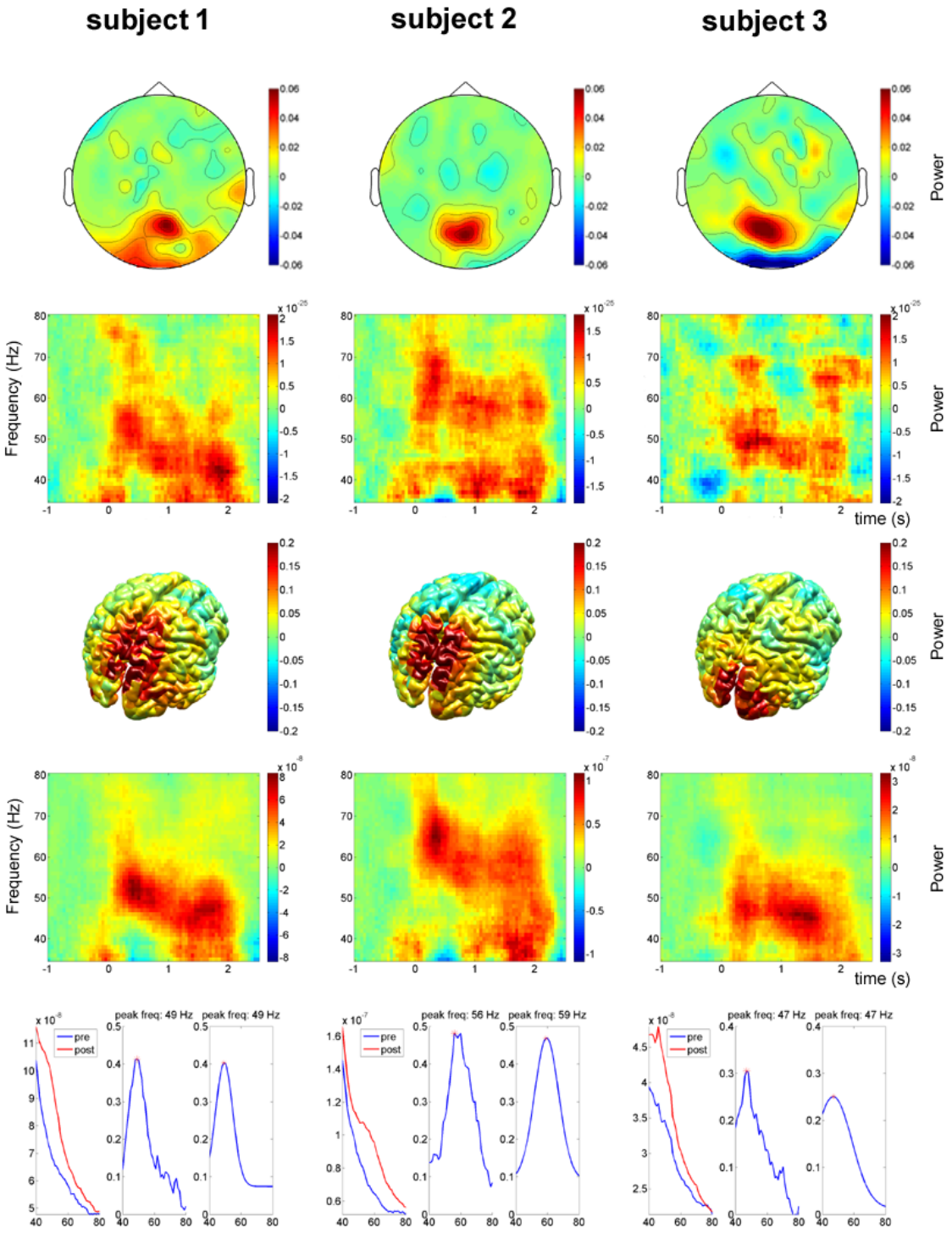

Figure 5.3: Gamma activation patterns of three representative subjects. The first row shows the topoplots based on the sensor space analysis, with the second row showing TFRs based in the sensor space analysis. The third row shows source localization of gamma band activity, with the fourth row showing the TFRs for the location of maximum activation. The final row of the figure shows the fitted peaks for each individual participant. The first part of the graph shows the spectrum before (blue) and during (red) the presentation of the grating. The second graph shows the difference between these two spectra and the peak activation for the subject. The third graph shows the fitted Gaussian curve.

We applied a beamformer spatial filtering technique to extract source-reconstructed gamma peak frequency and amplitude from the occipital lobe. Individual participants showed clear gamma responses in visual regions, as can be seen in Figure 5.3.
Even though there was individual variation, there was clear gamma activation visible in both the sensor and source space analyses, which was sustained for the duration of the stimulus (0-2s) and visible at the same peak frequency in both sensor and source space (Figure 5.3). For each individual participant, Fourier spectra for the gamma range (40-80Hz) were obtained with a fast Fourier transform. We used both the peak of the gamma activity and the location of the MRS voxel as regions of interest for the extraction of gamma frequency and amplitude. Spectra were plotted relative to baseline, and peak frequency and amplitude information extracted. Besides taking the highest value from the 'raw' spectra, we also fitted Gaussian curves to the spectra to establish the existence of unambiguous peaks for all individual subjects. Representative spectra for individual participants, based on the peak of the gamma activation, can be seen in Figure 5.3.

Gamma peak frequency based on the raw spectra and gamma peak frequency based on the Gaussian fit showed a strong correlation of $r=.892$, $p<.001$, as did our estimates based on the peak activity ROI and the MRS voxel ROI ($r=.690$, $p<.001$). To confirm the quality of the data and the reliability of the estimates, we estimated gamma peak frequencies for independent datasets based on activation induced by left and right gratings separately, which were strongly correlated ($r=.714$, $p<.001$). Figure 5.4 shows the correlation between the estimates based on the left and right gratings as well as the lateralised activation patterns induced by left and right gratings only. These could be seen at the group level as well as in single subjects.

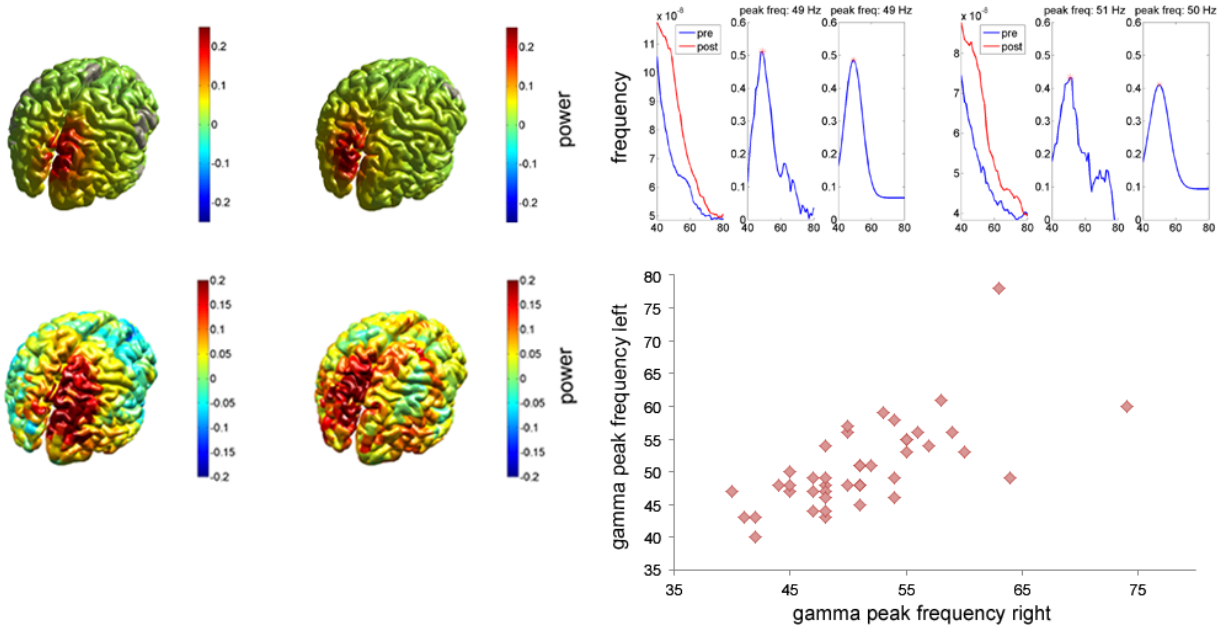

Figure 5.4: The upper left part of the figure shows lateralised activation at the group level, with the lower left part of the figure depicting lateralised activation in a representative subject (subject 1). The presentation of gratings on the left side of the screen led to activation in the right occipital cortex, whereas presentation of gratings on the right side of the screen led to activation in the left occipital cortex. The upper right part of the figure shows the fitted peaks (left and right) for this same subject. The lower right part shows the strong correlation between gamma peak frequency estimates for the left and right gratings.

5.3.3 Functional magnetic resonance imaging

Presentation of the gratings led to clear BOLD responses in occipital areas, as can been seen in the upper part of Figure 5.5. When looking at the effects of left and right gratings separately, we saw a clear lateralization of activation in occipital regions (lower part Figure 5.5).

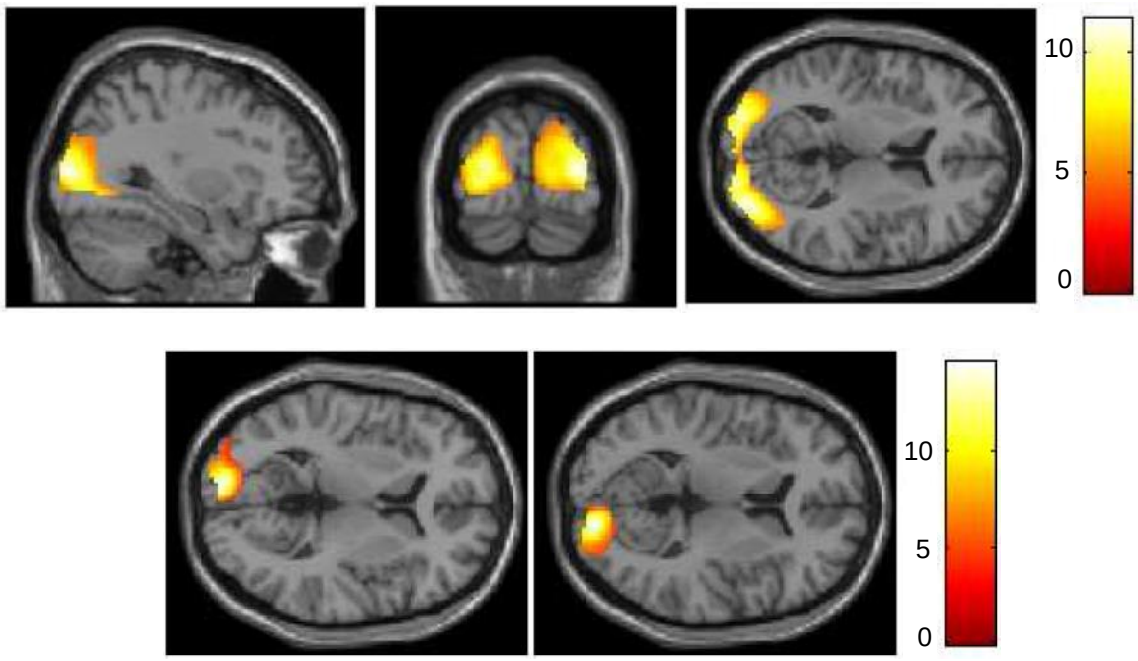

Figure 5.5: The upper part of the figure shows the BOLD response induced by the gratings at the group level (p=.05, FWE-corrected). The lower part of the figure shows that right gratings lead to activation in the left hemisphere (left image, p=.05, FWE-corrected) and left gratings lead to activation in the right hemisphere (right image, p=.05, FWE-corrected).

The first approach we took to extract percent signal change was to use these activations as a region of interest and extract percent signal change from those. In four participants there was no clear activation and therefore percent signal change could not be extracted. We were able to extract percent signal change based on the peak voxel from 46 participants and percent signal change based on the peak voxel from left gratings only from 48 participants. Percent signal change based on all voxels activated correlated well with percent signal change based on the peak voxel $r=.724$, $p<.001$ and with percent signal change based on the left grating $r=.592$, $p<.001$. Also percent signal change based on the peak voxel correlated well with percent signal change based on the left gratings only $r=.556$, $p<.001$.

5.3.4 Correlations between data from different imaging modalities

We found no correlations between GABA and any of our gamma peak frequency measures (GABA - gamma based on peak activation: r=-.114, p=.473; GABA - gamma based on left stimulus: r=-.132, p=.404; GABA - gamma based on MRS voxel: r=-.053, p=.737).

We applied further controls by subsampling participants, based on the line width and signal to noise ratio of the MRS data as well as the clarity of the peak in the MEG data. However, even when we sub-selected the participants with the best data quality (n=22), we did not find any significant correlations (GABA - gamma based on peak: r=-.160, p=.477; GABA - gamma left: r=-.130, p=.565; GABA - gamma based on MRS: r=-.155, p=.492). Scatter plots for all these correlations can be found in figure 5.6. No correlations were found between GABA and gamma amplitude (r=.151, p=.341.) or between glutamate and gamma frequency (r=-.105, p=.509), glutamate and gamma amplitude (r=.120, p=.449), GABA/glutamate and gamma frequency (r=-.055, p=.729), or GABA/glutamate and gamma amplitude (r=.060, p=.705).

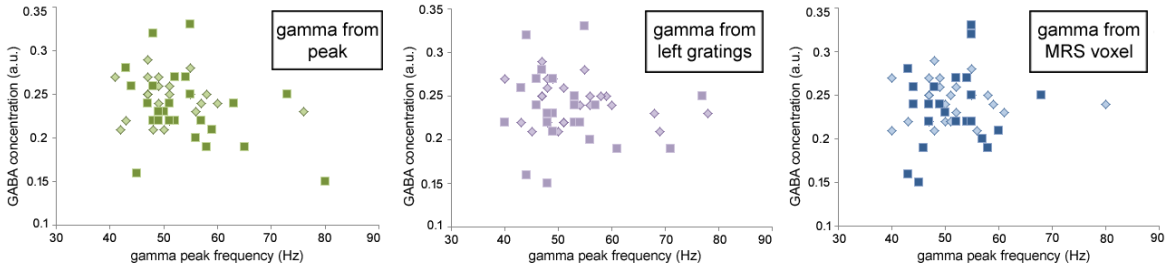

Figure 5.6: No correlations were observed between GABA and gamma based on the peak activation (left), between GABA and gamma based on left gratings only (middle), or between GABA and gamma from the location of the MRS voxel (right). Diamonds represent the participants with the best data quality.

We also did not observe any correlations between GABA and any of our BOLD measures (GABA - all activated voxels: r=-.080, p=.601; GABA - peak voxel: r=-.180, p=.227; GABA - peak voxel based on left gratings: r=-.053, p=.737). Also in this case, when we sub-selected the participants with the best data quality (n=24), based on the line

width and signal to noise ratio of the MRS data as well as the clear presence of a visual BOLD signal in the MRI data, we did not find any significant correlations (GABA - all activated voxels: r=-.109, p=.613; GABA - peak voxel: r=.135, p=.530; GABA - peak voxel based on left grating: r=-.192, p=.368). These scatter plots have been depicted in Figure 5.7. Furthermore, no correlation was found between glutamate and the BOLD signal (r=.088, p=.622).

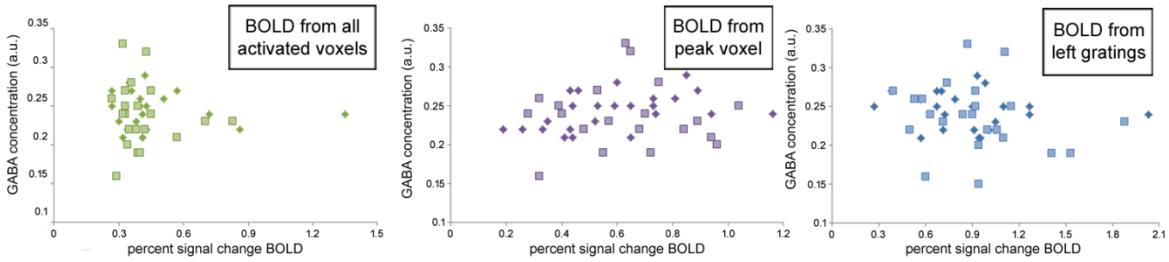

Figure 5.7: No correlations were observed between GABA and the BOLD signal in all activated voxels (left), between GABA and BOLD signal in the peak voxel (middle), or between GABA and BOLD in response to the left gratings only (right). Diamonds represent the participants with the best data quality.

Lastly, we correlated gamma frequency and amplitude based on the peak of the activation in occipital cortex with percent signal change in the voxel showing the strongest BOLD response and found no correlation (frequency: r=.273, p.088, Figure 5.8; amplitude: r= -.185, p=.274).

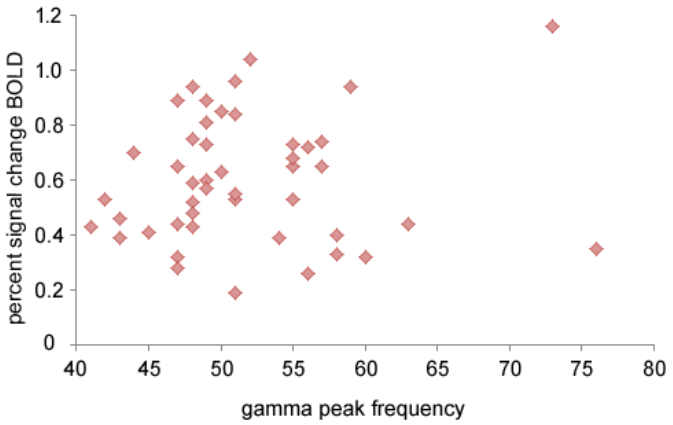

Figure 5.8: No correlation was observed between gamma peak frequency and percent signal change in the BOLD signal of the voxel with peak activation.

5.4 Discussion

With the study described in this chapter, we had two goals. First of all, we wanted to establish the best analysis methods for our multimodal dataset, especially for the MEG data where methods are less established than for fMRI. Secondly, we attempted to replicate the finding of Muthukumaraswamy et al. (2009) of correlations between resting GABA concentrations, gamma peak frequency, and BOLD fMRI in the occipital lobe. We were able to analyse all three types of data and developed an analysis pipeline for the MEG data that allowed us to show clear visual gamma in almost all participants. The methods described in this chapter will also be applied in chapter 6, where they will be used to address the question whether *ZNF804A* genotype affects prefrontal function. However, we did not replicate the findings of Muthukumaraswamy et al. (2009), because no correlations were found between GABA and gamma, gamma and BOLD, and GABA and BOLD. This is an important finding in itself, and I will discuss possible explanations and implications of this, focusing in more detail on the lack of correlation between GABA and gamma peak frequency, which was the most novel finding in the Muthukumaraswamy et al. (2009) paper and has received most attention in the literature.

In order to find not only the best way to analyse individual datasets, but also analysis methods that would enable us to link results from the different imaging modalities, the data were analysed using several methods. We initially attempted to assess the relationship between MRS GABA and gamma oscillations in a more direct way by taking both measurements from the same anatomical location. We also extracted frequency and amplitude from the spatial peak of the activity for each individual participant, so that our measures would be derived from the strongest gamma oscillations present. To make our study as comparable as possible to the study of Muthukumaraswamy et al. (2009), we also analysed the data based on the left gratings only. In addition to using the maximum

value of the FFT spectra, we fitted a Gaussian curve to the spectra to assess peak frequency. This makes explicit the assumption that there is a peak and is less susceptive to incorrect detection of a spurious incorrect local maximum. All these different measures of gamma activity correlated with each other, but none correlated with the measured GABA concentrations. With respect to the BOLD fMRI data, we extracted percent signal change from several ROIs, including all voxels activated by the gratings, the voxel showing peak activation, and the voxel showing peak activation in response to left gratings only. Also in this case, the different measures correlated with each other, but not with GABA or gamma peak frequency.

Gamma oscillations are generated within complex networks of inhibitory GABAergic and excitatory glutamatergic cells, with recorded gamma waves largely corresponding to synchronous IPSPs in pyramidal cells brought about by fast-spiking interneurons (Buzsaki & Wang, 2012). Therefore, synaptic GABA is crucial for the generation of gamma oscillations. Under basal conditions, the MRS GABA signal arises mostly or almost entirely from the large cytoplasmic GABA pool in GABAergic neurons, the functional significance of which is not known (Maddock & Buonocore, 2012). Therefore, MRS GABA seems unlikely to reflect primarily the activity of GABAergic interneurons, including those within gamma-generating networks (Stagg et al., 2011a). Studies have tried to address this issue by correlating MRS GABA measures with TMS measures of synaptic GABA-A and GABA-B (Stagg et al., 2011b; Tremblay et al., 2013), because different TMS protocols can be used to specifically assess GABA-A and GABA-B activity. No correlation between MRS GABA measures and TMS measures of synaptic GABA-A and GABA-B activity was found, supporting the view that MRS-derived GABA levels do not reflect specific synaptic activity. Given that gamma oscillations most likely mediate the relationship between GABA signalling and BOLD (Logothetis et al., 2001;

Buzsaki et al., 2007), this problem extends to possible correlations between GABA as measured by MRS and BOLD fMRI.

Moreover, whilst there is evidence that gamma peak frequency is heritable (van Pelt et al., 2012), which would indicate that it is a relatively stable characteristic, many factors seem to affect gamma frequency making it highly variable within individual subjects. Visual gamma frequency depends on several stimulus parameters such as stimulus contrast (Ray & Maunsell, 2010), velocity (Swettenham et al., 2009), size (Ray & Maunsell, 2011), and eccentricity (van Pelt & Fries, 2013). Recently, it has also been shown to depend on cognitive processes such as attention (Bosman et al., 2012). This variability of the gamma peak frequency makes it less plausible that gamma frequency would correlate with a relatively stable property (i.e. resting GABA levels), even if the latter could be measured selectively in terms of synaptic rather than total GABA. Studies such as those by Muthukumaraswamy & Singh (2008; 2009) also indicate that whereas gamma depends on changes in stimulus characteristics, this is not necessarily true for the BOLD signal.

There are several experimental differences that might have contributed to the discrepancy between our results and results from previous studies. When looking at studies addressing the correlation between gamma oscillations and BOLD amplitude, these studies have all reported correlations with gamma power rather than peak frequency (Zaehle et al., 2009; Zumer et al., 2010; Scheeringa et al., 2011), making this the more established correlation. We did not find this correlation with gamma power, but this might be due to the fact that we did not record the datasets simultaneously. As discussed, gamma oscillations are variable, making it important to keep the recording sessions as closely linked as possible. Furthermore, most of the studies discussed here that found correlations between gamma power and the BOLD signal either deconvolved the BOLD signal or

convolved the gamma signal with the hemodynamic response function. This might be important to make the data comparable (Zumer et al., 2010). When looking at reported correlations between BOLD and GABA as measured by MRS, the three previous studies were small, ranging from 10 to 15 subjects (Muthukumaraswamy et al., 2009; 2012; Donahue et al., 2010), compared to 50 subjects in our study. The positive findings in other studies could have been false positives, or alternatively, we might not have used the most optimal task for the generation of a BOLD response in visual areas. We decided to use the same task as in the MEG session to make those datasets as comparable as possible, but did not pilot the task separately for use in our fMRI study. It may have been possible to develop a more appropriate task that would have allowed us to detect an effect.

To conclude, previous studies have provided convincing evidence that in principal, GABAergic signalling underlies gamma oscillations and that gamma oscillations contribute to the BOLD signal. However, the results of the study described in this chapter are a reason to question how these relationships can be assessed. Gamma oscillations are sensitive and many studies observe intra-individual variation. Therefore, simultaneous fMRI and electrophysiological recordings might be necessary to study the relationship between BOLD and gamma. As explained in the discussion, GABA as measured by MRS does most likely not reflect synaptic GABA. Therefore, if possible, other methods might need to be developed to measure GABA concentrations in human brain. To date, most evidence that GABA underlies gamma oscillations comes from in vitro studies and computational models, indicating that it is by no means trivial to quantify this relationship in human brain. Therefore, it makes sense from a theoretical point of view that two larger studies (this study and Shaw et al., 2013) than the study by Muthukumaraswamy et al., (2009) have provided no evidence for a correlation between GABA and gamma peak frequency. These methodological limitations also mean that the methods we will apply in

chapter 6 are unlikely to provide evidence for correlations between measures of prefrontal function from different modalities. However, the methods described in this chapter can be applied to assess DLPFC function using MRS, fMRI, and MEG in order to study the effects of *ZNF804A* genotype on prefrontal brain activity.

Chapter 6 - The effect of *ZNF804A* genotype on prefrontal activity

6.1 Introduction

In this chapter, I will describe experiments conducted to assess the effect of *ZNF804A* genotype on prefrontal activity using the methods described in chapter 5. MEG and fMRI datasets were acquired during an N-back working memory task, while MRS was used to measure prefrontal metabolite concentrations during rest. In addition to the methods described in chapter 5, functional connectivity during the N-back task was assessed. Even though I will not carry out any case-control comparisons, in the introduction to this chapter I will describe experiments that have shown the importance of prefrontal functioning in schizophrenia using fMRI, MEG, and MRS and will discuss evidence for the use of these prefrontal measurements as intermediate phenotypes.

6.1.1 Schizophrenia and prefrontal function

The advent of functional imaging has allowed investigation of patterns of regional brain activity in schizophrenia both at rest and during task performance. The most robust of these findings concern abnormalities of the prefrontal cortex. One of the earliest functional abnormalities to be observed in patients with schizophrenia is the phenomenon of hypofrontality, a decrease in regional cerebral blood flow in the frontal lobes relative to posterior areas in the brains of patients with schizophrenia compared with controls (Ingvar & Franzen, 1974). Ingvar and Franzen also showed that this abnormality correlates with the severity of the patient's disorder, particularly with the negative symptoms.

Working memory tasks have been used in fMRI studies as a tool to assess activity in the DLPFC, because this area has been shown to be preferentially impacted by the biology of the illness (Meyer-Lindenberg & Bullmore, 2011). Particularly the N-back task, which requires people to constantly monitor a sequence of stimuli and react to stimuli that

match the one presented N stimuli previously, has been a very popular method to elicit a DLPFC response (Owen et al., 2005). The majority of early imaging studies as well as a recent meta-analysis have indicated hypofrontality at rest and during working memory tasks (Minzenberg et al., 2009). These abnormalities in DLPFC activation during working memory tasks have been found to be independent of performance level (Honey et al., 2002), motivation (Berman et al., 1988), or stimulus material used (Stevens et al., 1998; Tek et al., 2002; Thermenos et al., 2004).

However, during the last decades, hypofrontality in schizophrenia has become controversial, and it is thought that descriptive terms such as hypo- and hyperfrontality underestimate the complexity of the issue (Callicott et al., 2003b). Even in healthy subjects, it has been shown that prefrontal activation increases until a capacity limit is reached, at which point the DLPFC will deactivate (Callicott et al., 1999). It is thought that this 'inverted U' functioning becomes shifted to the left in schizophrenia. Put simply, when the demands of the task exceed processing capacity the DLPFC disengages, resulting in hypofrontality, which happens sooner in patients with schizophrenia than in controls. In contrast, when the task is within the processing capacity of the patients, they show an elevated prefrontal response relative to controls, as if their DLPFC is functioning less efficiently than that of controls (Weinberger et al., 2001).

6.1.2 Prefrontal oscillations

Another way to assess prefrontal activity during a working memory task is through electrophysiological methods. These provide a more direct measure of neuronal activity and have superior temporal resolution. However, finding the source of these activations, especially with EEG methods, is difficult. In this regard, MEG provides some advantages when the source of the activation is of interest. At the time of writing, there was only one

report of activation patterns during an N-back task as measured with MEG, which showed decreased alpha power in occipital regions (Ciesielski et al., 2010). Even though the current literature is limited, I will briefly discuss the patterns of working memory related oscillations that have been reported in frontal regions in electrophysiological studies.

The theta rhythm has been found to be particularly prominent in the hippocampus (see chapter 7), but several EEG studies have indicated that theta oscillations also arise in frontal midline structures, particularly during attention and working memory tasks (Gevins et al., 1997; Winterer et al., 1999). Using intracranial recordings, Meltzer et al. (2008) reported increased frontal midline activity during a working memory task, in line with findings from working memory EEG (Deiber et al., 2007) and MEG (Brookes et al., 2011a) studies. However, the gamma rhythm has been reported most often in relation to prefrontal working memory related activations. Using delayed match-to-sample tasks, Tallon-Baudry et al. (1998), Palva et al. (2010), and Roux et al. (2012) have all reported increases in gamma power with increasing working memory load. Roux et al (2012) even showed in their MEG study that gamma power is predictive of the number of items retained in working memory. Barr et al. (2009) have also reported an increase in gamma power with higher working memory load using an N-back task.

Neural oscillations are thought to be a fundamental mechanism for the coordination of neuronal responses throughout the cortex, and impairments in these oscillations are a candidate mechanism for network impairments in schizophrenia (Uhlhaas & Singer, 2010). Several studies have investigated whether in particular gamma oscillations are altered in schizophrenia. The gamma rhythm is thought to be important for neural synchronization and binding of information from multiple processing streams (Fries et al., 2007). Thereby, it plays an important role in functional connectivity in the brain. Studies using perceptual feature-binding tasks to assess endogenously generated gamma found that gamma

oscillations related to visual feature-binding are not present in patients with schizophrenia (Spencer et al., 2003; 2004). During a perceptual organization task, it was found that impaired performance in patients with schizophrenia was accompanied by a widespread reduction in the power of gamma band oscillations in the right temporal lobe (Tillmann C. et al., 2008). Additionally, patients with schizophrenia have been shown to have reduced amplitude of gamma -as well as theta- oscillations in frontal regions during working memory tasks (Schmiedt et al., 2005; Cho et al., 2006; Haenschel et al., 2009). Several studies have shown that in patients with schizophrenia the phase synchronization of oscillations in the higher frequency bands, during visuoperceptual organization and auditory processing, is reduced (Symond et al., 2005; Uhlhaas et al., 2006). Gamma band abnormalities can be detected in unmedicated patients (Gallinat et al., 2004) and it has been suggested that modern anti-psychotics can reverse the abnormalities (Hong et al., 2004). These abnormalities in the gamma band are already present in first-episode patients (Spencer et al., 2008). These findings suggest that impaired synchronization of high frequency oscillations might underlie functional dysconnectivity of cortical networks in schizophrenia.

6.1.3 MRS measurements in schizophrenia

The use of proton magnetic resonance spectroscopy allows investigation of several metabolites, including glutamate, GABA, and N-acetyl aspartate (NAA), a molecule found in mature neurons, particularly pyramidal neurons, and thought to be a marker of neuronal integrity (Bertolino & Weinberger, 1999; Weinberger et al., 2001). This potentially allows MRS studies to bridge the gap between neuroimaging studies and findings at the molecular and cellular level. Early MRS sequences were not yet able to resolve GABA and glutamate spectra, so most studies to date investigated changes in NAA levels related to

schizophrenia. NAA levels are decreased in the hippocampus and dorsolateral prefrontal cortex in schizophrenia (Bertolino et al., 1998a; Bertolino et al., 1998b), implying a loss of neuronal integrity in these regions. This has been confirmed in a meta-analysis (Steen et al., 2005) with NAA being equally reduced in grey and white matter. The changes in NAA are found to a similar extent in chronic and acute patients, as well as those who are medication-free and medication-naïve (Bertolino et al., 1998a; Weinberger et al., 2001; Steen et al., 2005). Interestingly, NAA in the DLPFC has been shown to correlate inversely with the severity of negative symptoms (Callicott et al., 2000a). Additionally, DLPFC NAA measures have been shown to correlate with abnormalities of DLPFC activation during working memory tasks (Bertolino et al., 2000; Callicott et al., 2000a; Callicott et al., 2000b). These relationships are not found in normal controls (Bertolino et al., 2000; Callicott et al., 2000b), suggesting that pathology in this region specifically affects the activity of a DLPFC network during task performance and is associated with schizophrenia (Weinberger et al, 2001).

Whereas the decrease in NAA is a well-established finding, results from studies looking at glutamate and/or glutamine changes in the DLPFC in schizophrenia are mixed. Some studies have reported changes in chronic but not first-episode or unmedicated patients (Stanley et al., 1996; Ohrmann et al., 2005; Rusch et al., 2008); others detected higher concentrations of glutamate in patients with schizophrenia (van Elst et al., 2005; Olbrich et al., 2008). One study has assessed neurotransmitter levels in the DLPFC during a working memory task and found GABA levels to be inversely related to the working memory related change in perfusion (Michels et al., 2012).

6.1.4 Prefrontal connectivity

Schizophrenia has often been described as a disorder of dysconnectivity. However, no meta-analyses of functional connectivity studies of schizophrenia are available, and both increased and decreased connectivity has been observed in studies comparing schizophrenia patients with controls. This indicates that there is no overall disruption of connectivity, but there are consistent findings in specific brain regions, one of those being the DLPFC (Meyer-Lindenberg & Bullmore, 2011). Studies of the DLPFC indicate that coupling with medial temporal lobe regions, particularly the hippocampus, is altered (Weinberger et al., 1992). The first study showing altered functional connectivity between the DLPFC and hippocampus was carried out by Meyer-Lindenberg et al. (2001) using positron emission tomography. A later study by Meyer-Lindenberg et al. (2005) replicated this finding and showed that while normally the DLPFC and hippocampus uncouple with increasing memory load, this is not the case in schizophrenia patients. Wolf et al. (2009) have also shown increased and persistent coupling of the DLPFC and hippocampus during working memory performance. This abnormality in prefrontal-temporal connectivity can already be detected in first-episode patients (Crossley et al., 2009).

6.1.5 DLPFC function and connectivity as intermediate phenotypes

It has been shown that the neural networks supporting working memory are heritable (Koten et al., 2009) and sibling studies indicate that abnormalities in prefrontal networks are present in the first-degree relatives of patients with schizophrenia (Unschuld et al., 2013). Rasetti et al. (2011) have shown that coupling between the DLPFC and hippocampus is compromised in both patients and siblings. Some of the most recently discovered schizophrenia risk genes have been shown to alter prefrontal-hippocampal connectivity, such as *CACNA1C* (Paulus et al., 2013a) and *ZNF804A*, discussed in more

detail in section 6.1.6. This indicates that prefrontal-hippocampal coupling is successfully being used as an intermediate phenotype in the study of schizophrenia risk genes.

Also DLPFC activity is an established intermediate phenotype in the study of schizophrenia risk genes. Blackwood et al. (1999) observed reduced prefrontal blood flow in first-degree relatives and also (Callicott et al., 2003a) found that comparable differences in DLPFC function to those seen in patients can be observed in the healthy siblings of patients with schizophrenia. By now, many studies looking at the effects of schizophrenia risk genes have already assessed DLPFC activity (e.g. Egan et al., 2001; Egan et al., 2004; McIntosh et al., 2007; Straub et al., 2007; Nicodemus et al., 2010; Nixon et al., 2011) and found effects of risk alleles. Additionally, it has been shown in a twin study that brain activation during an N-back working memory task is genetically influenced (Blokland et al., 2008).

The evidence for the use of MRS metabolite measures as intermediate phenotypes is somewhat mixed. A decrease in NAA can already be observed in people with early and late at-risk syndrome (Jessen et al., 2006). However, sibling studies of NAA have indicated that the decreases observed in patients with schizophrenia are not present in this genetically similar group (Callicott et al., 1998; Block et al., 2000). Studies looking at glutamate and/or glutamine changes in schizophrenia have found changes in chronic but not first-episode or unmedicated patients, indicating that these changes might be associated with progression of the disease or medication rather than any genetic factors (Stanley et al., 1996; Ohrmann et al., 2005). This is in line with a study by (Yoo et al., 2009), who found no glutamate alterations in first-degree relatives of patients with schizophrenia. On the other hand, Lutkenhoff et al. (2010) have shown that the unaffected twins of schizophrenia patients have significantly lower glutamate in prefrontal regions than healthy controls.

Gamma peak frequency has been shown to be heritable (van Pelt et al. 2012) and oscillatory activity in the gamma range is emerging as a possible intermediate phenotype (Egan & Cannon, 2011). A twin study has indicated that early auditory gamma band responses are heritable (Hall et al., 2011a) and several schizophrenia risk genes, such as DRD4 and DAT1, have been shown to affect gamma power (Demiralp et al., 2007).

6.1.6 *ZNF804A* genotype affects functional connectivity

Before the data discussed in this chapter were analysed, four studies had assessed the effect of rs1344706 on working memory related functional connectivity. As discussed in chapter 1, the first study assessing the effects of *ZNF804A* genotype on human brain function used an N-back working memory task to probe DLPFC function as well as functional connectivity (Esslinger et al., 2009). They reported increased functional connectivity between the right DLPFC and left hippocampus and decreased interhemispheric prefrontal coupling between the right and left DLPFC in healthy subjects carrying the risk allele. No effect of *ZNF804A* genotype on activity in the DLPFC was found. To assess whether these effects are state-dependent, the same group (Esslinger et al., 2011) scanned healthy subjects during rest, a working memory task, and an emotional processing task. They found an effect of rs1344706 on DLPFC-hippocampal coupling during the WM-task only, while interhemispheric prefrontal coupling was consistently altered and is therefore thought to be state-independent. Paulus et al. (2013b) attempted to replicate these findings and found no changes in coupling between the bilateral DLPFCs dependent on *ZNF804A* genotype. They did report altered DLPFC-hippocampal coupling during the N-back task, where they observed increased coupling in risk carriers. However, the genotype difference was only detected at very low thresholds and not at all when a different method for determining the seed voxels was used. To assess the usefulness of this

coupling as an intermediate phenotype, Rasetti et al. (2011) looked at patients, unaffected siblings, and healthy controls and found impaired coupling between the DLPFC and hippocampus in both patients and unaffected siblings - but not healthy controls. Furthermore, this coupling was modified by *ZNF804A* genotype in all experimental groups. They used not only a seed-based connectivity method, but reported the same finding using a psycho-physiological interaction (PPI) analysis.

The aim of the experiments described in this chapter is to assess the effect of rs1344706 on prefrontal function using fMRI, MEG, and MRS measurements. fMRI data were obtained during an N-back working memory task to allow replication of the reported alterations in prefrontal-hippocampal coupling. Additionally, we obtained MEG recordings during the same task from the same subjects. This allows us to investigate whether particular brain rhythms might underlie the previously reported changes in connectivity and to assess possible correlations between the imaging modalities. We also acquired MRS data during rest from a voxel placed in the DLPFC to assess possible effects of *ZNF804A* genotype on NAA, GABA, and glutamate and to correlate these measurements with the functional activations in the fMRI and MEG studies.

6.2 Methods

6.2.1 Participants

Fifty healthy right-handed participants between 18 and 35 participated in this study (described in section 5.2.1). Around 200 potential participants were approached, and fifty participants were pre-selected based on their genotype (section 6.2.2) so that 25 participants were risk homozygotes (AA) and 25 non-risk homozygotes (CC). The AA group consisted of 11 men and 14 women, while the CC group consisted of 12 men and 13 women. Several questionnaires, including the State-Trait Anxiety Questionnaire and a

Visual Analogue Scale were administered on the day of the MEG session. This information was obtained to ensure that any differences in brain activity between groups were not due to differences in mood or anxiety levels. The groups did not differ in terms of age (p=.331), scores on the State-Trait Anxiety Questionnaire (p=.650), scores on a Visual Analogue Scale (Alert p=.231; Drowsy p=.907; Anxious p=.547; Happy p=.490; Nauseous p=.846; Sad p=.962), alcohol consumption the night before the experiment (p=.500), or hours of sleep the night before the experiment (p=.941). All participants first took part in the MEG session, followed by the MR session, which took place on another day.

6.2.2 Genotyping

Participants in this study provided two cheek swabs for genotyping purposes. DNA was extracted using a Chargeswitch gDNA buccal cell kit (Invitrogen). Genotyping for each sample was undertaken using RT-qPCR with a taqman genotyping assay (C___2834835_10) using a7900HT qPCR system (Applied Biosystems) as described in section 3.2.4. Samples were loaded in duplicate.

6.2 3 N-back working memory task

In both the MEG and fMRI sessions, participants completed an N-back working memory task. Participants were required to monitor a sequence of letters continuously and to detect letters that matched the letter presented N stimuli previously. The task consisted of 14 blocks of 15 letters that were sequentially presented in the centre of the screen. In half the blocks, subjects responded when they saw the same letter as they saw 2 letters back (2-back condition) and in the other half of the blocks subjects responded when they were presented with an X (0-back condition). The presentation of the letters was randomised, and each block contained two, three, or four targets, with participants being

presented with on average three targets per block. Participants practiced two 0-back and two 2-back blocks before starting the task. Percent correct responses and reaction times were recorded.

6.2.4 Magnetic resonance spectroscopy

For MR data acquisition, a 3T Siemens scanner with a 32-channel head coil was used. Sagittal and axial T1 scout images were acquired and used to place a 2 x 2 x 2cm voxel of interest manually in the dorsolateral prefrontal cortex. The placement of the voxel is shown in Figure 6.1. The data were acquired and analysed as described in section 5.2.3. In short, the SPECIAL sequence, originally developed by Mlynarik et al. (2006) and adapted for humans by Mekle et al. (2009) was used for data acquisition. The spectra were quantitatively analysed using Linear Combination Model. This analyses the *in vivo* spectrum as a linear combination of a basis set of simulated metabolite spectra (Provencher, 1993).

Given our interest in NAA, GABA, and glutamate, we extracted the estimated concentrations for these neurotransmitters. Scans for which the uncertainty was more than 20% or line width more than 10Hz (Near et al., 2013) were excluded from further analyses. Furthermore, we extracted absolute levels of Creatine (Cr+PCr), which is a measure of cellular integrity and the standard reference resonance (Stagg et al., 2009). We then normalised our NAA, GABA, and glutamate values by dividing them by Creatine levels.

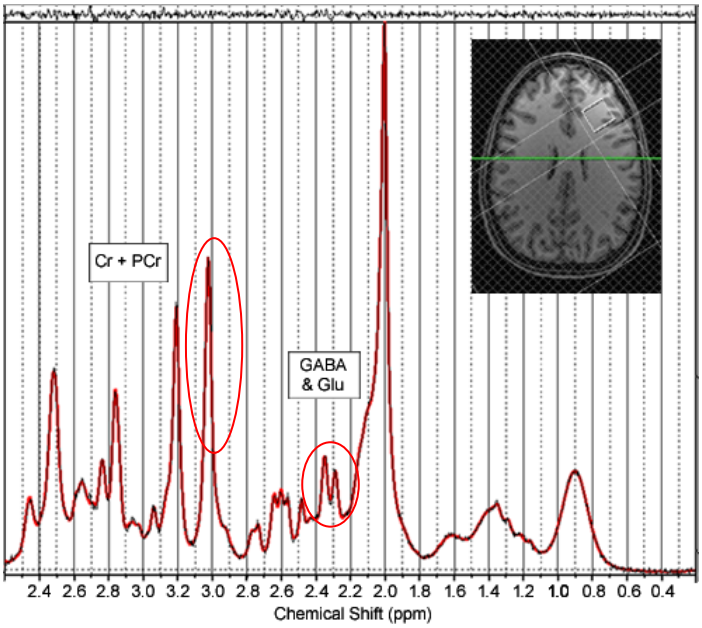

Figure 6.1: A typical spectrum acquired with the SPECIAL sequence from the voxel in the DLPFC (placement shown). Data were analysed with LCModel and the quality of the fit is represented by the small residual remaining after the fitting, shown as the little black line at the top of the figure. Peaks for GABA and glutamate as well as creatine (Cr+PCr) are indicated. Two more GABA peaks, at 3ppm and 1.9ppm, are present in the spectrum, but these are hidden by the larger peaks of other metabolites.

6.2.5 Magnetoencephalography

Whole-head MEG recordings were acquired using the Elekta NeuroMag MEG System. Data from the 204 gradiometers were analysed. The signal was digitised at a sampling rate of 1000Hz, with a high-pass filter of 0.03Hz and a low-pass filter of 330Hz. A magnetic digitizer (Polhemus FastTrach 3D) was used to measure the relative positions of four head-position indicator (HPI) coils and three anatomical landmarks (nasion, left and right auricular points). These coordinates were used for coregistration of the sensor montage to the participant's structural MRI scan. The data were analysed using the Matlab-based Fieldtrip toolbox (Oostenveld et al., 2011). The data were preprocessed and the sensor level analysis was carried out as described in chapter 5, except that we also investigated activity in the theta (4-8Hz) and beta (13-30Hz) band. Average spectral power was computed as the average across trials and tapers (time window between 0.2 and 1.2s),

with 2-back being contrasted with 0-back. All trials, except the ones following a response, were analysed.

We applied a frequency-domain beamformer technique (Gross et al., 2001; Schoffelen et al., 2008) to localise the sources of theta, alpha, beta, and gamma frequencies for the whole brain. This adaptive spatial filtering technique uses the Fourier spectra, which were obtained by applying a multitaper FFT approach to the 1s data segments. For the gamma band, this multitaper FFT approach was centred around 60Hz with 39 Slepian tapers, for the beta band around 23Hz with 13 Slepian multitapers, for the alpha band around 10Hz with 3 Slepian tapers, and for the theta band around 6Hz using 3 Slepian tapers. Using the individual anatomical MRI, we constructed a realistically shaped single-shell description of the brain for each subject. Lead fields were calculated for all grid points (Nolte, 2003). With the lead fields and the Fourier spectra, a spatial filter was constructed for each grid point. Using this filter, the spatial distribution of power was estimated for each trial separately and then averaged per condition so that 2-back could be contrasted with 0-back.

Statistical analysis to test the main effects was carried out using a cluster-based randomization procedure (Maris & Oostenveld, 2007) on both sensor and source level. By clustering neighbouring sensors (or grid points in the source analysis) that show the same effect, this test deals with the multiple-comparisons problem and at the same time takes into account the dependency of the data.

Additionally, the power and peak frequency of oscillatory brain activity were analysed for regions of interest in the left and right DLPFC. Regions of interest were generated in two ways. To directly assess the relationship of GABA and glutamate with gamma and theta oscillations in the same location in the brain, we took the MNI coordinates of the centre of the MRS voxel of each individual subject and generated a

sphere with a radius of 17.5mm which was used as a spatial mask to extract gamma and theta amplitude and frequency data. Furthermore, we used the functional MRI results by taking the coordinates of the peak voxels within the left and right DLPFC and drawing a sphere with a radius of 17.5mm around the peak voxels. This allowed us to extract frequency and amplitude information from prefrontal areas engaged in the task. In the ROI analyses, we focused on oscillations in the gamma and theta band, because these have been observed in prefrontal regions during working memory tasks (Uhlhaas & Singer, 2010). To establish individual peak frequency and amplitude in these regions of interest, an LCMV beamformer was applied. This procedure was the same as described in chapter 5, expect that both the gamma (40-80Hz) and theta (4-8Hz) band were studied. Spectra were plotted relative to baseline and peak frequency and amplitude information extracted.

6.2.6 Functional magnetic resonance imaging

During the N-back task, whole brain T2*-weighted BOLD fMRI data were acquired using EPI and an interleaved slice acquisition sequence [32 axial slices, volume repetition time (TR) = 2s, echo time (TE) = 28ms, flip angle = 76°, slice matrix size = 64 × 64, slice thickness = 3.0mm, field of view (FOV) = 192mm]. Three hundred and thirty five images were acquired.

Image processing and statistical analyses were conducted using SPM8 following the protocol described in chapter 5. Contrast parameter images generated at the single subject level (2-back vs. 0-back) were submitted to second-level group analysis. Additionally, MarsBaR (Brett et al., 2002) was used to obtain β-estimates for the voxel with peak activation within a mask of the left DLPFC and for the voxel with peak activation within a mask of the right DLPFC. Based on the extraction methods that were

tested in chapter 5, this seemed the best method to estimate prefrontal activity. Masks consisted of BA46 and the lateral part of BA9.

6.2.7 Connectivity

We performed a psycho-physiological interaction analysis as implemented in SPM8 to examine the functional connectivity pattern of the right DLPFC and the differences in this pattern between genotype groups. This part of the project was carried out together with a medical student whose FHS project I supervised. The method we used is comparable to the one described by Rasetti et al. (2011), in that we used PPI to explore the way in which brain activity in the right DLPFC modulated activity in other regions specifically in response to the working memory task.

To determine the seed voxel coordinates, we constrained the search space to a right DLPFC mask that consisted of BA46 and the lateral part of BA9. For removal of the medial regions of BA9, the MarsBaR toolbox was used (Brett et al., 2002).Within this mask, we determined the MNI coordinates of the DLPFC peak voxel at the group level in the 2-back vs. 0-back contrast [34 42 34]. Starting from the peak activation at the group level, we identified the coordinates of the next local maximum for each subject within the 2-back vs. 0-back contrast at $p<.01$ uncorrected. Additionally, we limited the next local maximum to clusters extending 10 voxels. Two subjects (CC) failed to show DLPFC activation within the aforementioned contrast and were therefore excluded from further analyses.

Seed time series were extracted as the first eigenvariate from a volume of interest which consisted of a sphere of 6 mm around the individual seed voxels, adjusting for effects-of-interest. We then used the PPI analysis toolbox (Friston et al., 1997) to assess functional connectivity. A general linear model was constructed at the first level using the

deconvolved BOLD signal (from right DLPFC VOI), the task-related predictor (2-Back vs. 0-Back), and the interaction term between the first and the second regressors. The movement parameter file, obtained in the realignment step during preprocessing, was also added as a regressor. At the group level, a one sample t-test was conducted to visualise the connectivity profile of the right DLPFC. We applied small volume corrections using a hippocampal mask and a prefrontal mask consisting of BA9+10+44+45+46+47.

In order to examine the differences in functional connectivity within the working memory task between genotype groups, a full factorial group analysis was carried out. Because we had a strong a priori hypothesis based on previous papers reporting findings on the effects of *ZNF804A* genotype on working memory related connectivity (Esslinger et al., 2009; Esslinger et al., 2011; Rasetti et al., 2011; Paulus et al., 2013b), we looked at effects of genotype within masks of the hippocampus and prefrontal cortex. Furthermore, we report results for an exploratory whole-brain analysis at $p<.001$ uncorrected.

6.2.8 Correlating data from different imaging modalities

Given our interest in linking data from different imaging modalities, we obtained measurements reflecting activity in the DLPFC from three different modalities. We used the same task for fMRI and MEG, and measured from the same location for MRS and MEG. To assess possible correlations between the three imaging modalities, Pearson's correlation coefficient was calculated using SPSS 21. $P\leq.05$ was considered significant. We correlated the β-estimate for the voxel with peak activation in the DLPFC (the same peak voxel as used in the connectivity analysis) with gamma peak frequency and amplitude, and with GABA, glutamate, and NAA concentrations. We also correlated GABA, glutamate, and NAA concentrations with gamma peak frequency and amplitude extracted from the location of the MRS voxel.

6.3 Results

6.3.1 N-back performance

Participants performed well on both the 0-back and 2-back tasks, with scores of over 90% correct. This indicates that participants understood and engaged in the task. There were no differences in percent correct or reaction times between genotype groups as assessed with ANOVAs. Table 6.1 shows the mean scores of the two groups for the N-back tasks carried out during the MEG and fMRI sessions.

Table 6.1: Percent correct and reaction times on the N-back task for both genotype groups during the MEG and fMRI sessions. Values are means (SEM) with reaction times in ms. P indicates the significance level

	N-Back MEG			N-back MRI		
	AA (N=25)	CC (N=25)	p=	AA (N=24)	CC (N=25)	p=
0-back % correct	98.3 (0.87)	99.1 (0.78)	.516	99.0 (0.64)	99.6 (0.26)	.376
2-back % correct	95.2 (1.46)	94.9 (1.06)	.833	93.5 (2.51)	96.0 (1.90)	.420
0-back RT	506 (16.0)	532 (16.2)	.256	463 (15.8)	537 (13.9)	.657
2-back RT	603 (29.3)	643 (21.1)	.279	537 (25.3)	531 (23.5)	.865

6.3.2 Magnetic resonance spectroscopy

The DLPFC spectra were less consistent than those obtained from the occipital cortex. A representative spectrum as acquired with the SPECIAL MRS sequence is shown in Figure 6.1. We were able to obtain estimates of NAA and glutamate for all participants, but GABA could only be estimated for 40 participants. In the other cases, the Cramer-Rao bounds were >20% and therefore the estimates were unreliable. All metabolites were normalised to Cr+PCr. No differences in NAA (p=.761), glutamate (p=.119), or GABA (p=.243) concentrations were detected between genotype groups.

6.3.3 Magnetoencephalography

Figure 6.2 shows localization of activation in the different frequency bands at the sensor level for the 2-back versus 0-back contrast. Clear deactivations can be observed in the theta (6.2B), alpha (6.2C), and beta (6.2D) bands. These deactivations are most

prominent in posterior areas. Additionally, frontal activations were observed in the gamma (6.2A) and theta (6.2B) band, but these did not reach significance.

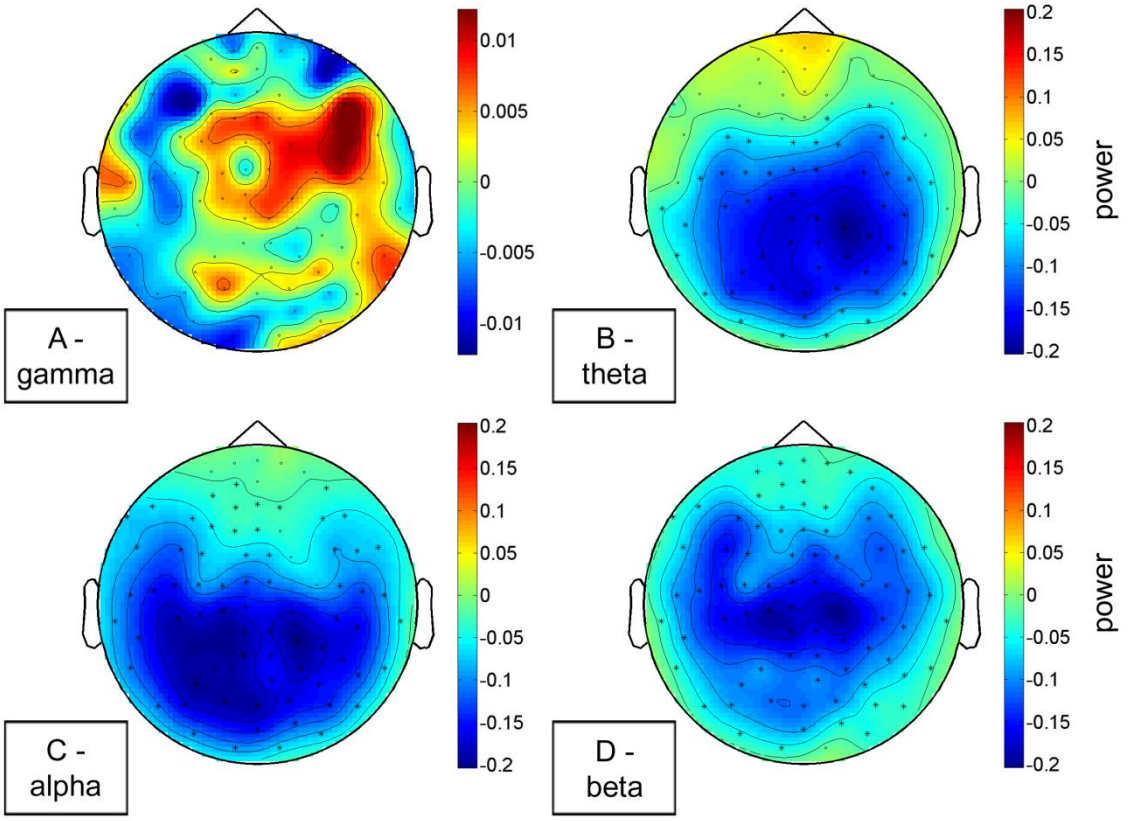

Figure 6.2: Sensor level activations for the 2-back>0-back contrast for the time window between 0.2 and 1.2s. Part A shows a hint of frontal activations in the gamma band (not significant); part B shows deactivation in the theta band with a hint of activation in medial frontal regions (not significant); part C shows deactivations in the alpha band; and part D shows deactivations in the beta band. The big black dots indicate sensors where there is a significant difference between the 2-back and 0-back conditions (smaller dots show sensors where there is no significant difference).

Figure 6.3 shows localization of activation in the different frequency bands at the source level for the 2-back versus 0-back contrast. A pattern similar to that seen at the sensor level was observed, with deactivations in the theta (6.3B), alpha (6.3C), and beta (6.3D) band. At the source level, the increase in theta power in frontal midline areas reached significance. However, gamma band power was not significantly different between the 2-back and 0-back conditions, but is plotted here to show a possible trend towards an increase.

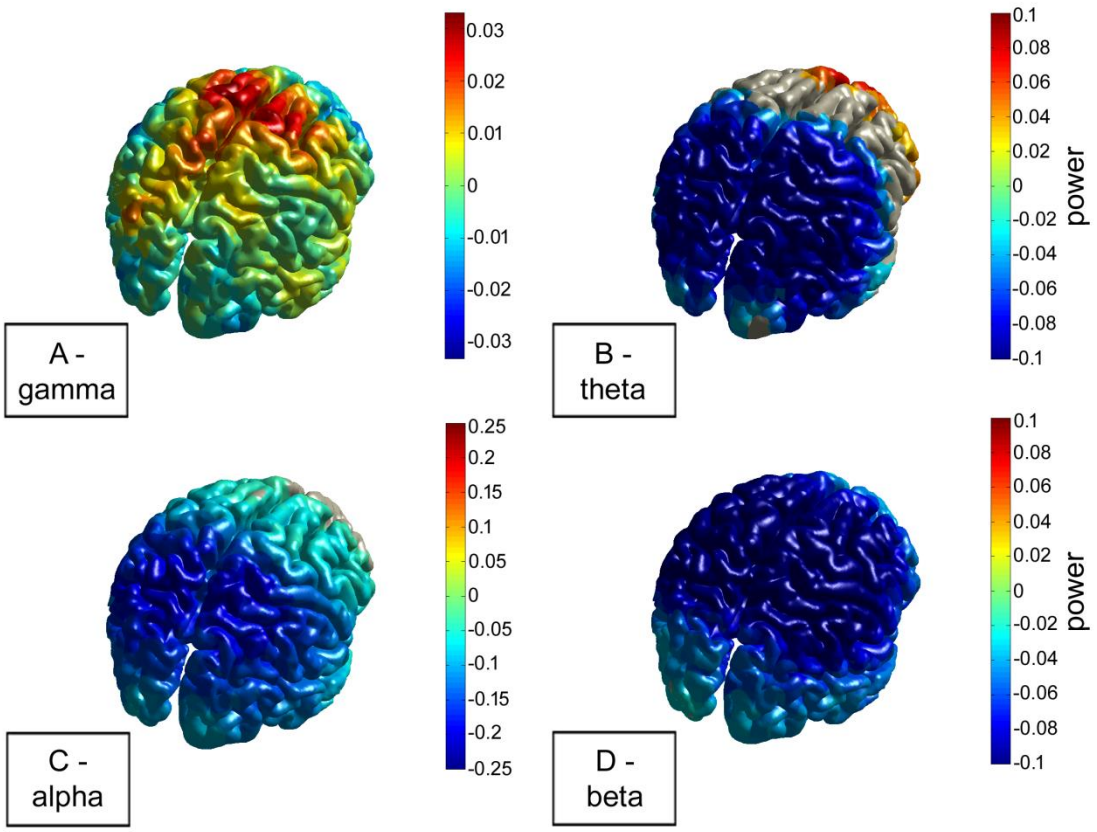

Figure 6.3: Source level activation for the 2-back>0-back contrast. Part A shows a hint of frontal activations in the gamma band (not significant); part B shows deactivation in the theta band together with activation in medial frontal regions ; part C shows deactivations in the alpha band; and part D shows deactivation in the beta band. In parts B, C, and D only significant differences have been plotted, whereas part A also shows differences that did not reach significance.

No differences between genotype groups were observed in the gamma, theta, and beta band at the level of the whole brain when studying activations in the 2-back > 0-back contrast. An effect was seen in the alpha band, with increased alpha power being observed in occipito-parietal regions in risk homozygotes. This between-group difference is depicted in Figure 6.4.

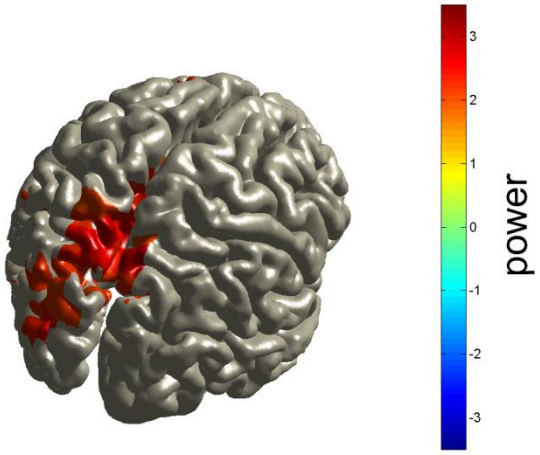

Figure 6.4: Effect of *ZNF804A* genotype on working memory related activation (2-back > 0-back). AA homozygotes showed more alpha power in occipito-parietal regions than CC homozygotes.

Given our a priori interest in prefrontal activation patterns, we carried out a region of interest analysis. Regions of interest were based on the location of the MRS voxel or on the peak of the activation observed in the DLPFC in the fMRI data. Figure 6.5 shows time-frequency representations for two of these regions of interest (left and right DLPFC based on BOLD activation pattern) for high and low frequencies separately. In these plots, zero represents the time of stimulus presentation. In the gamma band, a slight increase in power can be seen at this point, particularly in the right DLPFC (upper right part of figure 6.5). In the theta band, a decrease in power was observed (lower part of figure 6.5).

Given that no increase in theta could be detected in our regions of interest during stimulus presentation, gamma peak frequency and amplitude were compared between genotype groups. Frequency and amplitude were extracted for the location of the MRS voxel, and for the left and right prefrontal areas that were activated in the fMRI study. No differences between the genotype groups were detected in peak frequency or amplitude (gamma peak frequency left ROI, p=.942; gamma amplitude left ROI, p=.433; gamma

peak frequency right ROI, p=.520; gamma amplitude right ROI, p=.619; gamma peak frequency MRS ROI, p=.868; gamma amplitude MRS ROI, p=.862).

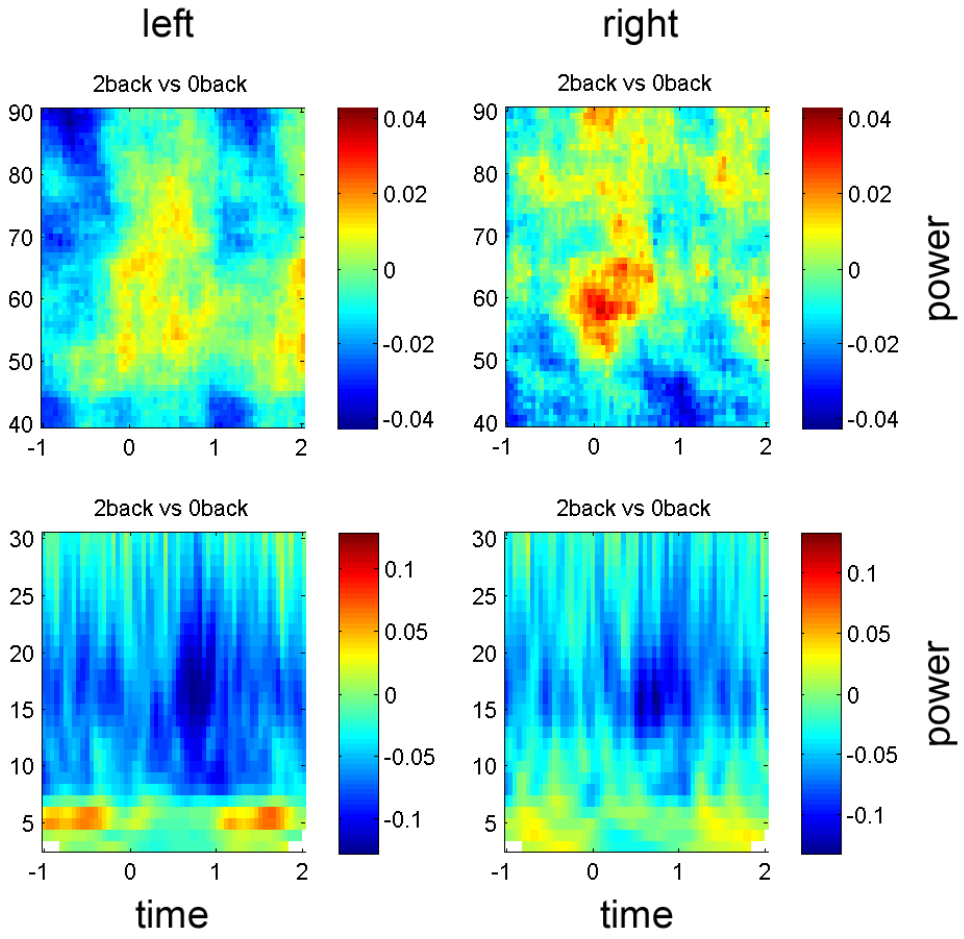

Figure 6.5: Time-frequency representations for the regions of interest based on the DLPFC activation patterns observed in the fMRI experiment. The two higher graphs show the higher frequencies, with activation in the left hemisphere on the left side and activation in the right hemisphere on the right side. A small increase in gamma power can be seen around the time of stimulus presentation (t=0). The two lower graphs show the lower frequencies, with activation in the left hemisphere on the left side and activation in the right hemisphere on the right side. There is a decrease in theta power in the retention period (t>0).

6.3.4 Functional magnetic resonance imaging

The working memory task activated (2-back > 0-back) a widespread network encompassing the bilateral DLPFC, inferior frontal cortex, inferior and superior parietal regions, intraparietal sulcus, precentral gyrus, and thalamus. Deactivations (0-back > 2-back) were observed in the superior medial frontal cortex, as well as in the posterior

cingulate, insula, and middle temporal, including parahippocampal, areas. These patterns of activation are depicted in Figure 6.6.

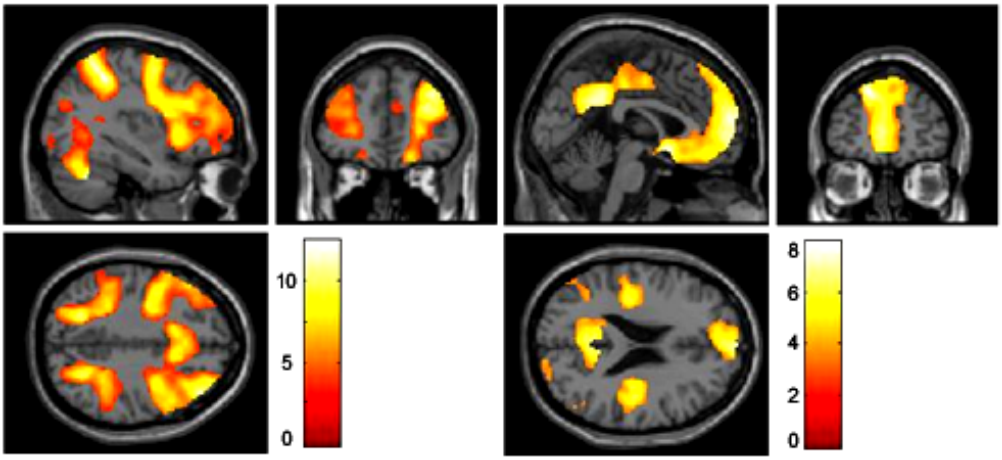

Figure 6.6: Patterns of activation observed during the N-back working memory task. The left hand panel shows an increase in activation with increased working memory load in a network including the DLPFC, inferior frontal cortex, and IPL ($p<.05$ FWE-corrected). The right panel shows the areas that become deactivated with increased working memory load, including superior medial frontal cortex, the posterior cingulate, insula, and medial temporal areas ($p<.001$, uncorrected).

No significant effect of the rs1344706 risk allele on working memory-related neural activation was observed for the whole brain at $p<.05$ (FWE-corrected), nor when small volume corrections were applied to the DLPFC.

6.3.5 Connectivity

The PPI group analysis indicated that a negative coupling exists between the right DLPFC seed region and the left hippocampus (SVC, peak voxel [-20 -36 6], $p=.019$). Additionally, we found positive coupling between the right DLPFC and the left middle frontal gyrus (SVC, peak coordinates [-44 18 26], $p=.037$). We found no evidence of connectivity between the right DLPFC and other brain regions.

We did not find a significant effect of rs1344706 genotype on functional connectivity at thresholds corrected for multiple comparisons in a whole brain analysis or in the ROI analyses. In an exploratory analysis, we therefore lowered the statistical

threshold and also examined the effects of rs1344706 genotype on functional connectivity at an uncorrected level (p<.05) within ROIs that were in line with our a priori hypothesis (left and right hippocampus, left prefrontal areas). This revealed an effect of rs1344706 on coupling between the right DLPFC and left hippocampus, with risk homozygotes displaying increased connectivity (Figure 6.7).

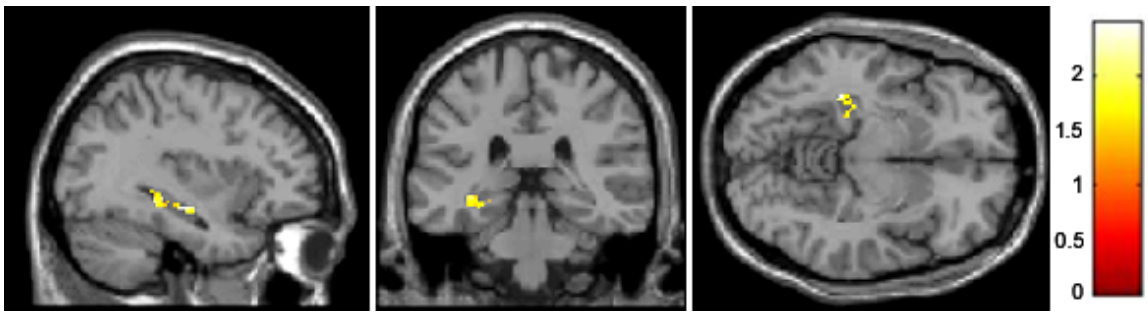

Figure 6.7: Effect of *ZNF804A* genotype on functional coupling as measured by PPI analysis. AA homozygotes show increased connectivity between the right DLPFC and left hippocampus compared to CC homozygotes. Contrast AA>CC, peak activation at [-34, -20, -12], within hippocampal mask significant at p<.05 uncorrected.

Table 6.2: MNI coordinates of voxels where there was increased coupling with the right DLPFC in *ZNF804A* risk allele homozygotes. The hippocampus and prefrontal ROIs were analysed at a p<.05 uncorrected threshold. Coordinates reported that are not in the aforementioned ROIs were analysed at the whole brain level, using a threshold of p<.001 uncorrected.

	MNI Coordinates				
	X	**Y**	**Z**	**Cluster size**	**P**
Left hippocampus	-34	-20	-12	14	0.009
	-36	-34	-8	10	0.011
	-28	-30	-12	3	0.027
Right hippocampus	38	-32	-8	5	0.036
	32	10	-16	3	0.001
Left Parahippocampal gyrus	-22	26	18	14	0.000
Right inferior temporal gyrus	52	-42	-12	13	0.001
Left Angular gyrus	-56	-60	34	13	0.000
Left superior temporal gyrus	-40	-30	12	16	0.000
Right angular gyrus	44	-72	40	3	0.001

Additionally, we carried out an exploratory whole brain analysis with thresholds set at p<.001 uncorrected. Table 6.2 reports coordinates where an effect of rs1344706 on coupling with the right DLPFC could be detected, with AA homozygotes showing more connectivity than CC homozygotes. No significant activations were detected in the CC vs. AA contrast.

6.3.6 Correlations

We found no evidence in favour of a correlation between BOLD activity in the left DLPFC and GABA (r=.111, p=.507), glutamate (r=-.186, p=.206), or NAA (r=-.155, p=.294) measured from a voxel in the left DLPFC. We also did not detect any correlations between gamma peak frequency and GABA (r=-.216, p=.187), glutamate (r=-.154, p=.290), or NAA (r=-.125, p=.394) or between gamma amplitude and GABA (r=-.170, p=.300), glutamate (r=.089, p=.541), or NAA (r=-.023, p=.875) measured from the same location in the left DLPFC. Lastly, there were no correlations between BOLD activation in the left DLPFC and gamma peak frequency (r=.041, p=.780) or gamma amplitude (r=.042, p=.776) measured from the same location in the left DLPFC; this was also true for activations measured in the right DLPFC, with no correlation being observed between the peak of the BOLD activity and gamma peak frequency (r=.136, p=.353) or gamma amplitude (r=.181, p=.213).

6.4 Discussion

In this study, we investigated the effect of rs1344706 on prefrontal function in healthy volunteers, using three different neuroimaging methods. We found no effect of the risk genotype on NAA, glutamate, and GABA concentrations in the DLPFC. Also in the MEG study, there was no effect of rs1344706 on prefrontal oscillations in any of the

frequency bands analysed. A difference between genotype groups was detected in occipito-parietal regions, with increased alpha band power in the AA group. As in other studies (Esslinger et al., 2009; 2011), our fMRI study revealed no effect of genotype on working memory related DLPFC activation. Our data show the previously described alteration in functional coupling between the right DLPFC and left hippocampus, albeit weaker than in some of the other studies (Esslinger et al., 2009; Rasetti et al., 2011).

The patterns of activation seen in our fMRI N-back dataset were comparable to results from other studies. No effects of rs1344706 on working memory related activation in the DLPFC were observed, nor in any other brain regions. As in the study by Paulus et al. (2013b), we could not replicate the previously reported alteration in connectivity between the DLPFC and hippocampus at thresholds corrected for multiple comparisons. However, both in their study and in ours, the effect could be seen when the threshold was lowered and the effects of rs1344706 were examined at uncorrected levels. In line with the initial finding by Esslinger et al. (2009), coupling was increased in double risk allele carriers. With increased working memory load, the DLPFC and hippocampus have been shown to decouple, in order to facilitate working memory related processing. In schizophrenia patients, coupling between the DLPFC and hippocampus persists (Meyer-Lindenberg et al., 2005), as has now also been observed for healthy subjects carrying two adenine alleles at rs1344706.

The first reason we did not replicate the effect of rs1344706 on functional connectivity when correcting for multiple comparisons might be the sample size of our study. In recent years, it has become apparent that even though effects of the gene may be more penetrant at the level of brain function, large sample sizes are important to detect effects of risk genes reliably (Munafo et al., 2008; Mier et al., 2010). We tried to maximise our power by specifically recruiting risk and non-risk homozygotes, and the sizes of these

groups in our study were comparable to those in other studies (Rasetti et al., 2011: 14 CC and 37 AA; Paulus et al., 2013b: 21 CC and 27 AA). Nevertheless, a larger sample size would have increased power, potentially allowing us to detect effects of rs1344706 when correcting for multiple comparisons. Additionally, we used a different type of N-back task than Esslinger et al. (2009; 2011) and Rasetti et al. (2011). In our study, stimuli were presented sequentially and participants only had to respond when a target appeared. In these other studies, several stimuli were presented simultaneously and a response was required on every trial. This more complicated task might have led to greater demands on executive processes and more working memory related activations, providing greater sensitivity to detect genotype effects. Furthermore, whereas Rasetti et al. (2011) also used a psycho-physiological interaction analysis to study the effects of *ZNF804A* genotype on functional connectivity, other studies to date carried out a seeded connectivity analysis without including a task parameter (Esslinger et al., 2009; 2011; Paulus et al., 2013b). PPI analyses test whether the correlation in activity between two distant brain areas is different in different psychological contexts, and therefore, whether there is an interaction between the psychological state and the functional coupling between two brain areas (O'Reilly et al., 2012). The seeded connectivity analysis as used by Esslinger et al. (2009; 2011) and Paulus et al. (2013b) only assesses correlations between the time courses of different brain regions. It is conceivable that some brain regions will share a time-course of activity with the seed region because regions are anatomically connected, share the same neuro-modulatory influences, or share sensory input. In all these cases, regions will all have correlated time-courses regardless of the experiment itself. Therefore, directly studying correlations between brain regions might be a less stringent way to study connectivity and effects of a risk gene on working memory related connectivity.

Whereas it is well established that increasing working memory load in an N-back task leads to increased DLPFC activity as measured with fMRI (Owen et al., 2005), very few studies to date have measured working memory related brain activity in a MEG study using the N-back task (Ciesielski et al., 2010). Therefore, it is not known whether gamma band power increases in the DLPFC can be measured during the N-back task. In our study, we observed a small increase in gamma band power in frontal areas, but this was not consistently seen in all participants, making it difficult to assess the effects of rs1344706. Given the positioning of the MEG coils, activity in the DLPFC is more difficult to measure than activity in posterior regions. This, in combination with the fact that power decreases when frequency increases, might have contributed to the weak gamma signal in prefrontal regions. Most of the studies that have reported increased gamma with increasing working memory load have used a delayed match-to-sample task (Tallon-Baudry et al., 1998; Palva et al., 2010; Roux et al., 2012), suggesting that this might be a more appropriate task when studying gamma oscillations in prefrontal regions. We did detect an effect of *ZNF804A* genotype on alpha band power in occipito-parietal regions, which was significant when correcting for multiple comparisons. No other studies have reported effects of rs1344706 in this region, but our study described in chapter 7 also suggests possible differences in this area.

ZNF804A genotype was not associated with NAA, glutamate, and GABA levels in the DLPFC. As discussed in section 6.1.4, there is only limited evidence for the use of MRS measures as intermediate phenotypes when studying schizophrenia risk genes, because alterations might be related to the disease state and/or use of medication. However, a few recent studies have found risk genes to have an effect on NAA and glutamate (Stern et al., 2008; Gruber et al., 2012; Wirth et al., 2012), suggesting it is possible to detect effects of polymorphisms on metabolites measured with MRS. As

mentioned in the discussion of chapter 5, the sequence and analysis methods used for this study are relatively new (Near et al., 2013) and have not been extensively assessed for use in the DLPFC. Therefore, it is conceivable that the method used here was not the most sensitive for detecting differences between concentrations of metabolites of interest in the DLPFC.

As in chapter 5, we did not observe any correlations between prefrontal BOLD, prefrontal gamma, and prefrontal GABA, glutamate, and NAA concentrations. Reasons why MRS might not be the most optimal tool to assess GABA and glutamate functioning have been described in the discussion of chapter 5. Given that we did not detect any clear working memory related prefrontal activation patterns in our MEG study, it was unlikely that we would find correlations with BOLD activations as measured by MRI. Other tasks or analysis methods might be required to assess such correlations.

The multimodal imaging study described in this chapter was designed to allow acquisition of corroborative evidence about the effects of *ZNF804A*. However, because of this goal, the study was very complex. Initial analyses have been carried out addressing our initial questions and hypotheses, but the data have not yet been fully explored. Therefore, it seems early to conclude that in our data set, *ZNF804A* genotype does not affect NAA, glutamate, and GABA, or oscillations in prefrontal regions. More sensitive analyses might still reveal differences based on rs1344706. Due to time constraints and the complexity of the dataset, these could not be carried out within the framework of this thesis. However, we did detect a previously reported alteration in prefrontal-hippocampal coupling in the fMRI data, which suggests that it will be of interest to continue the investigation of underlying mechanisms.

Chapter 7 - The effect of *ZNF804A* genotype on resting state networks

7.1 Introduction

7.1.1 Resting state networks

In early functional magnetic resonance imaging studies, it became apparent that even when the brain is at rest, meaningful patterns of activation still occur (Raichle et al., 2001). Biswal et al. (1995) were the first to show that spontaneous fluctuations in different parts of the brain are temporally correlated. Several networks have since been identified, and these distinct networks can be separated because they all have their own specific temporal characteristics (Cordes et al., 2000; Beckmann et al., 2005). An early combined MRI-EEG study (Goldman et al., 2002) showed that variation in EEG rhythms is correlated with the fMRI measurements, which suggests a neuronal basis for the fluctuations. Resting state networks (RSNs) jointly characterise the neuronal baseline activity of the human brain in the absence of deliberate and/or externally stimulated neuronal activity, and reflect functionally distinct networks (Beckmann et al., 2005). Next to task-positive networks, which consist of brain regions usually activated in response to stimuli, a task-negative network, which deactivates during tasks, was also discovered. Usually called the default-mode network (DMN), it includes medial frontal (including anterior cingulate), parietal (including posterior cingulate, precuneus and inferior parietal) and medial temporal (including hippocampus) areas of the brain (Raichle et al., 2001; Fox et al., 2005).

Independent component analysis is one of the methods that has been most successfully applied to the estimation of the low-frequency patterns making up RSNs (Goldman & Cohen, 2003; Beckmann et al., 2005), because it has the ability to identify various types of signal fluctuations by virtue of their spatial and/or temporal characteristics without the need to specify an explicit temporal model. It has been shown that the patterns

of activity measured in the resting brain with ICA are fairly consistent across sessions and subjects (Damoiseaux et al., 2006). More recently, it was also shown that RSNs measured with ICA correspond to the functional networks used by the active brain when engaged in a comprehensive set of task types (Smith et al., 2009), which confirms the validity of the approach. Importantly, not only do resting state networks provide information about how the healthy brain functions, they have also been shown to be of clinical value in studies investigating abnormalities in neurological and psychiatric diseases.

7.1.2 Schizophrenia and resting state networks

According to the dysconnectivity hypothesis of schizophrenia, the disorder is associated with abnormalities in neuronal connectivity (Friston & Frith, 1995; Bullmore et al., 1997; Friston, 1999) which result from a combination of genetic and environmental risk factors that affect normal brain development (Maynard et al., 2001; Karlsgodt et al., 2008). This may be one manifestation of changes observed in neuropathological studies, which show decreases in synaptic markers and cortical neuropil. Task-based approaches targeting a particular region of interest, such as the analyses discussed in chapter 6, can be used to assess such abnormalities in functional connectivity, but always require specific a priori hypotheses. However, investigations into RSNs, which are assumed to measure intrinsic properties of functional brain organization, do not require specific regions of interest, and provide a relatively hypothesis-free way of assessing possible changes in connectivity in schizophrenia.

As explained in previous chapters, I will discuss findings observed in schizophrenia patients because these provide an indication of possible intermediate phenotypes. In general, studies seem to report a decrease in connectivity in schizophrenia patients compared to healthy controls (Fornito & Bullmore, 2010). However, results are

not always consistent, with some studies reporting increased connectivity between key RSNs in schizophrenia (Jafri et al., 2008). Another reasonably consistent finding is that schizophrenia patients have difficulties deactivating the default mode network (Williamson & Allman, 2012). However, both increased and decreased connectivity have been reported within the default-mode network, perhaps reflecting reduced distal and enhanced local connectivity in cognitive control networks in schizophrenia patients (Repovs et al., 2011). Because simply measuring RSNs has not clearly shown which networks are abnormal in schizophrenia patients, a recent study developed a classification algorithm that used RSN connectivity to differentiate between groups with an accuracy of 75% (Venkataraman et al., 2012). Relative to controls, schizophrenia patients exhibited co-existing patterns of increased connectivity between parietal and frontal regions, and decreased connectivity between parietal and temporal regions, and between the temporal cortices bilaterally. Resting state connectivity patterns have also been shown to be associated with specific symptomatology, with, for example, an increase in hippocampal-prefrontal connectivity in patients who have visual hallucinations (Amad et al., 2013). Altered resting state connectivity can already be detected in drug-naïve first-episode patients, specifically in fronto-parietal and default mode networks (Ren et al., 2013), indicating that these alterations are not just related to long-term illness or use of medication. Taken together, these studies indicate that there are abnormalities in resting state networks in schizophrenia, but the inconsistent findings do not allow clear predictions.

7.1.3 Genetic influences on resting state networks

Establishing the heritability of functional connectivity and RSNs makes it possible to use resting state networks as intermediate phenotypes in the search for the genetic roots

of illnesses that have been associated with altered connectivity patterns, such as schizophrenia (Glahn et al., 2010). To date, no gene discovery experiments (e.g. linkage or GWAS) have been reported using resting state functional MRI or PET derived traits (Thompson et al., 2013). However, there is substantial evidence that RSNs are heritable. In 333 subjects, Glahn et al. (2010) found that ~40% of the between subject variance in functional connectivity within the default-mode network is under genetic control. Although neuroanatomical variation in this network was also heritable, the genetic factors that influenced default-mode functional connectivity and grey matter density seem to be distinct, suggesting that unique genes influence the function of the network. Fornito et al. (2011) developed optimised cost-efficiency networks from resting state functional MRI data in 58 healthy twins (16 monozygotic pairs and 13 dizygotic pairs).While there was little evidence for genetic control of BOLD signal fluctuations in the 0.02–0.04Hz, 0.04–0.09Hz, or 0.18–0.35Hz ranges, the heritability estimate for network connectivity in the 0.09–0.18Hz range was h2 = 0.60, suggesting substantial heritability. Van den Heuvel et al. (2013), using 21 monozygotic and 22 dizygotic healthy twin-pairs, also reported significant heritability (h2 = 0.42).

In addition to establishing heritability, several studies have also compared schizophrenia patients, first-degree relatives, and healthy controls to assess the use of resting state networks as an intermediate phenotype. Meda et al. (2012) and Khadka et al. (2013) studied the same group of schizophrenia patients with their first-degree relatives and compared their activity in RSNs to that of 118 healthy controls. Using functional network connectivity analysis, Meda et al. found no abnormalities in RSNs that were shared between schizophrenia patients and their relatives. However, Khadka et al., who used ICA, showed that abnormalities in fronto-occipital, frontal-thalamic-basal ganglia, and sensorimotor networks during rest were shared by schizophrenia patients and their

relatives. Liu et al. (2012) tested 25 schizophrenia patients and their siblings and found that they share increased resting state connectivity in the task-negative (default-mode) network, but not in task-positive networks.

Some initial studies have provided evidence for the effect of specific genes on resting state networks. Both Filippini et al. (2009) and Trachtenberg et al. (2012) have shown that *APOE* genotype affects resting state networks. Tunbridge et al. (2013) showed an effect of *COMT* genotype, another candidate gene for schizophrenia, on connectivity in the prefrontal cortex during rest. These studies indicate that resting state networks can be studied as an intermediate phenotype for schizophrenia.

7.1.4 MEG resting state networks

The spontaneous fluctuations that underlie resting state networks, as identified using fMRI, can also be detected with MEG. de Pasquale et al. (2010) showed that seed-based connectivity measures give similar networks to those measured with MRI, with the added advantage that it is possible to assess which frequency underlies activity in a particular network (Hillebrand et al., 2012). Additionally, MEG provides a more direct measure of neuronal activity, resolving questions about the physiological mechanisms underlying resting state networks. Brookes et al. (2011b) implemented independent component analysis for MEG data, making it possible to assess resting state networks in MEG data without any prior assumptions about spatial locations and patterns of the networks. In their study, they compared MEG and MRI data and showed that this analysis method gives a similar pattern of networks in MEG and MRI datasets. This approach has now also been adapted to test for between-group differences in resting state networks (Luckhoo et al., submitted) using a dual regression approach on spatial basis sets, which can be derived from both MEG and fMRI data. A first study has applied this method to

assess the effects of APOE on resting state networks (Heise et al., in prep.) and found effects similar to those reported in fMRI studies.

Independent component analysis of resting state networks provides a hypothesis-free way of assessing potential differences in connectivity between groups. It has been shown that schizophrenia is associated with alterations in functional connectivity and initial neuroimaging studies of *ZNF804A* also indicate that rs1344706 might affect functional connectivity, as discussed in chapter 6. Therefore, we studied the effect of *ZNF804A* genotype on resting state networks measured by MEG using the methods as developed by Brookes et al. (2011b) and extended by Luckhoo et al. (submitted). We specifically compared risk homozygotes with non-risk homozygotes to maximise the chances of detecting differences between genotype groups. Based on the initial *ZNF804A* studies discussed in chapter 6, we hypothesised that changes might occur in networks involving prefrontal or medial temporal cortices.

7.2 Methods

7.2.1 Data acquisition

During the measurement of resting state activity, participants (n=50, with 25 AA homozygotes and 25 CC homozygotes, described in more detail in chapters 5 and 6) were seated in the MEG scanner. They were asked to keep their eyes open and to fixate on a white cross in the centre of a grey screen. Resting state activity was measured for 6 minutes. Whole-head MEG recordings were acquired using the Elekta NeuroMag MEG System. Data from both the 204 gradiometers and the 102 magnetometers were analysed. The signal was digitised at a sampling rate of 1000Hz, with a high-pass filter of 0.03Hz and a low-pass filter of 330Hz. A magnetic digitizer (Polhemus FastTrach 3D) was used to measure the relative positions of four head-position indicator coils and three anatomical

landmarks (nasion, left and right auricular points). These coordinates were used for coregistration of the sensor montage to the participant's structural MRI scan.

7.2.2 Preprocessing

For this dataset, MEG data analysis was carried out using the MATLAB-based toolbox Statistical Parametric Mapping 8 and OHBAs Software Library (OSL). OSL contains a specific resting state analysis pipeline. The preprocessing pipeline consisted of the following steps. First, channels containing excessive noise were identified manually in OSLview, before applying MaxFilter 2.2, a tool provided by Elekta, with signal space separation and movement compensation (Taulu et al., 2004). MaxFilter separates signal from sources outside the helmet and thereby reduces noise from external sources. Additionally, MaxFilter processes the continuous head positioning measurements and uses these to compensate for the effects of head movement. After applying MaxFilter, the data were downsampled to 250Hz and epochs containing artefacts associated with body movement or external sources were removed manually. A semi-automatic artefact rejection method was applied using independent component analysis that identified noise components associated with line noise (50Hz), eyeblinks, and heartbeat. Additionally, all components were inspected manually and based on their spatial topography, timecourse and frequency spectrum, it was decided whether these components represented noise and had to be removed from the data. The last steps of preprocessing consisted of applying a high-pass filter at 1Hz to remove low-frequency fluctuations and carrying out a further manual check of the data to remove epochs with artefacts that were still present after the other artefact removal steps.

7.2.3 Source reconstruction

The source reconstruction of MEG data consisted of several steps. First, the subject's headshape, measured with the Polhemus Isotrack, was co-registered to the structural MRI and to the MNI template brain using an automatic algorithm implemented in OSL. An overlapping local spheres forward model implemented in FieldTrip was chosen as head model to define the head shape of each subject (Huang et al., 1999). The forward model was then used to calculate lead fields, in order to model the MEG signal at each grid point. Subsequently, as in the analysis described in chapter 5, a linearly constrained minimum variance beamformer was applied (Van Veen et al., 1997; Woolrich et al., 2011). MEG data in different frequency bands of interest (alpha (8-12), theta (4-8), beta (13-30), and broadband (4-30Hz)) were projected into source space. For each 6x6x6mm voxel, a time course of oscillatory activity in the frequency band of interest was computed.

7.2.4 Hilbert enveloping and ICA

Following application of the LCMV beamformer, a Hilbert transform was applied to each voxel time course to derive the amplitude of oscillatory activity, termed the Hilbert envelope. The envelope was downsampled temporally by dividing each envelope time course into 2s non-overlapping windows and averaging the data within those windows. This has consistently been shown to be a robust way of detecting stationary functional connectivity (Brookes et al., 2011a; Brookes et al., 2011b; Luckhoo et al., 2012). Envelope data were spatially smoothed with a 4mm Gaussian kernel and the voxel size was resampled to an 8mm grid. Data were transformed to MNI space using FLIRT before datasets from all subjects were temporally concatenated. After Hilbert enveloping, the MEG data were analysed using two different spatial basis sets. First, ICA was run on the

MEG data across all subjects to decompose the concatenated envelopes into 25 temporally independent timecourses (implemented using fastICA) (Hyvarinen, 1999) which generated 25 resting state networks. This number was chosen based on pilot studies carried out at OHBA. Additionally, a set of RSN ICA maps based on fMRI datasets (Smith et al., 2009) was used for comparison purposes and to look at potential genotype differences within these networks. For both approaches, a frequency band of 4-30Hz was chosen. Again, pilot studies at the Oxford Centre for Human Brain Activity have shown that analysis of this frequency band gives the most reliable networks. Also, a previous study has reported that higher frequencies (30-60Hz) are least optimal for detecting functional connectivity (Luckhoo et al., 2012). Furthermore, we investigated the three frequency bands contained within this broadband analysis, theta, alpha, and beta, separately to assess the contribution of each of these bands to potential differences between *ZNF804A* genotype groups. These analyses were carried out within the MRI spatial basis set.

7.2.5 Regression

To compare the two genotype groups, the between-subject analysis of the resting data was carried out using a regression technique that allows for voxel-wise comparisons of MEG data. Using a dual-regression approach, the subject-specific spatial maps were estimated by using the time-course of the ICA maps in a linear model fit against the subject's MEG dataset. A voxel-wise general linear model was applied using non-parametric permutation testing with 5000 permutations and correcting for multiple comparisons across space using Threshold-Free Cluster Enhancement (TFCE). A difference between groups was considered significant if the networks differed at $p<.05$.

7.3 Results

7.3.1 Resting state networks in the 4-30Hz range

Of the 25 components generated in the ICA analysis, 15 were non-overlapping and are presented in Figure 7.1. We observed the following components: a frontal component, a fronto-parietal component, right and left auditory components, right and left parietal components, a posterior cingulate cortex component, an executive control component, a sensori-motor component, a motor component, a medial visual component, a visual component located in the occipital pole, right and left medial temporal lobe components, and a cerebellar component. The prefrontal, PCC, parietal, and medial temporal lobe components generally appear in fMRI studies as one component representing the default-mode network.

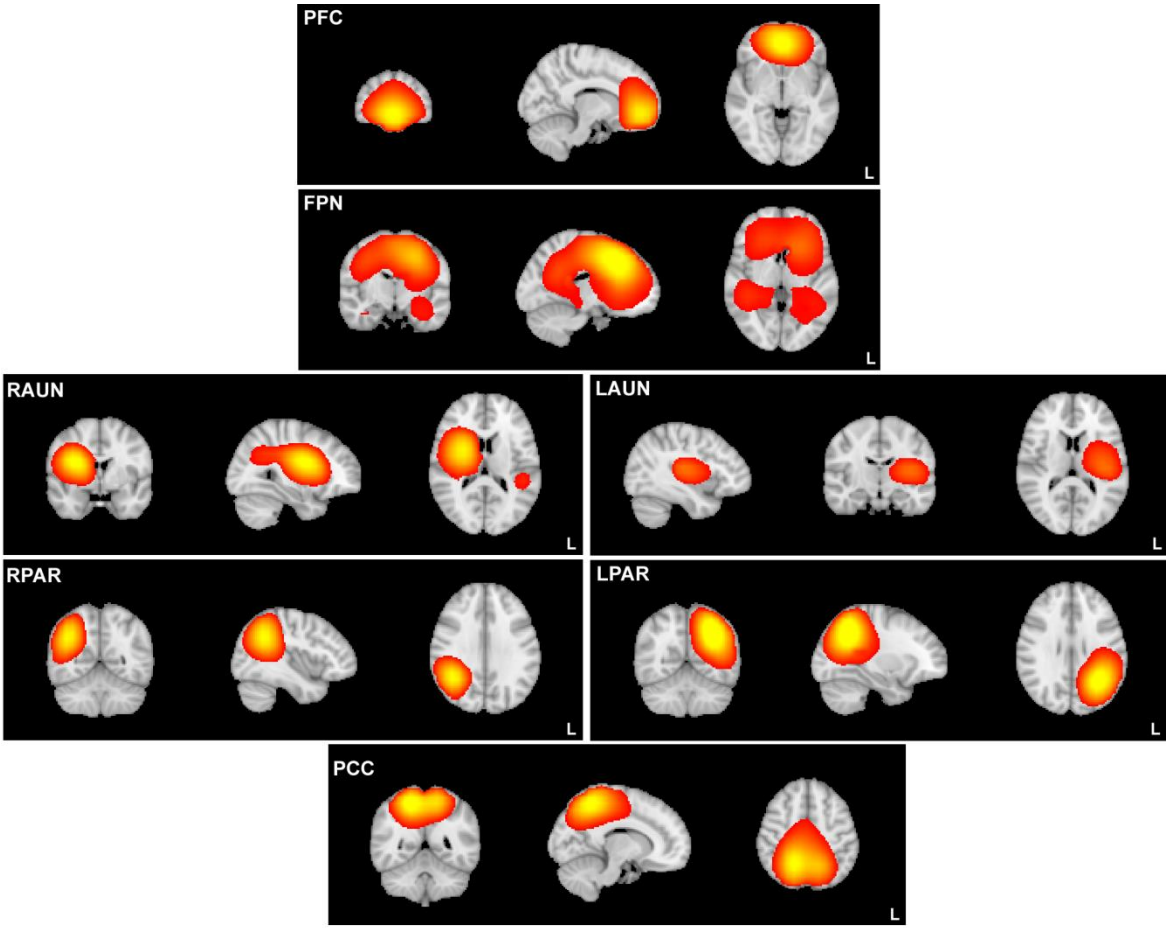

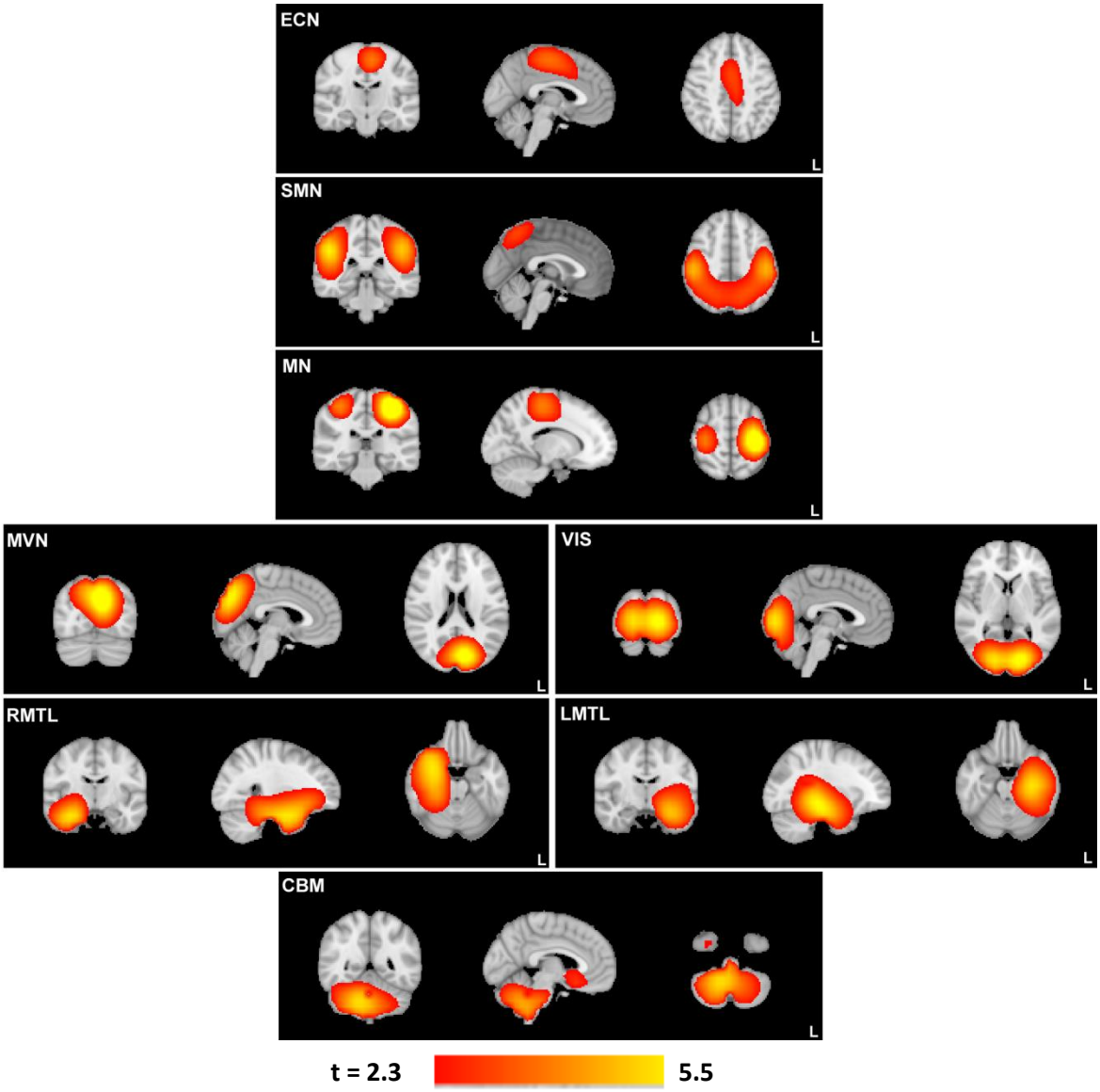

Figure 7.1: The MEG resting state analysis showed the following components: a frontal network (PFC), a fronto-parietal network (FPN), right (RAUN) and left (LAUN) auditory networks, right (RPAR) and left (LPAR) parietal networks, a posterior cingulate cortex network (PCC), a executive control network (ECN), a sensori-motor network (SMN), a motor network (MN), a medial visual network (MVN), a visual network located in the occipital pole (VIS), right (RMTL) and left (LMTL) medial temporal lobe networks, and a cerebellar network (CBM). The L indicates the left side of the brain. Images are thresholded at t>2.3.

7.3.2 Effects of *ZNF804A* genotype on resting state networks

The between genotype group comparison carried out within the 25 MEG components we observed in the 4-30Hz range indicated that there were three components that were affected by rs1344706. These components are depicted on the left side of Figure 7.2. In all three networks, there was evidence of increased connectivity for CC

homozygotes compared to AA homozygotes. An additional analysis using a spatial basis set consisting of fMRI-based RSNs was carried out and indicated genotype differences within the same three networks (right side of Figure 7.2).

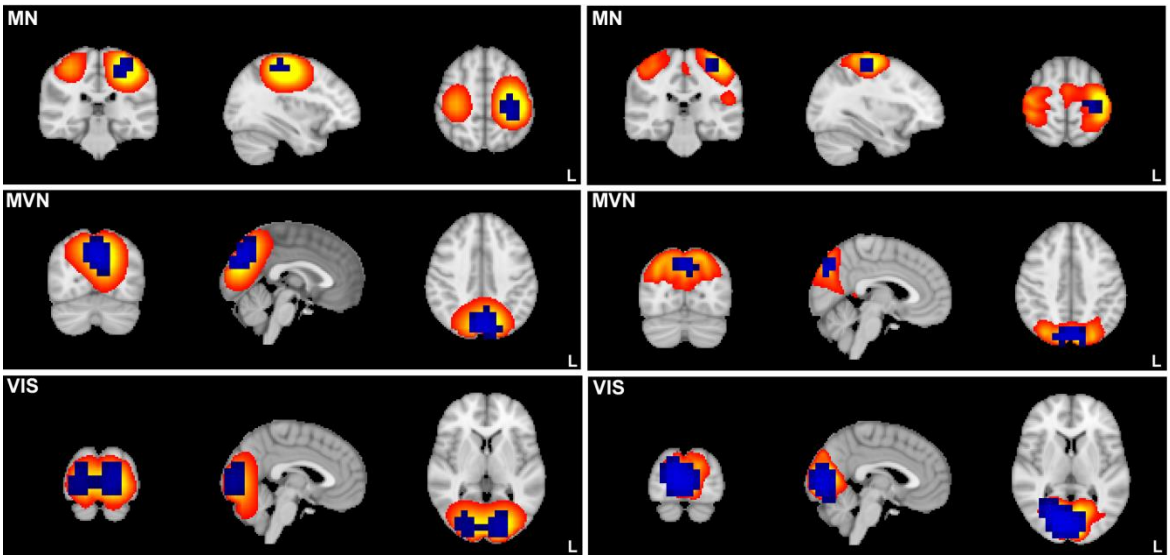

Figure 7.2: Genotype differences within RSNs. Non-risk homozygotes showed more connectivity within three networks: the motor network, the medial visual network, and the visual network in the occipital pole. The left panels show the analysis within the networks presented in Figure 7.1, with the panels on the right showing the analysis within the spatial basis set of fMRI networks. Blue indicates significant genotype differences at $p<.05$.

7.3.3 Alpha and beta analysis

Separate analyses were carried out per frequency band to establish which frequency band was the main contributor to the observed genotype differences. These analyses were done within the spatial basis set consisting of fMRI networks. We found that the observed difference within the motor network was mainly due to differences within the beta band, whereas the observed effects in the two posterior components were mainly due to differences in the alpha band. These results are depicted in Figure 7.3.

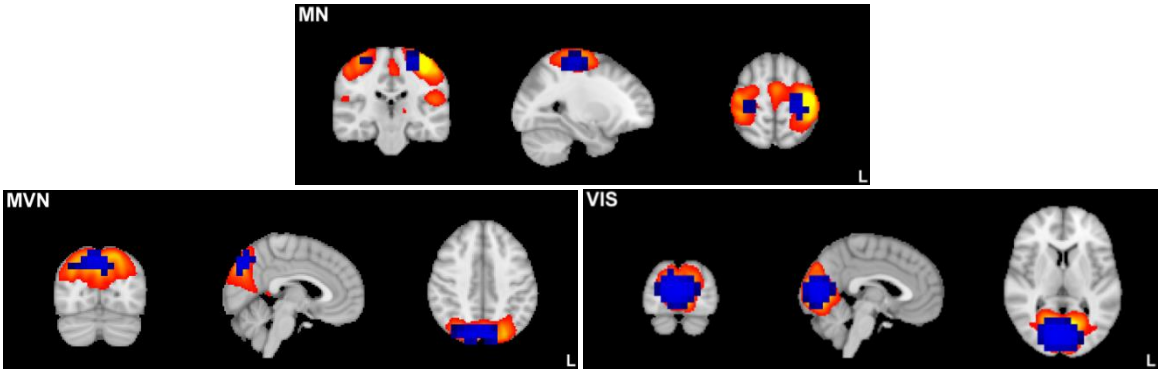

Figure 7.3: The observed genotype differences depicted in Figure 7.2 can be narrowed down to specific frequency bands. The effect of rs1344706 on the motor network was due to an effect in the beta band, whereas the effects on the two occipital networks could be narrowed down to the alpha band. Blue indicates significant genotype differences at p<.05.

7.3.4 Theta analysis

Assessing the effects of rs1344706 on theta band activity within the spatial basis set of fMRI networks revealed a difference in the right hippocampus (Figure 7.4). Specifically, we found an increase in theta in the right hippocampus of CC homozygotes, indicating increased connectivity with the other structures in the medial temporal lobe network.

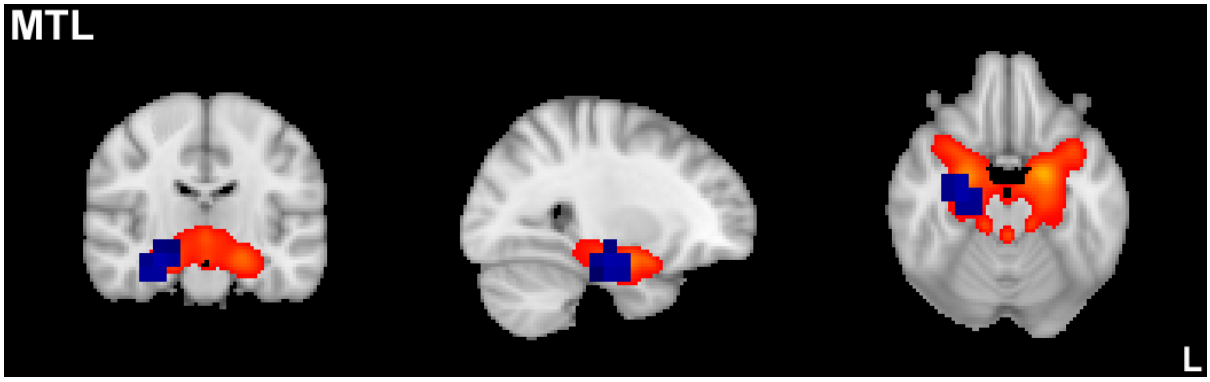

Figure 7.4: Rs1344706 affects connectivity within a hippocampal network, with non-risk homozygotes displaying more connectivity within the theta band. Blue indicates significant genotype differences at p<.05.

7.4 Discussion

In this experiment, we applied a novel analysis approach based on independent component analysis to assess resting state networks in an MEG dataset. Looking at the 4-30Hz range, we observed a set of components including prefrontal, fronto-parietal,

parietal, motor, auditory, executive, PCC, occipital, medial-temporal, and cerebellar networks which were similar to the networks observed by Brookes et al. (2011b), Luckhoo et al. (submitted) and Heise et al. (in prep.). We applied a dual regression approach to both those networks as well as to a general spatial basis set based on fMRI networks to assess differences associated with *ZNF804A* genotype. We observed differences in both motor and occipital areas, with CC homozygotes demonstrating more connectivity. Post-hoc tests revealed that occipital differences were caused by differences in the alpha band (8-12Hz), whereas the effects in the motor cortex could be narrowed down to the beta band (13-30Hz). Most notably, we found an effect of *ZNF804A* genotype on hippocampal connectivity in the theta band (4-8Hz), with non-risk homozygotes displaying more connectivity.

The finding that rs1344706 is associated with a change in connectivity in the hippocampus is particularly interesting given earlier findings from fMRI studies. Esslinger et al. (2009, 2011), Paulus et al. (2013b) and Rasetti et al. (2011) have all reported that *ZNF804A* genotype is associated with a change in hippocampal-prefrontal coupling during a working memory task. Even though we did not find a similar change in hippocampal-prefrontal coupling in our MEG data, the finding that the theta rhythm in the hippocampus is altered could provide a first clue as to the mechanisms that might underlie the previously observed alterations in hippocampal-prefrontal coupling. Whether hippocampal signals can be detected using scalp MEG has been a topic of debate, but the hippocampal theta rhythm was detected using MEG as early as 1997 (Tesche, 1997) and has been reported in many other studies, including other MEG studies (Tesche & Karhu, 2000; Cornwell et al., 2008; Quraan et al., 2011) and studies using intracranial recordings in humans (Axmacher et al., 2010; Foster & Parvizi, 2012) and animals (Jones & Wilson, 2005). More recently, Luckhoo et al (2012) have shown that the ICA method applied in this study is capable of

detecting hippocampal network activity. Hippocampal theta activity is thought to have an important role in cognitive processing (Tesche & Karhu, 2000; Cornwell et al., 2008) and particularly when coupled to prefrontal gamma (Colgin, 2011). Spiking of individual neurons in the prefrontal cortex has been shown to become entrained to the hippocampal theta rhythm (Hyman et al., 2011). The theta-entrained activity across cortico-hippocampal circuits is thought be important for information flow and guiding the changes that are believed to underlie the storage of information across these networks (Siapas et al., 2005). Several studies have suggested that this coupling between hippocampal theta and prefrontal gamma is disturbed in schizophrenia (Sigurdsson et al., 2010; Lisman, 2012).

The differences in connectivity we observed in motor and occipital components based on rs1344706 genotype are more difficult to explain. No studies to date have reported any functional or structural changes in these areas associated with rs1344706. However, no other studies looking at *ZNF804A* have used electrophysiological methods, so it is conceivable that these effects can only be picked up using MEG or EEG. The fact that the effects could be narrowed down to differences in the frequency bands that are generally most prominent in these areas (alpha in occipital regions and beta in motor regions) makes the findings more plausible. Given that we have two additional MEG datasets from the same subjects, it would be of interest to investigate whether similar differences can be observed in the other datasets. Initial analyses looking at power differences in the other datasets indicate that there might be a power difference in the alpha band in occipito-parietal regions.

At this point, it is difficult to be completely certain about the robustness of the findings, because the technique used here was developed very recently, and very few studies to date have applied it to between-group comparisons. Two important questions should be considered. First of all, how reliable are the networks that come out of the ICA

analysis, and secondly, how reliable is the comparison of the two genotype groups based on dual regression? Brookes et al. (2011b) validated the use of ICA for the detection of resting state networks and showed that these networks are comparable to the networks usually found in fMRI studies. Despite the good correspondence between networks, they also reported that the MEG networks are generally larger, possibly due to signal leakage, and have a lesser spatial resolution. This is also the case in our study, with our networks generally comprising less spatially separated areas than the networks observed in the Brookes et al. 2011a and 2011b study. This might be due to the use of a different MEG system, because their data were recorded with a CTF system instead of an Elekta system. Luckhoo et al. (submitted) addressed the validity of the dual regression approach by carrying out several simulations. They found that the procedure is robust against false positives and can accurately localise group differences and associate these with specific RSNs. However, complementary analyses are needed to elucidate the physiological basis of the observed differences. Additionally, it seems encouraging that an independent study assessing effects of another gene on connectivity within resting state networks found very similar networks and was able to detect previously reported genotype differences (Heise et al., in prep.).

Additional analyses, such as assessing differences in theta power in the hippocampus, might be necessary to elucidate the physiological basis of the observed effects. If the mean signal intensity and variance of the signal are found to be the same in both groups, then the finding can most likely be interpreted as a change in connectivity, with the right hippocampus being more connected with the rest of the MTL network in non-risk than in risk homozygotes. Furthermore, it would be interesting to carry out a seed-based connectivity analysis on the data to see if a similar pattern of connectivity is found; or whether it might even be possible to detect a genotype associated change in

connectivity between the hippocampus and DLPFC. Given that we also recorded an N-back working memory dataset using MEG, maybe the most interesting additional analysis would be to apply the same ICA analysis described here to the N-back data, which has previously been shown to be feasible (Luckhoo et al., 2012). If we find a similar change in the hippocampus in this independent dataset, it would provide convincing evidence that hippocampal connectivity in the theta band is associated with *ZNF804A* genotype.

Chapter 8 - General discussion

8.1 Summary of results

Rs1344706 in *ZNF804A* was the first SNP to show genome-wide significant association with schizophrenia, but when this thesis began, very little was known about the expression or function of the gene, or about the effects of the SNP. The main goal of this thesis was to investigate aspects of both these issues, in order to clarify the biological and pathophysiological significance of the genetic association to schizophrenia. To this end, I used both a genetic neuropathology and a genetic neuroimaging approach.

The first part of my thesis characterised ZNF804A expression in human brain and studied how this is affected by genotype and by diagnosis. In chapter 2, using western blotting and immunohistochemistry, I provided the first evidence that ZNF804A immunoreactivity is present in human brain. ZNF804A immunoreactivity could be detected in both adult and foetal human brain and was mainly localised to layer III pyramidal cells. This was true for all cortical regions studied. Within the cell, we observed granular staining throughout the cytoplasm. In chapter 3, I compared ZNF804A mRNA and immunoreactivity in schizophrenia with expression in healthy controls, and between risk and non-risk allele carriers at rs1344706 using qPCR and immunohistochemical techniques. No differences were observed between risk and non-risk carriers or between cases and controls, at both the mRNA and protein level.

The second question I addressed, using both volumetry and voxel-based morphometry, is whether *ZNF804A* genotype affects macroscopic brain structure. In chapter 4, in collaboration with the Donders institute (Nijmegen, the Netherlands), I investigated a large structural MRI dataset of 922 healthy volunteers to assess effects of rs1344706 on total brain volume, grey and white matter, and several cortical and

subcortical regions of interest. No effect of rs1344706 could be detected at the whole brain level, nor on any of the regions of interest.

In the last chapters of my thesis, I studied the functional correlates of rs1344706 genotype in the living human brain using MEG and MR methods. The purpose of the multimodal scanning experiments was twofold: first, and primarily, to provide convergent and multifaceted evidence about the impact of *ZNF804A* genotype on brain function. Secondly, to show the extent to which these different indices correlate within subjects, an issue of broad relevance to multimodal neuroimaging. In contrast to an earlier study, no correlations were found between gamma oscillations, BOLD response, and GABA or glutamate levels in occipital regions raising several questions, which were discussed in chapter 5 and are not considered further here. However, the findings of chapter 5 were valuable for developing methods to assess the effects of rs1344706 on prefrontal function using MEG and fMRI. As shown in chapter 6, using these methods, we were unable to detect an effect of *ZNF804A* genotype on prefrontal GABA, glutamate, or NAA, and on prefrontal gamma oscillations. However, we did detect the previously observed alteration in prefrontal-hippocampal coupling in our fMRI study, with risk homozygotes displaying increased connectivity during a working memory task. Additionally, in chapter 7, when studying resting state networks in our MEG dataset using independent component analysis, we found an effect of rs1344706 on hippocampal theta, with non-risk homozygotes showing increased connectivity within a hippocampal network.

8.2 Genetic neuropathology studies of *ZNF804A*

In this thesis, I described effects of rs1344706 on several neuroimaging phenotypes, but found no effects on mRNA and protein expression levels. This raises the question how this polymorphism can alter brain activity, given that the first steps on the

pathway between the gene and disease (mRNA and protein) were not found to be affected by the SNP. As mentioned in chapter 3, it is conceivable that rs1344706 does affect expression levels, but possibly of another isoform or at a different developmental stage. Recent studies by our collaborators from the Lieber Institute for Brain Development (Tao, Cousijn et al., submitted) indicate that both explanations are true for *ZNF804A*. Using RNA-Seq, a powerful technology for identifying novel splice variants (Griffith et al., 2010; Ameur et al., 2011), and confirmed by 5'-RACE, they discovered a truncated isoform denoted ZNF804A^{E3E4} which lacks exons 1 and 2, and with a novel 5' extension of exon 3. This transcript is abundant and together with the fact that it remains in frame, suggests that it represents an alternative protein-coding transcript of potential functional significance. Both full-length and truncated mRNAs are highly expressed in foetal brain and continue to be expressed throughout life. As discussed in chapter 2, on some of our western blots we detected two instead of one band using a ZNF804A antibody. The two mRNA transcripts identified by our collaborators suggest that two bands should be detected in western blot studies, with the smaller band representing the truncated variant. However, the predicted size of the truncated variant is 121 kDa, which is bigger than the bands observed on our western blots (estimated at ~100 kDa) and close to the band representing the full-length transcript. Future studies will have to clarify whether the second band detected is indeed the truncated form of ZNF804A, which could be done using mass spectrometry or by selective transfection of cells with ZNF804A^{E3E4}.

Another crucial finding by Tao, Cousijn et al. (submitted) is that rs1344706 specifically affects expression of the truncated variant, doing so selectively during foetal but not postnatal life. As discussed in chapter 3, a recent study by Hill and Bray (2012) provided initial evidence that rs1344706 might have an effect in foetal but not in adult brain. The data from this study (Tao, Cousijn et al., submitted) confirm this observation

and, critically, show that the effect of rs1344706 is upon ZNF804A^{E3E4} mRNA, not full-length ZNF804A. The primers used in the earlier study by Hill and Bray (2012) amplify both variants, and so these new findings are both a replication and an important clarification. The finding that a schizophrenia risk SNP selectively affects expression of a splice variant adds to an increasing list of such findings (Law et al., 2006; Law et al., 2007; Straub et al., 2007; Sartorius et al., 2008; Huffaker et al., 2009; Nakata et al., 2009; Hyde et al., 2011). For example, metabotropic glutamate receptor 3 (GRM3) was associated with schizophrenia and the implicated SNPs were intronic and had no known function. Sartorius et al. (2008) found splice variants of GRM3 mRNA in human brain, including one that lacked exon 4 downstream from the implicated SNP. The abundance of this isoform relative to full-length GRM3 was then shown to be affected by two of the risk-associated intronic SNPs, supporting the hypothesis that this might be a mechanism underlying the clinical association. It has now been proposed that this specific effect of risk SNPs on particular isoforms may be a common feature, particularly for isoforms that are foetally enriched (Kleinman et al., 2011). This specific effect in foetal brain is also in line with the idea that schizophrenia is a disorder with neurodevelopmental origins.

Furthermore, it is notable that ZNF804A^{E3E4} is predicted to lack the zinc finger domain of ZNF804A and so is a strong candidate to have other roles. However, the ZNF804A^{E3E4} amino-acid sequence has no strong motifs, nor homologies to other proteins, precluding meaningful predictions as to its functions. This might also explain the cytoplasmic, granular immunoreactivity we observed in our immunohistochemistry experiments, which seemed unusual for a transcription factor. This pattern of staining, together with the fact that the truncated variant does not contain the zinc finger domain, suggests that more studies are needed to elucidate the roles of ZNF804A.

Taken together, the results from the studies carried out for this thesis and the results from studies carried out by our collaborators show that ZNF804A mRNA and immunoreactivity can be detected in both adult and foetal brain, but that the effects of rs1344706 take place during early development rather than in the adult brain. Furthermore, the newly identified variant ZNF804A^{E3E4} rather than full length ZNF804A is affected by rs13440706. However, there is no unique part to the amino acid sequence of ZNF804A^{E3E4} precluding specific investigations of ZNF804A^{E3E4} immunoreactivity. In terms of the function of ZNF804A protein, the finding that ZNF804A immunoreactivity is not localised to the nucleus but can be detected throughout the cytoplasm, together with the fact that ZNF804A^{E3E4} lacks the predicted zinc finger domain, suggests that ZNF804A might not function as a transcription factor but has other, yet unknown, roles.

8.3 Genetic neuroimaging studies of *ZNF804A*

As discussed in chapter 6, several studies have now shown that rs1344706 alters connectivity between the dorsolateral prefrontal cortex and the hippocampus, which makes this the most established functional correlate of *ZNF804A* to date. Even though in the experiment described here we could only detect the effect at uncorrected thresholds, the direction of the effect was the same as in previous studies (Esslinger et al., 2009; 2011;Paulus et al., 2013b). Risk homozygotes showed more connectivity between the right DLPFC and left hippocampus during a working memory task as compared to non-risk homozygotes. This same pattern has been found in patients with schizophrenia (Meyer-Lindenberg et al., 2001; 2005), who do not show the decoupling between the DLPFC and hippocampus that is normally observed with increased working memory load. Therefore, the finding that this functional connectivity is also altered in risk homozygotes shows that the SNP affects processes that are affected in the brains of patients with schizophrenia, and

thereby provides first clues about the neurobiological pathways between *ZNF804A* and schizophrenia.

We additionally assessed effects of rs1344706 on GABA, glutamate, and NAA concentrations as well as on gamma oscillations in prefrontal regions in an attempt to clarify the mechanisms by which prefrontal-hippocampal connectivity might be altered. None of these parameters showed an effect of rs1344706 genotype, although, as discussed in chapter 6, it is conceivable that additional analyses of these datasets might still reveal effects. However, when analyzing the MEG resting state dataset, we did detect an effect of rs1344706 on hippocampal theta. Theta is the rhythm most prominent in the hippocampus and several studies have shown that spiking of individual neurons in the prefrontal cortex becomes entrained to the hippocampal theta rhythm (Hyman et al., 2011) and that the theta-entrained activity across cortico-hippocampal circuits is important for information flow (Siapas et al., 2005). Therefore, it is conceivable that this observed increase in hippocampal theta in non-risk homozygotes could lead to alterations in prefrontal-hippocampal connectivity. The theta rhythm as measured by MEG provides a much more direct measure of neuronal activity than the BOLD signal, and can thereby provide an indication that the observed BOLD changes are indeed due to changes in neuronal firing patterns.

What should also be noted is the important role of layer III pyramidal cells in corticocortical connectivity. These pyramidal neurons are suspected to be of particular relevance to the pathophysiology of schizophrenia, given this role in connectivity, and in light of neuropathological findings in the disorder (Lewis et al., 2003). Our finding that ZNF804A immunoreactivity is particularly localised to these neurons provides another clue as to the neurobiological pathway via which ZNF804A might be involved in the observed alterations in functional connectivity in the brain.

8.4 Future directions

As discussed in the respective chapters, several interesting analyses could still be carried out on the data acquired for this thesis. In particular, it would be of interest to further investigate the effects of rs1344706 on oscillations. Most of the genetic neuroimaging studies to date looking at schizophrenia risk genes have used MRI methods, while electrophysiological methods provide richer datasets with good temporal resolution that are a better reflection of neural activity. I expect that future genetic neuroimaging studies will start to include magnetoencephalography measurements more often, in order to obtain new insights and explain previously observed differences in BOLD fMRI.

Several genetic neuroimaging studies investigating the effects of rs1344706 on brain function have appeared over the last years, in which different tasks were used and in which different brain regions were studied. Our studies have added to these neuroimaging findings, but it should be noted that most of these findings remain to be replicated. As in our study, sample sizes are often too small to draw conclusion that are beyond reasonable doubt. For the studies described here, we tried to maximise our power by specifically recruiting risk and non-risk homozygotes and by using different imaging techniques to allow acquisition of corroborative evidence about the effects of *ZNF804A* genotype. Nevertheless, replications in larger cohorts will be necessary to establish the robustness of the effects.

Additionally, I think that it is important that future studies look at well-established intermediate phenotypes for schizophrenia, which have been shown to be heritable and are present in family members of patients with schizophrenia. First of all, this is important to maximise the chances of detecting effects of schizophrenia risk genes, but also because those findings can actually elucidate the pathway between gene and disease. As mentioned in section 8.3, altered prefrontal-hippocampal connectivity has been reported in

schizophrenia patients and by now also several times in studies investigating effects of *ZNF804A* genotype in healthy volunteers. Our finding of an effect of rs1344706 on hippocampal theta provides a first clue as to the mechanisms that might underlie the observed alteration in prefrontal-hippocampal coupling. However, replications and additional analyses are needed to establish this finding and clarify whether the change in hippocampal theta truly reflects connectivity within the hippocampal network. The finding that *ZNF804A* genotype might affect occipito-parietal activations will be more difficult to interpret, because no imaging studies comparing schizophrenia patients with controls have reported abnormalities in occipito-parietal alpha power.

One of the most important remaining questions concerns the function of ZNF804A. In vitro studies have started to address this by looking at overexpression and knockdown of ZNF804A and its effects on other genes (Hill et al., 2012; Girgenti et al., 2012). However, at the time of writing, no animal models of ZNF804A had been developed, even though these are crucial for answering questions about the function of ZNF804A. When I started studying *ZNF804A* I expected one would become available before I finished this thesis – which would also have allowed additional validation of the antibody used in this thesis – but this has not happened, which might be a reflection of the time it takes to develop a good animal model. A complete knockout of a gene in mice is a reliable approach to test or validate the functions of the gene in vivo, and could therefore give a first indication of the function of ZNF804A. Given that *ZNF804A* might have its effects during development, conditional knockout of *ZNF804A* at a particular time during development could elucidate why a change in ZNF804A expression during development might be associated with schizophrenia later in life. It would also be of interest to see whether mice possess the truncated variant, and if not, study the effects of the human truncated form in a mouse model.

However, even if such studies would completely elucidate the path between this gene and schizophrenia, the clinical relevance would still be limited. *ZNF804A* has generated a lot of excitement because it was the first genome-wide significant gene, but it only has an OR of 1.10. Therefore, the most important questions about *ZNF804A* might revolve around its interactions with other risk genes and environmental risk factors, because being exposed to several of these risk factors might ultimately lead to schizophrenia. In vitro studies have indicated several schizophrenia risk genes *ZNF804A* might interact with, which provides some first clues about gene-gene interactions that could be studied. However, large-scale computational studies, including pathway analyses, might be needed to identify genes *ZNF804A* interacts with. Epidemiological studies as well as animal models could begin to identify *ZNF804A*-environment interactions that increase the chance of schizophrenia. We might need to study all schizophrenia risk genes one by one to unravel the pathways that they are involved in, but ultimately we will need to understand how interactions between multiple genes and multiple environmental factors increase the chance of schizophrenia. Only then will genes have predictive value and aid in prevention, and can medication target particular pathways.

8.5 Conclusions

The experiments described in this thesis were carried out to elucidate the neurobiological pathways in which schizophrenia risk gene *ZNF804A* and in particular risk SNP rs1344706 are involved. These experiments showed for the first time that ZNF804A immunoreactivity can be detected in both foetal and adult brain and that it is mainly localised to layer III pyramidal cells, with a granular subcellular distribution throughout the cytoplasm. No effect of rs1344706 on mRNA and protein expression was found, but experiments by collaborators have now shown that rs1344706 affects expression of a

truncated variant of ZNF804A during development. Rs1344706 was not found to affect macroscopic brain structure as measured by volumetry and VBM; given the large sample size of the study, this seems a convincing negative. It seems more likely that any pathophysiological correlates of rs1344706 in *ZNF804A* occur via modulation of brain function or connectivity. Earlier studies, as well as our study, have indicated that rs1344706 alters prefrontal-hippocampal connectivity, with increased connectivity in risk homozygotes. Our finding of increased hippocampal theta in non-risk homozygotes provides a first clue as to the mechanisms that might underlie this change in connectivity. Future studies will need to elucidate the actual function(s) of the ZNF804A protein, in order to bridge the gap between the molecular and neuroimaging findings described in this thesis.

References

Aleman A, Hijman R, de Haan EH, Kahn RS. (1999). Memory impairment in schizophrenia: a meta-analysis. *Am J Psychiatry* 156: 1358-66

Amad A, Cachia A, Gorwood P, Pins D, Delmaire C, Rolland B, Mondino M, Thomas P, Jardri R. (2013). The multimodal connectivity of the hippocampal complex in auditory and visual hallucinations. *Mol Psychiatry*, advanced online publication, Jan.2013

Ameur A, Zaghlool A, Halvardson J, Wetterbom A, Gyllensten U, Cavelier L, Feuk L. (2011). Total RNA sequencing reveals nascent transcription and widespread co-transcriptional splicing in the human brain. *Nat Struct Mol Biol* 18: 1435-40

Andreasen NC. (1995). Symptoms, signs, and diagnosis of schizophrenia. *Lancet* 346: 477-81

Arango C, Carpenter WT. (2011). The schizophrenia construct: symptomatic presentation. In: *Schizophrenia*, ed. DR Weinberger, PJ Harrison, pp. 9-23. Oxford: Blackwell

Ashburner J, Friston KJ. (2000). Voxel-based morphometry--the methods. *Neuroimage* 11: 805-21

Axmacher N, Cohen MX, Fell J, Haupt S, Dumpelmann M, Elger CE, Schlaepfer TE, Lenartz D, Sturm V, Ranganath C. (2010). Intracranial EEG correlates of expectancy and memory formation in the human hippocampus and nucleus accumbens. *Neuron* 65: 541-9

Barch DM, Ceaser A. (2012). Cognition in schizophrenia: core psychological and neural mechanisms. *Trends Cogn Sci* 16: 27-34

Barr MS, Farzan F, Rusjan PM, Chen R, Fitzgerald PB, Daskalakis ZJ. (2009). Potentiation of gamma oscillatory activity through repetitive transcranial magnetic stimulation of the dorsolateral prefrontal cortex. *Neuropsychopharmacology* 34: 2359-67

Bartos M, Vida I, Jonas P. (2007). Synaptic mechanisms of synchronized gamma oscillations in inhibitory interneuron networks. *Nat Rev Neurosci* 8: 45-56

Bassett AS, Scherer SW, Brzustowicz LM. (2010). Copy number variations in schizophrenia: critical review and new perspectives on concepts of genetics and disease. *Am J Psychiatry* 167: 899-914

Beckmann CF, DeLuca M, Devlin JT, Smith SM. (2005). Investigations into resting-state connectivity using independent component analysis. *Philos Trans R Soc Lond B Biol Sci* 360: 1001-13

Bergmann O, Haukvik UK, Brown AA, Rimol LM, Hartberg CB, Athanasiu L, Melle I, Djurovic S, Andreassen OA, Dale AM, Agartz I. (2013). ZNF804A and cortical thickness in schizophrenia and bipolar disorder. *Psychiatry Res* 212: 154-7

Berman KF, Illowsky BP, Weinberger DR. (1988). Physiological dysfunction of dorsolateral prefrontal cortex in schizophrenia. IV. Further evidence for regional and behavioral specificity. *Arch Gen Psychiatry* 45: 616-22

Berrios GE. (1985). Positive and negative symptoms and Jackson. A conceptual history. *Arch Gen Psychiatry* 42: 95-7

Bertolino A, Callicott JH, Elman I, Mattay VS, Tedeschi G, Frank JA, Breier A, Weinberger DR. (1998a). Regionally specific neuronal pathology in untreated patients with schizophrenia: a proton magnetic resonance spectroscopic imaging study. *Biol Psychiatry* 43: 641-8

Bertolino A, Callicott JH, Nawroz S, Mattay VS, Duyn JH, Tedeschi G, Frank JA, Weinberger DR. (1998b). Reproducibility of proton magnetic resonance

spectroscopic imaging in patients with schizophrenia. *Neuropsychopharmacology* 18: 1-9
Bertolino A, Weinberger DR. (1999). Proton magnetic resonance spectroscopy in schizophrenia. *Eur J Radiol* 30: 132-41
Bertolino A, Esposito G, Callicott JH, Mattay VS, Van Horn JD, Frank JA, Berman KF, Weinberger DR. (2000). Specific relationship between prefrontal neuronal N-acetylaspartate and activation of the working memory cortical network in schizophrenia. *Am J Psychiatry* 157: 26-33
Bilder RM, Goldman RS, Robinson D, Reiter G, Bell L, Bates JA, Pappadopulos E, Willson DF, Alvir JM, Woerner MG, Geisler S, Kane JM, Lieberman JA. (2000). Neuropsychology of first-episode schizophrenia: initial characterization and clinical correlates. *Am J Psychiatry* 157: 549-59
Biswal B, Yetkin FZ, Haughton VM, Hyde JS. (1995). Functional connectivity in the motor cortex of resting human brain using echo-planar MRI. *Magnetic Resonance in Medicine* 34: 537-41
Blackwood DH, Glabus MF, Dunan J, O'Carroll RE, Muir WJ, Ebmeier KP. (1999). Altered cerebral perfusion measured by SPECT in relatives of patients with schizophrenia. Correlations with memory and P300. *Br J Psychiatry* 175: 357-66
Block W, Bayer TA, Tepest R, Traber F, Rietschel M, Muller DJ, Schulze TG, Honer WG, Maier W, Schild HH, Falkai P. (2000). Decreased frontal lobe ratio of N-acetyl aspartate to choline in familial schizophrenia: a proton magnetic resonance spectroscopy study. *Neurosci Lett* 289: 147-51
Blokland GA, McMahon KL, Hoffman J, Zhu G, Meredith M, Martin NG, Thompson PM, de Zubicaray GI, Wright MJ. (2008). Quantifying the heritability of task-related brain activation and performance during the N-back working memory task: a twin fMRI study. *Biol Psychol* 79: 70-9
Bosman CA, Schoffelen JM, Brunet N, Oostenveld R, Bastos AM, Womelsdorf T, Rubehn B, Stieglitz T, De Weerd P, Fries P. (2012). Attentional stimulus selection through selective synchronization between monkey visual areas. *Neuron* 75: 875-88
Bralten J, Arias-Vasquez A, Makkinje R, Veltman JA, Brunner HG, Fernandez G, Rijpkema M, Franke B. (2011a). Association of the Alzheimer's gene SORL1 with hippocampal volume in young, healthy adults. *Am J Psychiatry* 168: 1083-9
Bralten J, Franke B, Arias-Vasquez A, Heister A, Brunner HG, Fernandez G, Rijpkema M. (2011b). CR1 genotype is associated with entorhinal cortex volume in young healthy adults. *Neurobiol Aging* 32: 2106.e7-11
Brayer KJ, Segal DJ. (2008). Keep your fingers off my DNA: protein-protein interactions mediated by C2H2 zinc finger domains. *Cell Biochem Biophys* 50: 111-31
Brembs B, Button K, Munafo M. (2013). Deep impact: unintended consequences of journal rank. *Front Hum Neurosci* 7: 291
Brett M, Anton JL, Valabregue R, Poline JB. (2002). *Region of interest analysis using an SPM toolbox. Available on CD-ROM in NeuroImage, Vol 16, No 2.* Presented at 8th International Conference on Functional Mapping of the Human Brain, Sendai, Japan
Bristow GC, Lane TA, Walker M, Chen L, Sei Y, Hyde TM, Kleinman JE, Harrison PJ, Eastwood SL. (2009). Expression of kinase interacting with stathmin (KIS, UHMK1) in human brain and lymphoblasts: Effects of schizophrenia and genotype. *Brain Res* 1301: 197-206
Brookes MJ, Wood JR, Stevenson CM, Zumer JM, White TP, Liddle PF, Morris PG. (2011a). Changes in brain network activity during working memory tasks: a magnetoencephalography study. *Neuroimage* 55: 1804-15

Brookes MJ, Woolrich M, Luckhoo H, Price D, Hale JR, Stephenson MC, Barnes GR, Smith SM, Morris PG. (2011b). Investigating the electrophysiological basis of resting state networks using magnetoencephalography. *Proc Natl Acad Sci U S A* 108: 16783-8

Buckholtz JW, Meyer-Lindenberg A, Honea RA, Straub RE, Pezawas L, Egan MF, Vakkalanka R, Kolachana B, Verchinski BA, Sust S, Mattay VS, Weinberger DR, Callicott JH. (2007). Allelic variation in RGS4 impacts functional and structural connectivity in the human brain. *Journal of Neuroscience* 27: 1584-93

Bullmore ET, Frangou S, Murray RM. (1997). The dysplastic net hypothesis: an integration of developmental and dysconnectivity theories of schizophrenia. *Schizophr Res* 28: 143-56

Buonocore F, Hill MJ, Campbell CD, Oladimeji PB, Jeffries AR, Troakes C, Hortobagyi T, Williams BP, Cooper JD, Bray NJ. (2010). Effects of cis-regulatory variation differ across regions of the adult human brain. *Hum Mol Genet* 19: 4490-6

Buzsaki G, Kaila K, Raichle M. (2007). Inhibition and brain work. *Neuron* 56: 771-83

Buzsaki G, Wang XJ. (2012). Mechanisms of gamma oscillations. *Annu Rev Neurosci* 35: 203-25

Callicott JH, Egan MF, Bertolino A, Mattay VS, Langheim FJ, Frank JA, Weinberger DR. (1998). Hippocampal N-acetyl aspartate in unaffected siblings of patients with schizophrenia: a possible intermediate neurobiological phenotype. *Biol Psychiatry* 44: 941-50

Callicott JH, Mattay VS, Bertolino A, Finn K, Coppola R, Frank JA, Goldberg TE, Weinberger DR. (1999). Physiological characteristics of capacity constraints in working memory as revealed by functional MRI. *Cereb Cortex* 9: 20-6

Callicott JH, Bertolino A, Egan MF, Mattay VS, Langheim FJ, Weinberger DR. (2000a). Selective relationship between prefrontal N-acetylaspartate measures and negative symptoms in schizophrenia. *Am J Psychiatry* 157: 1646-51

Callicott JH, Bertolino A, Mattay VS, Langheim FJ, Duyn J, Coppola R, Goldberg TE, Weinberger DR. (2000b). Physiological dysfunction of the dorsolateral prefrontal cortex in schizophrenia revisited. *Cereb Cortex* 10: 1078-92

Callicott JH, Egan MF, Mattay VS, Bertolino A, Bone AD, Verchinksi B, Weinberger DR. (2003a). Abnormal fMRI response of the dorsolateral prefrontal cortex in cognitively intact siblings of patients with schizophrenia. *Am J Psychiatry* 160: 709-19

Callicott JH, Mattay VS, Verchinski BA, Marenco S, Egan MF, Weinberger DR. (2003b). Complexity of prefrontal cortical dysfunction in schizophrenia: more than up or down. *Am J Psychiatry* 160: 2209-15

Callicott JH, Straub RE, Pezawas L, Egan MF, Mattay VS, Hariri AR, Verchinski BA, Meyer-Lindenberg A, Balkissoon R, Kolachana B, Goldberg TE, Weinberger DR. (2005). Variation in DISC1 affects hippocampal structure and function and increases risk for schizophrenia. *Proc Natl Acad Sci U S A* 102: 8627-32

Cannon M, Jones PB, Murray RM. (2002). Obstetric complications and schizophrenia: historical and meta-analytic review. *Am J Psychiatry* 159: 1080-92

Cardno AG, Marshall EJ, Coid B, Macdonald AM, Ribchester TR, Davies NJ, Venturi P, Jones LA, Lewis SW, Sham PC, Gottesman, II, Farmer AE, McGuffin P, Reveley AM, Murray RM. (1999). Heritability estimates for psychotic disorders: the Maudsley twin psychosis series. *Arch Gen Psychiatry* 56: 162-8

Censits DM, Ragland JD, Gur RC, Gur RE. (1997). Neuropsychological evidence supporting a neurodevelopmental model of schizophrenia: a longitudinal study. *Schizophr Res* 24: 289-98

Chakirova G, Whalley HC, Thomson PA, Hennah W, Moorhead TW, Welch KA, Giles S, Hall J, Johnstone EC, Lawrie SM, Porteous DJ, Brown VJ, McIntosh AM. (2011). The effects of DISC1 risk variants on brain activation in controls, patients with bipolar disorder and patients with schizophrenia. *Psychiatry Res* 192: 20-8

Cho RY, Konecky RO, Carter CS. (2006). Impairments in frontal cortical gamma synchrony and cognitive control in schizophrenia. *Proc Natl Acad Sci U S A* 103: 19878-83

Chubb JE, Bradshaw NJ, Soares DC, Porteous DJ, Millar JK. (2008). The DISC locus in psychiatric illness. *Mol Psychiatry* 13: 36-64

Chung HJ, Lee JY, Deocaris CC, Min H, Kim SH, Kim MH. (2010). Mouse Homologue of the Schizophrenia Susceptibility Gene ZNF804A as a Target of Hoxc8. *J Biomed Biotechnol* 2010: 231708

Ciesielski KT, Ahlfors SP, Bedrick EJ, Kerwin AA, Hamalainen MS. (2010). Top-down control of MEG alpha-band activity in children performing Categorical N-Back Task. *Neuropsychologia* 48: 3573-9

Colantuoni C, Lipska BK, Ye T, Hyde TM, Tao R, Leek JT, Colantuoni EA, Elkahloun AG, Herman MM, Weinberger DR, Kleinman JE. (2011). Temporal dynamics and genetic control of transcription in the human prefrontal cortex. *Nature* 478: 519-23

Colgin LL. (2011). Oscillations and hippocampal-prefrontal synchrony. *Curr Opin Neurobiol* 21: 467-74

Consortium IS. (2009). Common polygenic variation contributes to risk of schizophrenia and bipolar disorder. *Nature* 460: 748-52

Cordes D, Haughton VM, Arfanakis K, Wendt GJ, Turski PA, Moritz CH, Quigley MA, Meyerand ME. (2000). Mapping functionally related regions of brain with functional connectivity MR imaging. *AJNR Am J Neuroradiol* 21: 1636-44

Cornwell BR, Johnson LL, Holroyd T, Carver FW, Grillon C. (2008). Human hippocampal and parahippocampal theta during goal-directed spatial navigation predicts performance on a virtual Morris water maze. *J Neurosci* 28: 5983-90

Cousijn H, Rijpkema M, Harteveld A, Harrison PJ, Fernandez G, Franke B, Arias-Vasquez A. (2012). Schizophrenia risk gene ZNF804A does not influence macroscopic brain structure: an MRI study in 892 volunteers. *Mol Psychiatry* 17: 1155-7

Crespo-Facorro B, Barbadillo L, Pelayo-Teran JM, Rodriguez-Sanchez JM. (2007). Neuropsychological functioning and brain structure in schizophrenia. *Int Rev Psychiatry* 19: 325-36

Crossley NA, Mechelli A, Fusar-Poli P, Broome MR, Matthiasson P, Johns LC, Bramon E, Valmaggia L, Williams SC, McGuire PK. (2009). Superior temporal lobe dysfunction and frontotemporal dysconnectivity in subjects at risk of psychosis and in first-episode psychosis. *Hum Brain Mapp* 30: 4129-37

Cuadra MB, Cammoun L, Butz T, Cuisenaire O, Thiran JP. (2005). Comparison and validation of tissue modelization and statistical classification methods in T1-weighted MR brain images. *IEEE Trans Med Imaging* 24: 1548-65

Cummings E, Donohoe G, McDonald C, Dinan TG, O'Neill FA, O'Callaghan E, Waddington JL, Murphy KC, Gill M, Morris DW, Corvin A. (2010). Clinical symptomatology and the psychosis risk gene ZNF804A. *Schizophr Res* 122: 273-5

Damoiseaux JS, Rombouts SA, Barkhof F, Scheltens P, Stam CJ, Smith SM, Beckmann CF. (2006). Consistent resting-state networks across healthy subjects. *Proc Natl Acad Sci U S A* 103: 13848-53

Davies G, Welham J, Chant D, Torrey EF, McGrath J. (2003). A systematic review and meta-analysis of Northern Hemisphere season of birth studies in schizophrenia. *Schizophr Bull* 29: 587-93

de Geus E, Goldberg T, Boomsma DI, Posthuma D. (2008). Imaging the genetics of brain structure and function. *Biol Psychol* 79: 1-8

de Pasquale F, Della Penna S, Snyder AZ, Lewis C, Mantini D, Marzetti L, Belardinelli P, Ciancetta L, Pizzella V, Romani GL, Corbetta M. (2010). Temporal dynamics of spontaneous MEG activity in brain networks. *Proc Natl Acad Sci U S A* 107: 6040-5

Deiber MP, Missonnier P, Bertrand O, Gold G, Fazio-Costa L, Ibanez V, Giannakopoulos P. (2007). Distinction between perceptual and attentional processing in working memory tasks: a study of phase-locked and induced oscillatory brain dynamics. *J Cogn Neurosci* 19: 158-72

Demiralp T, Herrmann CS, Erdal ME, Ergenoglu T, Keskin YH, Ergen M, Beydagi H. (2007). DRD4 and DAT1 polymorphisms modulate human gamma band responses. *Cereb Cortex* 17: 1007-19

Donahue MJ, Near J, Blicher JU, Jezzard P. (2010). Baseline GABA concentration and fMRI response. *Neuroimage* 53: 392-8

Donohoe G, Rose E, Frodl T, Morris D, Spoletini I, Adriano F, Bernardini S, Caltagirone C, Bossu P, Gill M, Corvin AP, Spalletta G. (2011). ZNF804A risk allele is associated with relatively intact gray matter volume in patients with schizophrenia. *Neuroimage* 54: 2132-7

Duncan NW, Enzi B, Wiebking C, Northoff G. (2011). Involvement of glutamate in rest-stimulus interaction between perigenual and supragenual anterior cingulate cortex: a combined fMRI-MRS study. *Hum Brain Mapp* 32: 2172-82

Dwyer S, Williams H, Holmans P, Moskvina V, Craddock N, Owen MJ, O'Donovan MC. (2010). No evidence that rare coding variants in ZNF804A confer risk of schizophrenia. *Am J Med Genet B Neuropsychiatr Genet* 153b: 1411-6

Eastwood SL, Burnet PW, Harrison PJ. (1995). Altered synaptophysin expression as a marker of synaptic pathology in schizophrenia. *Neuroscience* 66: 309-19

Edden RA, Muthukumaraswamy SD, Freeman TC, Singh KD. (2009). Orientation discrimination performance is predicted by GABA concentration and gamma oscillation frequency in human primary visual cortex. *J Neurosci* 29: 15721-6

Egan MF, Goldberg TE, Kolachana BS, Callicott JH, Mazzanti CM, Straub RE, Goldman D, Weinberger DR. (2001). Effect of COMT Val108/158 Met genotype on frontal lobe function and risk for schizophrenia. *Proc Natl Acad Sci U S A* 98: 6917-22

Egan MF, Straub RE, Goldberg TE, Yakub I, Callicott JH, Hariri AR, Mattay VS, Bertolino A, Hyde TM, Shannon-Weickert C, Akil M, Crook J, Vakkalanka RK, Balkissoon R, Gibbs RA, Kleinman JE, Weinberger DR. (2004). Variation in GRM3 affects cognition, prefrontal glutamate, and risk for schizophrenia. *Proc Natl Acad Sci U S A* 101: 12604-9

Egan MF, Cannon TD. (2011). Intermediate phenotypes in genetic studies of schizophrenia. In: *Schizophrenia*, ed. DR Weinberger, PJ Harrison, pp. 289-310. Oxford: Blackwell

Esslinger C, Walter H, Kirsch P, Erk S, Schnell K, Arnold C, Haddad L, Mier D, Opitz von Boberfeld C, Raab K, Witt SH, Rietschel M, Cichon S, Meyer-Lindenberg A. (2009). Neural mechanisms of a genome-wide supported psychosis variant. *Science* 324: 605

Esslinger C, Kirsch P, Haddad L, Mier D, Sauer C, Erk S, Schnell K, Arnold C, Witt SH, Rietschel M, Cichon S, Walter H, Meyer-Lindenberg A. (2011). Cognitive state and connectivity effects of the genome-wide significant psychosis variant in ZNF804A. *Neuroimage* 54: 2514-23

Falkenberg LE, Westerhausen R, Specht K, Hugdahl K. (2012). Resting-state glutamate level in the anterior cingulate predicts blood-oxygen level-dependent response to cognitive control. *Proc Natl Acad Sci U S A* 109: 5069-73

Filippini N, MacIntosh BJ, Hough MG, Goodwin GM, Frisoni GB, Smith SM, Matthews PM, Beckmann CF, Mackay CE. (2009). Distinct patterns of brain activity in young carriers of the APOE-epsilon4 allele. *Proc Natl Acad Sci U S A* 106: 7209-14

Fornito A, Yucel M, Patti J, Wood SJ, Pantelis C. (2009). Mapping grey matter reductions in schizophrenia: an anatomical likelihood estimation analysis of voxel-based morphometry studies. *Schizophr Res* 108: 104-13

Fornito A, Bullmore ET. (2010). What can spontaneous fluctuations of the blood oxygenation-level-dependent signal tell us about psychiatric disorders? *Curr Opin Psychiatry* 23: 239-49

Fornito A, Zalesky A, Bassett DS, Meunier D, Ellison-Wright I, Yucel M, Wood SJ, Shaw K, O'Connor J, Nertney D, Mowry BJ, Pantelis C, Bullmore ET. (2011). Genetic influences on cost-efficient organization of human cortical functional networks. *J Neurosci* 31: 3261-70

Foster BL, Parvizi J. (2012). Resting oscillations and cross-frequency coupling in the human posteromedial cortex. *Neuroimage* 60: 384-91

Fox MD, Snyder AZ, Vincent JL, Corbetta M, Van Essen DC, Raichle ME. (2005). The human brain is intrinsically organized into dynamic, anticorrelated functional networks. *Proc Natl Acad Sci U S A* 102: 9673-8

Franck N, O'Leary DS, Flaum M, Hichwa RD, Andreasen NC. (2002). Cerebral blood flow changes associated with Schneiderian first-rank symptoms in schizophrenia. *J Neuropsychiatry Clin Neurosci* 14: 277-82

Franke B, Vasquez AA, Veltman JA, Brunner HG, Rijpkema M, Fernandez G. (2010). Genetic variation in CACNA1C, a gene associated with bipolar disorder, influences brainstem rather than gray matter volume in healthy individuals. *Biol Psychiatry* 68: 586-8

Freedman D, Brown AS. (2011). The developmental course of executive functioning in schizophrenia. *Int J Dev Neurosci* 29: 237-43

Freedman R. (2003). Schizophrenia. *N Engl J Med* 349: 1738-49

Fries P, Nikolic D, Singer W. (2007). The gamma cycle. *Trends Neurosci* 30: 309-16

Friston KJ, Frith CD. (1995). Schizophrenia: a disconnection syndrome? *Clin Neurosci* 3: 89-97

Friston KJ, Buechel C, Fink GR, Morris J, Rolls E, Dolan RJ. (1997). Psychophysiological and modulatory interactions in neuroimaging. *Neuroimage* 6: 218-29

Friston KJ. (1999). Schizophrenia and the disconnection hypothesis. *Acta Psychiatr Scand Suppl* 395: 68-79

Gaetz W, Edgar JC, Wang DJ, Roberts TP. (2011). Relating MEG measured motor cortical oscillations to resting gamma-aminobutyric acid (GABA) concentration. *Neuroimage* 55: 616-21

Gallinat J, Winterer G, Herrmann CS, Senkowski D. (2004). Reduced oscillatory gamma-band responses in unmedicated schizophrenic patients indicate impaired frontal network processing. *Clin Neurophysiol* 115: 1863-74

Gamsjaeger R, Liew CK, Loughlin FE, Crossley M, Mackay JP. (2007). Sticky fingers: zinc-fingers as protein-recognition motifs. *Trends Biochem Sci* 32: 63-70

Garey LJ, Ong WY, Patel TS, Kanani M, Davis A, Mortimer AM, Barnes TR, Hirsch SR. (1998). Reduced dendritic spine density on cerebral cortical pyramidal neurons in schizophrenia. *J Neurol Neurosurg Psychiatry* 65: 446-53

Gaser C, Volz HP, Kiebel S, Riehemann S, Sauer H. (1999). Detecting structural changes in whole brain based on nonlinear deformations-application to schizophrenia research. *Neuroimage* 10: 107-13

Geddes JR, Verdoux H, Takei N, Lawrie SM, Bovet P, Eagles JM, Heun R, McCreadie RG, McNeil TF, O'Callaghan E, Stober G, Willinger U, Murray RM. (1999). Schizophrenia and complications of pregnancy and labor: an individual patient data meta-analysis. *Schizophr Bull* 25: 413-23

Gerritsen L, Comijs HC, Deeg DJ, Penninx BW, Geerlings MI. (2011). Salivary cortisol, APOE-epsilon4 allele and cognitive decline in a prospective study of older persons. *Neurobiol Aging* 32: 1615-25

Gershon ES, Goldin LR. (1986). Clinical methods in psychiatric genetics. I. Robustness of genetic marker investigative strategies. *Acta Psychiatr Scand* 74: 113-8

Gevins A, Smith ME, McEvoy L, Yu D. (1997). High-resolution EEG mapping of cortical activation related to working memory: effects of task difficulty, type of processing, and practice. *Cereb Cortex* 7: 374-85

Ghose S, Crook JM, Bartus CL, Sherman TG, Herman MM, Hyde TM, Kleinman JE, Akil M. (2008). Metabotropic glutamate receptor 2 and 3 gene expression in the human prefrontal cortex and mesencephalon in schizophrenia. *Int J Neurosci* 118: 1609-27

Girgenti MJ, LoTurco JJ, Maher BJ. (2012). ZNF804a regulates expression of the schizophrenia-associated genes PRSS16, COMT, PDE4B, and DRD2. *PLoS One* 7: e32404

Gittins R, Harrison PJ. (2004). Neuronal density, size and shape in the human anterior cingulate cortex: a comparison of Nissl and NeuN staining. *Brain Res Bull* 63: 155-60

Gittins RA, Harrison PJ. (2011). A morphometric study of glia and neurons in the anterior cingulate cortex in mood disorder. *J Affect Disord* 133: 328-32

Glahn DC, Winkler AM, Kochunov P, Almasy L, Duggirala R, Carless MA, Curran JC, Olvera RL, Laird AR, Smith SM, Beckmann CF, Fox PT, Blangero J. (2010). Genetic control over the resting brain. *Proc Natl Acad Sci U S A* 107: 1223-8

Glantz LA, Lewis DA. (1997). Reduction of synaptophysin immunoreactivity in the prefrontal cortex of subjects with schizophrenia. Regional and diagnostic specificity. *Arch Gen Psychiatry* 54: 660-9

Glantz LA, Lewis DA. (2000). Decreased dendritic spine density on prefrontal cortical pyramidal neurons in schizophrenia. *Arch Gen Psychiatry* 57: 65-73

Goense JB, Logothetis NK. (2008). Neurophysiology of the BOLD fMRI signal in awake monkeys. *Curr Biol* 18: 631-40

Goldman AL, Pezawas L, Mattay VS, Fischl B, Verchinski BA, Zoltick B, Weinberger DR, Meyer-Lindenberg A. (2008). Heritability of brain morphology related to schizophrenia: a large-scale automated magnetic resonance imaging segmentation study. *Biol Psychiatry* 63: 475-83

Goldman AL, Pezawas L, Mattay VS, Fischl B, Verchinski BA, Chen Q, Weinberger DR, Meyer-Lindenberg A. (2009). Widespread reductions of cortical thickness in schizophrenia and spectrum disorders and evidence of heritability. *Arch Gen Psychiatry* 66: 467-77

Goldman RI, Stern JM, Engel J, Jr., Cohen MS. (2002). Simultaneous EEG and fMRI of the alpha rhythm. *Neuroreport* 13: 2487-92

Goldman RI, Cohen MS. (2003). *Tomographic distribution of resting alpha rhythm sources revealed by independent component analysis. Printed in NeuroImage 19, S412.* Presented at Ninth International Conference on Functional Mapping of the Human Brain, New York

Goldstein JM, Goodman JM, Seidman LJ, Kennedy DN, Makris N, Lee H, Tourville J, Caviness VS, Jr., Faraone SV, Tsuang MT. (1999). Cortical abnormalities in schizophrenia identified by structural magnetic resonance imaging. *Arch Gen Psychiatry* 56: 537-47

Good CD, Johnsrude I, Ashburner J, Henson RN, Friston KJ, Frackowiak RS. (2001). Cerebral asymmetry and the effects of sex and handedness on brain structure: a voxel-based morphometric analysis of 465 normal adult human brains. *Neuroimage* 14: 685-700

Gottesman, II, Shields J. (1973). Genetic theorizing and schizophrenia. *Br J Psychiatry* 122: 15-30

Gottesman, II, Gould TD. (2003). The endophenotype concept in psychiatry: etymology and strategic intentions. *Am J Psychiatry* 160: 636-45

Gottesman I. (1991). *Schizophrenia Genesis*. New York: WH Freeman.

Green AE, Munafo MR, DeYoung CG, Fossella JA, Fan J, Gray JR. (2008). Using genetic data in cognitive neuroscience: from growing pains to genuine insights. *Nat Rev Neurosci* 9: 710-20

Griffith M, Griffith OL, Mwenifumbo J, Goya R, Morrissy AS, Morin RD, Corbett R, Tang MJ, Hou YC, Pugh TJ, Robertson G, Chittaranjan S, Ally A, Asano JK, Chan SY, Li HI, McDonald H, Teague K, Zhao Y, Zeng T, Delaney A, Hirst M, Morin GB, Jones SJ, Tai IT, Marra MA. (2010). Alternative expression analysis by RNA sequencing. *Nat Methods* 7: 843-7

Gross J, Kujala J, Hamalainen M, Timmermann L, Schnitzler A, Salmelin R. (2001). Dynamic imaging of coherent sources: Studying neural interactions in the human brain. *Proc Natl Acad Sci U S A* 98: 694-9

Gruber O, Hasan A, Scherk H, Wobrock T, Schneider-Axmann T, Ekawardhani S, Schmitt A, Backens M, Reith W, Meyer J, Falkai P. (2012). Association of the brain-derived neurotrophic factor val66met polymorphism with magnetic resonance spectroscopic markers in the human hippocampus: in vivo evidence for effects on the glutamate system. *Eur Arch Psychiatry Clin Neurosci* 262: 23-31

Gschwandtner U, Aston J, Borgwardt S, Drewe M, Feinendegen C, Lacher D, Lanzarone A, Stieglitz RD, Riecher-Rossler A. (2003). Neuropsychological and neurophysiological findings in individuals suspected to be at risk for schizophrenia: preliminary results from the Basel early detection of psychosis study - Fruherkennung von Psychosen (FEPSY). *Acta Psychiatr Scand* 108: 152-5

Habl G, Zink M, Petroianu G, Bauer M, Schneider-Axmann T, von Wilmsdorff M, Falkai P, Henn FA, Schmitt A. (2009). Increased D-amino acid oxidase expression in the bilateral hippocampal CA4 of schizophrenic patients: a post-mortem study. *J Neural Transm* 116: 1657-65

Habl G, Schmitt A, Zink M, von Wilmsdorff M, Yeganeh-Doost P, Jatzko A, Schneider-Axmann T, Bauer M, Falkai P. (2012). Decreased reelin expression in the left prefrontal cortex (BA9) in chronic schizophrenia patients. *Neuropsychobiology* 66: 57-62

Haenschel C, Bittner RA, Waltz J, Haertling F, Wibral M, Singer W, Linden DE, Rodriguez E. (2009). Cortical oscillatory activity is critical for working memory as revealed by deficits in early-onset schizophrenia. *J Neurosci* 29: 9481-9

Hall MH, Taylor G, Sham P, Schulze K, Rijsdijk F, Picchioni M, Toulopoulou T, Ettinger U, Bramon E, Murray RM, Salisbury DF. (2011a). The early auditory gamma-band response is heritable and a putative endophenotype of schizophrenia. *Schizophr Bull* 37: 778-87

Hall SD, Barnes GR, Furlong PL, Seri S, Hillebrand A. (2010). Neuronal network pharmacodynamics of GABAergic modulation in the human cortex determined using pharmaco-magnetoencephalography. *Hum Brain Mapp* 31: 581-94
Hall SD, Stanford IM, Yamawaki N, McAllister CJ, Ronnqvist KC, Woodhall GL, Furlong PL. (2011b). The role of GABAergic modulation in motor function related neuronal network activity. *Neuroimage* 56: 1506-10
Halliday GM. (2001). A review of the neuropathology of schizophrenia. *Clin Exp Pharmacol Physiol* 28: 64-5
Hambrecht M, Lammertink M, Klosterkotter J, Matuschek E, Pukrop R. (2002). Subjective and objective neuropsychological abnormalities in a psychosis prodrome clinic. *Br J Psychiatry Suppl* 43: s30-7
Hariri AR, Weinberger DR. (2003). Imaging genomics. *Br Med Bull* 65: 259-70
Harrison PJ. (1996). Advances in post mortem molecular neurochemistry and neuropathology: examples from schizophrenia research. *Br Med Bull* 52: 527-38
Harrison PJ. (1999). The neuropathology of schizophrenia. A critical review of the data and their interpretation. *Brain* 122 (Pt 4): 593-624
Harrison PJ, Freemantle N, Geddes JR. (2003). Meta-analysis of brain weight in schizophrenia. *Schizophr Res* 64: 25-34
Harrison PJ, Owen MJ. (2003). Genes for schizophrenia? Recent findings and their pathophysiological implications. *Lancet* 361: 417-9
Harrison PJ. (2005). Neuropathology of schizophrenia. *Psychiatry* 4: 18-21
Harrison PJ, Weinberger DR. (2005). Schizophrenia genes, gene expression, and neuropathology: on the matter of their convergence. *Mol Psychiatry* 10: 40-68; image 5
Harrison PJ, Lewis DA, Kleinman JE. (2011). Neuropathology of schizophrenia. In: *Schizophrenia*, ed. DR Weinberger, PJ Harrison, pp. 372-92. Oxford: Blackwell
Hashimoto R, Ohi K, Yasuda Y, Fukumoto M, Iwase M, Iike N, Azechi M, Ikezawa K, Takaya M, Takahashi H, Yamamori H, Okochi T, Tanimukai H, Tagami S, Morihara T, Okochi M, Tanaka T, Kudo T, Kazui H, Iwata N, Takeda M. (2010). The impact of a genome-wide supported psychosis variant in the ZNF804A gene on memory function in schizophrenia. *Am J Med Genet B Neuropsychiatr Genet* 153b: 1459-64
Heckers S. (1997). Neuropathology of schizophrenia: cortex, thalamus, basal ganglia, and neurotransmitter-specific projection systems. *Schizophr Bull* 23: 403-21
Heise V, Luckhoo H, Trachtenberg AJ, Ebmeier KP, Nobre AC, Woolrich MW, Mackay CE. (in prep.). The electrophysiological basis of APOE genotype effects on neuronal function at rest.
Heston LL. (1966). Psychiatric disorders in foster home reared children of schizophrenic mothers. *Br J Psychiatry* 112: 819-25
Highley JR, McDonald B, Walker MA, Esiri MM, Crow TJ. (1999). Schizophrenia and temporal lobe asymmetry. A post-mortem stereological study of tissue volume. *Br J Psychiatry* 175: 127-34
Hill MJ, Bray NJ. (2011). Allelic differences in nuclear protein binding at a genome-wide significant risk variant for schizophrenia in ZNF804A. *Mol Psychiatry* 16: 787-9
Hill MJ, Bray NJ. (2012). Evidence that schizophrenia risk variation in the ZNF804A gene exerts its effects during fetal brain development. *Am J Psychiatry* 169: 1301-8
Hill MJ, Jeffries AR, Dobson RJ, Price J, Bray NJ. (2012). Knockdown of the psychosis susceptibility gene ZNF804A alters expression of genes involved in cell adhesion. *Hum Mol Genet* 21: 1018-24

Hillebrand A, Barnes GR, Bosboom JL, Berendse HW, Stam CJ. (2012). Frequency-dependent functional connectivity within resting-state networks: an atlas-based MEG beamformer solution. *Neuroimage* 59: 3909-21

Hirschhorn JN, Daly MJ. (2005). Genome-wide association studies for common diseases and complex traits. *Nat Rev Genet* 6: 95-108

Honea RA, Meyer-Lindenberg A, Hobbs KB, Pezawas L, Mattay VS, Egan MF, Verchinski B, Passingham RE, Weinberger DR, Callicott JH. (2008). Is gray matter volume an intermediate phenotype for schizophrenia? A voxel-based morphometry study of patients with schizophrenia and their healthy siblings. *Biol Psychiatry* 63: 465-74

Honey GD, Bullmore ET, Sharma T. (2002). De-coupling of cognitive performance and cerebral functional response during working memory in schizophrenia. *Schizophr Res* 53: 45-56

Hong LE, Summerfelt A, McMahon RP, Thaker GK, Buchanan RW. (2004). Gamma/beta oscillation and sensory gating deficit in schizophrenia. *Neuroreport* 15: 155-9

Huang MX, Mosher JC, Leahy RM. (1999). A sensor-weighted overlapping-sphere head model and exhaustive head model comparison for MEG. *Phys Med Biol* 44: 423-40

Huber G. (1997). The heterogeneous course of schizophrenia. *Schizophr Res* 28: 177-85

Huffaker SJ, Chen J, Nicodemus KK, Sambataro F, Yang F, Mattay V, Lipska BK, Hyde TM, Song J, Rujescu D, Giegling I, Mayilyan K, Proust MJ, Soghoyan A, Caforio G, Callicott JH, Bertolino A, Meyer-Lindenberg A, Chang J, Ji Y, Egan MF, Goldberg TE, Kleinman JE, Lu B, Weinberger DR. (2009). A primate-specific, brain isoform of KCNH2 affects cortical physiology, cognition, neuronal repolarization and risk of schizophrenia. *Nat Med* 15: 509-18

Hutcheson NL, Reid MA, White DM, Kraguljac NV, Avsar KB, Bolding MS, Knowlton RC, den Hollander JA, Lahti AC. (2012). Multimodal analysis of the hippocampus in schizophrenia using proton magnetic resonance spectroscopy and functional magnetic resonance imaging. *Schizophr Res* 140: 136-42

Hyde TM, Lipska BK, Ali T, Mathew SV, Law AJ, Metitiri OE, Straub RE, Ye T, Colantuoni C, Herman MM, Bigelow LB, Weinberger DR, Kleinman JE. (2011). Expression of GABA signaling molecules KCC2, NKCC1, and GAD1 in cortical development and schizophrenia. *J Neurosci* 31: 11088-95

Hyman JM, Hasselmo ME, Seamans JK. (2011). What is the Functional Relevance of Prefrontal Cortex Entrainment to Hippocampal Theta Rhythms? *Front Neurosci* 5: 24

Hyvarinen A. (1999). Fast and robust fixed-point algorithms for independent component analysis. *IEEE Trans Neural Netw* 10: 626-34

II G, Shields J. (1972). *Schizophrenia and Genetics: A Twin Study Vantage Point*. New York: Academic Press.

Ingraham LJ, Kety SS. (2000). Adoption studies of schizophrenia. *Am J Med Genet* 97: 18-22

Ingvar DH, Franzen G. (1974). Abnormalities of cerebral blood flow distribution in patients with chronic schizophrenia. *Acta Psychiatr Scand* 50: 425-62

Iuchi S. (2001). Three classes of C2H2 zinc finger proteins. *Cell Mol Life Sci* 58: 625-35

Jafri MJ, Pearlson GD, Stevens M, Calhoun VD. (2008). A method for functional network connectivity among spatially independent resting-state components in schizophrenia. *Neuroimage* 39: 1666-81

Jessen F, Scherk H, Traber F, Theyson S, Berning J, Tepest R, Falkai P, Schild HH, Maier W, Wagner M, Block W. (2006). Proton magnetic resonance spectroscopy in subjects at risk for schizophrenia. *Schizophr Res* 87: 81-8

Job DE, Whalley HC, McConnell S, Glabus M, Johnstone EC, Lawrie SM. (2002). Structural gray matter differences between first-episode schizophrenics and normal controls using voxel-based morphometry. *Neuroimage* 17: 880-9

Jones MW, Wilson MA. (2005). Theta rhythms coordinate hippocampal-prefrontal interactions in a spatial memory task. *PLoS Biol* 3: e402

Jovicich J, Czanner S, Han X, Salat D, van der Kouwe A, Quinn B, Pacheco J, Albert M, Killiany R, Blacker D, Maguire P, Rosas D, Makris N, Gollub R, Dale A, Dickerson BC, Fischl B. (2009). MRI-derived measurements of human subcortical, ventricular and intracranial brain volumes: Reliability effects of scan sessions, acquisition sequences, data analyses, scanner upgrade, scanner vendors and field strengths. *Neuroimage* 46: 177-92

Jung TP, Makeig S, Westerfield M, Townsend J, Courchesne E, Sejnowski TJ. (2000). Removal of eye activity artifacts from visual event-related potentials in normal and clinical subjects. *Clin Neurophysiol* 111: 1745-58

Kallmann FJ. (1946). The Genetic Theory of Schizophrenia. An Analysis of 691 Schizophrenic Twin Index Families. *Am J Psychiatry* 103

Karlsgodt KH, Sun D, Jimenez AM, Lutkenhoff ES, Willhite R, van Erp TG, Cannon TD. (2008). Developmental disruptions in neural connectivity in the pathophysiology of schizophrenia. *Dev Psychopathol* 20: 1297-327

Khadka S, Meda SA, Stevens MC, Glahn DC, Calhoun VD, Sweeney JA, Tamminga CA, Keshavan MS, O'Neil K, Schretlen D, Pearlson GD. (2013). Is aberrant functional connectivity a psychosis endophenotype? A resting state functional magnetic resonance imaging study. *Biol Psychiatry* 74: 458-66

Kim AH, Parker EK, Williamson V, McMichael GO, Fanous AH, Vladimirov VI. (2012). Experimental validation of candidate schizophrenia gene ZNF804A as target for hsa-miR-137. *Schizophr Res* 141: 60-4

Kleinman JE, Casanova MF, Jaskiw GE. (1988). The neuropathology of schizophrenia. *Schizophr Bull* 14: 209-16

Kleinman JE, Law AJ, Lipska BK, Hyde TM, Ellis JK, Harrison PJ, Weinberger DR. (2011). Genetic neuropathology of schizophrenia: new approaches to an old question and new uses for postmortem human brains. *Biol Psychiatry* 69: 140-5

Koten JW, Jr., Wood G, Hagoort P, Goebel R, Propping P, Willmes K, Boomsma DI. (2009). Genetic contribution to variation in cognitive function: an FMRI study in twins. *Science* 323: 1737-40

Kuswanto CN, Woon PS, Zheng XB, Qiu A, Sitoh YY, Chan YH, Liu J, Williams H, Ong WY, Sim K. (2012). Genome-wide supported psychosis risk variant in ZNF804A gene and impact on cortico-limbic WM integrity in schizophrenia. *Am J Med Genet B Neuropsychiatr Genet* 159b: 255-62

Ladomery M, Dellaire G. (2002). Multifunctional zinc finger proteins in development and disease. *Ann Hum Genet* 66: 331-42

Laufs H, Kleinschmidt A, Beyerle A, Eger E, Salek-Haddadi A, Preibisch C, Krakow K. (2003). EEG-correlated fMRI of human alpha activity. *Neuroimage* 19: 1463-76

Law AJ, Harrison PJ. (2003). The distribution and morphology of prefrontal cortex pyramidal neurons identified using anti-neurofilament antibodies SMI32, N200 and FNP7. Normative data and a comparison in subjects with schizophrenia, bipolar disorder or major depression. *J Psychiatr Res* 37: 487-99

Law AJ, Lipska BK, Weickert CS, Hyde TM, Straub RE, Hashimoto R, Harrison PJ, Kleinman JE, Weinberger DR. (2006). Neuregulin 1 transcripts are differentially expressed in schizophrenia and regulated by 5' SNPs associated with the disease. *Proc Natl Acad Sci U S A* 103: 6747-52

Law AJ, Kleinman JE, Weinberger DR, Weickert CS. (2007). Disease-associated intronic variants in the ErbB4 gene are related to altered ErbB4 splice-variant expression in the brain in schizophrenia. *Hum Mol Genet* 16: 129-41

Lawrie SM, Abukmeil SS. (1998). Brain abnormality in schizophrenia. A systematic and quantitative review of volumetric magnetic resonance imaging studies. *Br J Psychiatry* 172: 110-20

Lawrie SM, Pantelis C. (2011). Structural brain imaging in schizophrenia and related populations. In: *Schizophrenia*, ed. DR Weinberger, PJ Harrison, pp. 334-52. Oxford: Blackwell

Lencz T, Szeszko PR, DeRosse P, Burdick KE, Bromet EJ, Bilder RM, Malhotra AK. (2010). A schizophrenia risk gene, ZNF804A, influences neuroanatomical and neurocognitive phenotypes. *Neuropsychopharmacology* 35: 2284-91

Lewis DA, Levitt P. (2002). Schizophrenia as a disorder of neurodevelopment. *Annu Rev Neurosci* 25: 409-32

Lewis DA, Glantz LA, Pierri JN, Sweet RA. (2003). Altered cortical glutamate neurotransmission in schizophrenia: evidence from morphological studies of pyramidal neurons. *Ann N Y Acad Sci* 1003: 102-12

Lin M, Pedrosa E, Shah A, Hrabovsky A, Maqbool S, Zheng D, Lachman HM. (2011). RNA-Seq of human neurons derived from iPS cells reveals candidate long non-coding RNAs involved in neurogenesis and neuropsychiatric disorders. *PLoS One* 6: e23356

Lisman J. (2012). Excitation, inhibition, local oscillations, or large-scale loops: what causes the symptoms of schizophrenia? *Curr Opin Neurobiol* 22: 537-44

Liu H, Kaneko Y, Ouyang X, Li L, Hao Y, Chen EY, Jiang T, Zhou Y, Liu Z. (2012). Schizophrenic patients and their unaffected siblings share increased resting-state connectivity in the task-negative network but not its anticorrelated task-positive network. *Schizophr Bull* 38: 285-94

Liu YL, Fann CS, Liu CM, Chang CC, Yang WC, Hung SI, Yu SL, Hwang TJ, Hsieh MH, Liu CC, Tsuang MM, Wu JY, Jou YS, Faraone SV, Tsuang MT, Chen WJ, Hwu HG. (2007). More evidence supports the association of PPP3CC with schizophrenia. *Mol Psychiatry* 12: 966-74

Logothetis NK, Pauls J, Augath M, Trinath T, Oeltermann A. (2001). Neurophysiological investigation of the basis of the fMRI signal. *Nature* 412: 150-7

Logothetis NK. (2008). What we can do and what we cannot do with fMRI. *Nature* 453: 869-78

Luckhoo H, Hale JR, Stokes MG, Nobre AC, Morris PG, Brookes MJ, Woolrich MW. (2012). Inferring task-related networks using independent component analysis in magnetoencephalography. *Neuroimage* 62: 530-41

Luckhoo H, Brookes MJ, Baker AB, Smith SM, Duff EP, Heise V, Mackay CE, Woolrich MW. (submitted). A framework for group comparisons of functional networks in MEG using ICA and Dual Regression.

Lutkenhoff ES, van Erp TG, Thomas MA, Therman S, Manninen M, Huttunen MO, Kaprio J, Lonnqvist J, O'Neill J, Cannon TD. (2010). Proton MRS in twin pairs discordant for schizophrenia. *Mol Psychiatry* 15: 308-18

Maddock RJ, Buonocore MH. (2012). MR Spectroscopic Studies of the Brain in Psychiatric Disorders. *Curr Top Behav Neurosci*

Malhotra AK, Goldman D. (1999). Benefits and pitfalls encountered in psychiatric genetic association studies. *Biol Psychiatry* 45: 544-50

Maris E, Oostenveld R. (2007). Nonparametric statistical testing of EEG- and MEG-data. *J Neurosci Methods* 164: 177-90

Maynard TM, Sikich L, Lieberman JA, LaMantia AS. (2001). Neural development, cell-cell signaling, and the "two-hit" hypothesis of schizophrenia. *Schizophr Bull* 27: 457-76

McIntosh A, Lawrie S. (2004). Structural magnetic resonance imaging. In: *Schizophrenia: From Neuroimaging to Neuroscience*, ed. S Lawrie, EC Johnstone, DR Weinberger, pp. 21-57. Oxford: Oxford University Press

McIntosh AM, Baig BJ, Hall J, Job D, Whalley HC, Lymer GK, Moorhead TW, Owens DG, Miller P, Porteous D, Lawrie SM, Johnstone EC. (2007). Relationship of catechol-O-methyltransferase variants to brain structure and function in a population at high risk of psychosis. *Biol Psychiatry* 61: 1127-34

McIntosh AM, Moorhead TW, Job D, Lymer GK, Munoz Maniega S, McKirdy J, Sussmann JE, Baig BJ, Bastin ME, Porteous D, Evans KL, Johnstone EC, Lawrie SM, Hall J. (2008). The effects of a neuregulin 1 variant on white matter density and integrity. *Mol Psychiatry* 13: 1054-9

Meda SA, Gill A, Stevens MC, Lorenzoni RP, Glahn DC, Calhoun VD, Sweeney JA, Tamminga CA, Keshavan MS, Thaker G, Pearlson GD. (2012). Differences in resting-state functional magnetic resonance imaging functional network connectivity between schizophrenia and psychotic bipolar probands and their unaffected first-degree relatives. *Biol Psychiatry* 71: 881-9

Mekle R, Mlynarik V, Gambarota G, Hergt M, Krueger G, Gruetter R. (2009). MR spectroscopy of the human brain with enhanced signal intensity at ultrashort echo times on a clinical platform at 3T and 7T. *Magn Reson Med* 61: 1279-85

Meltzer JA, Zaveri HP, Goncharova, II, Distasio MM, Papademetris X, Spencer SS, Spencer DD, Constable RT. (2008). Effects of working memory load on oscillatory power in human intracranial EEG. *Cereb Cortex* 18: 1843-55

Meyer-Lindenberg A, Poline JB, Kohn PD, Holt JL, Egan MF, Weinberger DR, Berman KF. (2001). Evidence for abnormal cortical functional connectivity during working memory in schizophrenia. *Am J Psychiatry* 158: 1809-17

Meyer-Lindenberg A, Weinberger DR. (2006). Intermediate phenotypes and genetic mechanisms of psychiatric disorders. *Nat Rev Neurosci* 7: 818-27

Meyer-Lindenberg A, Nicodemus KK, Egan MF, Callicott JH, Mattay V, Weinberger DR. (2008). False positives in imaging genetics. *Neuroimage* 40: 655-61

Meyer-Lindenberg A, Bullmore E. (2011). Functional brain imaging in schizophrenia. In: *Schizophrenia*, ed. DR Weinberger, PJ Harrison, pp. 353-71. Oxford: Blackwell

Meyer-Lindenberg AS, Olsen RK, Kohn PD, Brown T, Egan MF, Weinberger DR, Berman KF. (2005). Regionally specific disturbance of dorsolateral prefrontal-hippocampal functional connectivity in schizophrenia. *Arch Gen Psychiatry* 62: 379-86

Michels L, Martin E, Klaver P, Edden R, Zelaya F, Lythgoe DJ, Luchinger R, Brandeis D, O'Gorman RL. (2012). Frontal GABA levels change during working memory. *PLoS One* 7: e31933

Mier D, Kirsch P, Meyer-Lindenberg A. (2010). Neural substrates of pleiotropic action of genetic variation in COMT: a meta-analysis. *Mol Psychiatry* 15: 918-27

Millar JK, Christie S, Semple CA, Porteous DJ. (2000). Chromosomal location and genomic structure of the human translin-associated factor X gene (TRAX; TSNAX) revealed by intergenic splicing to DISC1, a gene disrupted by a translocation segregating with schizophrenia. *Genomics* 67: 69-77

Minzenberg MJ, Laird AR, Thelen S, Carter CS, Glahn DC. (2009). Meta-analysis of 41 functional neuroimaging studies of executive function in schizophrenia. *Arch Gen Psychiatry* 66: 811-22

Mitkus SN, Hyde TM, Vakkalanka R, Kolachana B, Weinberger DR, Kleinman JE, Lipska BK. (2008). Expression of oligodendrocyte-associated genes in dorsolateral prefrontal cortex of patients with schizophrenia. *Schizophr Res* 98: 129-38

Mlynarik V, Gambarota G, Frenkel H, Gruetter R. (2006). Localized short-echo-time proton MR spectroscopy with full signal-intensity acquisition. *Magn Reson Med* 56: 965-70

Morris HM, Stopczynski RE, Lewis DA. (2009). NPY mRNA expression in the prefrontal cortex: Selective reduction in the superficial white matter of subjects with schizoaffective disorder. *Schizophr Res* 115: 261-9

Munafo MR, Brown SM, Hariri AR. (2008). Serotonin transporter (5-HTTLPR) genotype and amygdala activation: a meta-analysis. *Biol Psychiatry* 63: 852-7

Murray RM, Lewis SW. (1987). Is schizophrenia a neurodevelopmental disorder? *Br Med J (Clin Res Ed)* 295: 681-2

Muthukumaraswamy SD, Singh KD. (2008). Spatiotemporal frequency tuning of BOLD and gamma band MEG responses compared in primary visual cortex. *Neuroimage* 40: 1552-60

Muthukumaraswamy SD, Edden RA, Jones DK, Swettenham JB, Singh KD. (2009). Resting GABA concentration predicts peak gamma frequency and fMRI amplitude in response to visual stimulation in humans. *Proc Natl Acad Sci U S A* 106: 8356-61

Muthukumaraswamy SD, Singh KD. (2009). Functional decoupling of BOLD and gamma-band amplitudes in human primary visual cortex. *Hum Brain Mapp* 30: 2000-7

Muthukumaraswamy SD, Evans CJ, Edden RA, Wise RG, Singh KD. (2012a). Individual variability in the shape and amplitude of the BOLD-HRF correlates with endogenous GABAergic inhibition. *Hum Brain Mapp* 33: 455-65

Muthukumaraswamy SD, Myers JF, Wilson SJ, Nutt DJ, Lingford-Hughes A, Singh KD, Hamandi K. (2012b). The effects of elevated endogenous GABA levels on movement-related network oscillations. *Neuroimage* 66c: 36-41

Nakata K, Lipska BK, Hyde TM, Ye T, Newburn EN, Morita Y, Vakkalanka R, Barenboim M, Sei Y, Weinberger DR, Kleinman JE. (2009). DISC1 splice variants are upregulated in schizophrenia and associated with risk polymorphisms. *Proc Natl Acad Sci U S A* 106: 15873-8

Narr KL, Bilder RM, Toga AW, Woods RP, Rex DE, Szeszko PR, Robinson D, Sevy S, Gunduz-Bruce H, Wang YP, DeLuca H, Thompson PM. (2005). Mapping cortical thickness and gray matter concentration in first episode schizophrenia. *Cereb Cortex* 15: 708-19

Near J, Andersson J, Maron E, Mekle R, Gruetter R, Cowen P, Jezzard P. (2013). Unedited in vivo detection and quantification of gamma-aminobutyric acid in the occipital cortex using short-TE MRS at 3 T. *NMR Biomed*

Nelson MD, Saykin AJ, Flashman LA, Riordan HJ. (1998). Hippocampal volume reduction in schizophrenia as assessed by magnetic resonance imaging: a meta-analytic study. *Arch Gen Psychiatry* 55: 433-40

Ng MY, Levinson DF, Faraone SV, Suarez BK, DeLisi LE, Arinami T, Riley B, Paunio T, Pulver AE, Irmansyah, Holmans PA, Escamilla M, Wildenauer DB, Williams NM, Laurent C, Mowry BJ, Brzustowicz LM, Maziade M, Sklar P, Garver DL, Abecasis GR, Lerer B, Fallin MD, Gurling HM, Gejman PV, Lindholm E, Moises HW, Byerley W, Wijsman EM, Forabosco P, Tsuang MT, Hwu HG, Okazaki Y, Kendler KS, Wormley B, Fanous A, Walsh D, O'Neill FA, Peltonen L, Nestadt G, Lasseter VK, Liang KY, Papadimitriou GM, Dikeos DG, Schwab SG, Owen MJ, O'Donovan MC, Norton N, Hare E, Raventos H, Nicolini H, Albus M, Maier W,

Nimgaonkar VL, Terenius L, Mallet J, Jay M, Godard S, Nertney D, Alexander M, Crowe RR, Silverman JM, Bassett AS, Roy MA, Merette C, Pato CN, Pato MT, Roos JL, Kohn Y, Amann-Zalcenstein D, Kalsi G, McQuillin A, Curtis D, Brynjolfson J, Sigmundsson T, Petursson H, Sanders AR, Duan J, Jazin E, Myles-Worsley M, Karayiorgou M, Lewis CM. (2009). Meta-analysis of 32 genome-wide linkage studies of schizophrenia. *Mol Psychiatry* 14: 774-85

Nicodemus KK, Law AJ, Radulescu E, Luna A, Kolachana B, Vakkalanka R, Rujescu D, Giegling I, Straub RE, McGee K, Gold B, Dean M, Muglia P, Callicott JH, Tan HY, Weinberger DR. (2010). Biological validation of increased schizophrenia risk with NRG1, ERBB4, and AKT1 epistasis via functional neuroimaging in healthy controls. *Arch Gen Psychiatry* 67: 991-1001

Niessing J, Ebisch B, Schmidt KE, Niessing M, Singer W, Galuske RA. (2005). Hemodynamic signals correlate tightly with synchronized gamma oscillations. *Science* 309: 948-51

Nixon DC, Prust MJ, Sambataro F, Tan HY, Mattay VS, Weinberger DR, Callicott JH. (2011). Interactive effects of DAOA (G72) and catechol-O-methyltransferase on neurophysiology in prefrontal cortex. *Biol Psychiatry* 69: 1006-8

Nolte G. (2003). The magnetic lead field theorem in the quasi-static approximation and its use for magnetoencephalography forward calculation in realistic volume conductors. *Phys Med Biol* 48: 3637-52

Northoff G, Walter M, Schulte RF, Beck J, Dydak U, Henning A, Boeker H, Grimm S, Boesiger P. (2007). GABA concentrations in the human anterior cingulate cortex predict negative BOLD responses in fMRI. *Nat Neurosci* 10: 1515-7

O'Connell G, Lawrie SM, McIntosh AM, Hall J. (2011). Schizophrenia risk genes: Implications for future drug development and discovery. *Biochem Pharmacol* 81: 1367-73

O'Donovan MC, Craddock N, Norton N, Williams H, Peirce T, Moskvina V, Nikolov I, Hamshere M, Carroll L, Georgieva L, Dwyer S, Holmans P, Marchini JL, Spencer CC, Howie B, Leung HT, Hartmann AM, Moller HJ, Morris DW, Shi Y, Feng G, Hoffmann P, Propping P, Vasilescu C, Maier W, Rietschel M, Zammit S, Schumacher J, Quinn EM, Schulze TG, Williams NM, Giegling I, Iwata N, Ikeda M, Darvasi A, Shifman S, He L, Duan J, Sanders AR, Levinson DF, Gejman PV, Cichon S, Nothen MM, Gill M, Corvin A, Rujescu D, Kirov G, Owen MJ, Buccola NG, Mowry BJ, Freedman R, Amin F, Black DW, Silverman JM, Byerley WF, Cloninger CR. (2008). Identification of loci associated with schizophrenia by genome-wide association and follow-up. *Nat Genet* 40: 1053-5

O'Reilly JX, Woolrich MW, Behrens TE, Smith SM, Johansen-Berg H. (2012). Tools of the trade: psychophysiological interactions and functional connectivity. *Soc Cogn Affect Neurosci* 7: 604-9

Ohrmann P, Siegmund A, Suslow T, Spitzberg K, Kersting A, Arolt V, Heindel W, Pfleiderer B. (2005). Evidence for glutamatergic neuronal dysfunction in the prefrontal cortex in chronic but not in first-episode patients with schizophrenia: a proton magnetic resonance spectroscopy study. *Schizophr Res* 73: 153-7

Okada T, Hashimoto R, Yamamori H, Umeda-Yano S, Yasuda Y, Ohi K, Fukumoto M, Ikemoto K, Kunii Y, Tomita H, Ito A, Takeda M. (2012). Expression analysis of a novel mRNA variant of the schizophrenia risk gene ZNF804A. *Schizophr Res* 141: 277-8

Olbrich HM, Valerius G, Rusch N, Buchert M, Thiel T, Hennig J, Ebert D, Van Elst LT. (2008). Frontolimbic glutamate alterations in first episode schizophrenia: evidence from a magnetic resonance spectroscopy study. *World J Biol Psychiatry* 9: 59-63

Ongur D, Drevets WC, Price JL. (1998). Glial reduction in the subgenual prefrontal cortex in mood disorders. *Proc Natl Acad Sci U S A* 95: 13290-5

Oostenveld R, Fries P, Maris E, Schoffelen JM. (2011). FieldTrip: Open source software for advanced analysis of MEG, EEG, and invasive electrophysiological data. *Comput Intell Neurosci* 2011: 156869

Owen AM, McMillan KM, Laird AR, Bullmore E. (2005). N-back working memory paradigm: a meta-analysis of normative functional neuroimaging studies. *Hum Brain Mapp* 25: 46-59

Owen AM, Schiff ND, Laureys S. (2009). A new era of coma and consciousness science. *Prog Brain Res* 177: 399-411

Pakkenberg B. (1993). Total nerve cell number in neocortex in chronic schizophrenics and controls estimated using optical disectors. *Biol Psychiatry* 34: 768-72

Palva JM, Monto S, Kulashekhar S, Palva S. (2010). Neuronal synchrony reveals working memory networks and predicts individual memory capacity. *Proc Natl Acad Sci U S A* 107: 7580-5

Patenaude B, Smith SM, Kennedy DN, Jenkinson M. (2011). A Bayesian model of shape and appearance for subcortical brain segmentation. *Neuroimage* 56: 907-22

Paulus FM, Bedenbender J, Krach S, Pyka M, Krug A, Sommer J, Mette M, Nothen MM, Witt SH, Rietschel M, Kircher T, Jansen A. (2013a). Association of rs1006737 in CACNA1C with alterations in prefrontal activation and fronto-hippocampal connectivity. *Hum Brain Mapp*

Paulus FM, Krach S, Bedenbender J, Pyka M, Sommer J, Krug A, Knake S, Nothen MM, Witt SH, Rietschel M, Kircher T, Jansen A. (2013b). Partial support for ZNF804A genotype-dependent alterations in prefrontal connectivity. *Hum Brain Mapp* 34: 304-13

Pedone PV, Ghirlando R, Clore GM, Gronenborn AM, Felsenfeld G, Omichinski JG. (1996). The single Cys2-His2 zinc finger domain of the GAGA protein flanked by basic residues is sufficient for high-affinity specific DNA binding. *Proc Natl Acad Sci U S A* 93: 2822-6

Pedrosa E, Sandler V, Shah A, Carroll R, Chang C, Rockowitz S, Guo X, Zheng D, Lachman HM. (2011). Development of patient-specific neurons in schizophrenia using induced pluripotent stem cells. *J Neurogenet* 25: 88-103

Pierri JN, Volk CL, Auh S, Sampson A, Lewis DA. (2001). Decreased somal size of deep layer 3 pyramidal neurons in the prefrontal cortex of subjects with schizophrenia. *Arch Gen Psychiatry* 58: 466-73

Plambeck CA, Kwan AH, Adams DJ, Westman BJ, van der Weyden L, Medcalf RL, Morris BJ, Mackay JP. (2003). The structure of the zinc finger domain from human splicing factor ZNF265 fold. *J Biol Chem* 278: 22805-11

Potash JB, Buervenich S, Cox NJ, Zandi PP, Akula N, Steele J, Rathe JA, Avramopoulos D, Detera-Wadleigh SD, Gershon ES, DePaulo JR, Jr., Feinberg AP, McMahon FJ. (2008). Gene-based SNP mapping of a psychotic bipolar affective disorder linkage region on 22q12.3: association with HMG2L1 and TOM1. *Am J Med Genet B Neuropsychiatr Genet* 147b: 59-67

Provencher SW. (1993). Estimation of metabolite concentrations from localized in vivo proton NMR spectra. *Magn Reson Med* 30: 672-9

Quraan MA, Moses SN, Hung Y, Mills T, Taylor MJ. (2011). Detection and localization of hippocampal activity using beamformers with MEG: a detailed investigation using simulations and empirical data. *Hum Brain Mapp* 32: 812-27

Raichle ME, MacLeod AM, Snyder AZ, Powers WJ, Gusnard DA, Shulman GL. (2001). A default mode of brain function. *Proc Natl Acad Sci U S A* 98: 676-82

Rajkowska G, Selemon LD, Goldman-Rakic PS. (1998). Neuronal and glial somal size in the prefrontal cortex: a postmortem morphometric study of schizophrenia and Huntington disease. *Arch Gen Psychiatry* 55: 215-24
Rapoport JL, Addington A, Frangou S. (2005). The neurodevelopmental model of schizophrenia: what can very early onset cases tell us? *Curr Psychiatry Rep* 7: 81-2
Rasetti R, Sambataro F, Chen Q, Callicott JH, Mattay VS, Weinberger DR. (2011). Altered cortical network dynamics: a potential intermediate phenotype for schizophrenia and association with ZNF804A. *Arch Gen Psychiatry* 68: 1207-17
Ray S, Maunsell JH. (2010). Differences in gamma frequencies across visual cortex restrict their possible use in computation. *Neuron* 67: 885-96
Ray S, Maunsell JH. (2011). Different origins of gamma rhythm and high-gamma activity in macaque visual cortex. *PLoS Biol* 9: e1000610
Redpath HL, Lawrie SM, Sprooten E, Whalley HC, McIntosh AM, Hall J. (2013). Progress in imaging the effects of psychosis susceptibility gene variants. *Expert Rev Neurother* 13: 37-47
Rees E, Kirov G, O'Donovan MC, Owen MJ. (2012). De novo mutation in schizophrenia. *Schizophr Bull* 38: 377-81
Ren W, Lui S, Deng W, Li F, Li M, Huang X, Wang Y, Li T, Sweeney JA, Gong Q. (2013). Anatomical and Functional Brain Abnormalities in Drug-Naive First-Episode Schizophrenia. *Am J Psychiatry*
Repovs G, Csernansky JG, Barch DM. (2011). Brain network connectivity in individuals with schizophrenia and their siblings. *Biol Psychiatry* 69: 967-73
Repovs G, Barch DM. (2012). Working memory related brain network connectivity in individuals with schizophrenia and their siblings. *Front Hum Neurosci* 6: 137
Riley B, Thiselton D, Maher BS, Bigdeli T, Wormley B, McMichael GO, Fanous AH, Vladimirov V, O'Neill FA, Walsh D, Kendler KS. (2010). Replication of association between schizophrenia and ZNF804A in the Irish Case-Control Study of Schizophrenia sample. *Mol Psychiatry* 15: 29-37
Rodriguez-Murillo L, Gogos JA, Karayiorgou M. (2012). The genetic architecture of schizophrenia: new mutations and emerging paradigms. *Annu Rev Med* 63: 63-80
Rosenthal D, Wender PH, Kety SS, Welner J, Schulsinger F. (1971). The adopted-away offspring of schizophrenics. *Am J Psychiatry* 128: 307-11
Ross CA, Margolis RL, Reading SA, Pletnikov M, Coyle JT. (2006). Neurobiology of schizophrenia. *Neuron* 52: 139-53
Roux F, Wibral M, Mohr HM, Singer W, Uhlhaas PJ. (2012). Gamma-band activity in human prefrontal cortex codes for the number of relevant items maintained in working memory. *J Neurosci* 32: 12411-20
Rusch N, Tebartz van Elst L, Valerius G, Buchert M, Thiel T, Ebert D, Hennig J, Olbrich HM. (2008). Neurochemical and structural correlates of executive dysfunction in schizophrenia. *Schizophr Res* 99: 155-63
Sartorius LJ, Weinberger DR, Hyde TM, Harrison PJ, Kleinman JE, Lipska BK. (2008). Expression of a GRM3 splice variant is increased in the dorsolateral prefrontal cortex of individuals carrying a schizophrenia risk SNP. *Neuropsychopharmacology* 33: 2626-34
Saxena N, Muthukumaraswamy SD, Diukova A, Singh K, Hall J, Wise R. (2013). Enhanced stimulus-induced gamma activity in humans during propofol-induced sedation. *PLoS One* 8: e57685
Saykin AJ, Shtasel DL, Gur RE, Kester DB, Mozley LH, Stafiniak P, Gur RC. (1994). Neuropsychological deficits in neuroleptic naive patients with first-episode schizophrenia. *Arch Gen Psychiatry* 51: 124-31

Scheeringa R, Bastiaansen MC, Petersson KM, Oostenveld R, Norris DG, Hagoort P. (2008). Frontal theta EEG activity correlates negatively with the default mode network in resting state. *Int J Psychophysiol* 67: 242-51

Scheeringa R, Petersson KM, Oostenveld R, Norris DG, Hagoort P, Bastiaansen MC. (2009). Trial-by-trial coupling between EEG and BOLD identifies networks related to alpha and theta EEG power increases during working memory maintenance. *Neuroimage* 44: 1224-38

Scheeringa R, Fries P, Petersson KM, Oostenveld R, Grothe I, Norris DG, Hagoort P, Bastiaansen MC. (2011). Neuronal dynamics underlying high- and low-frequency EEG oscillations contribute independently to the human BOLD signal. *Neuron* 69: 572-83

Schmiedt C, Brand A, Hildebrandt H, Basar-Eroglu C. (2005). Event-related theta oscillations during working memory tasks in patients with schizophrenia and healthy controls. *Brain Res Cogn Brain Res* 25: 936-47

Schnell K, Heekeren K, Daumann J, Schnell T, Schnitker R, Moller-Hartmann W, Gouzoulis-Mayfrank E. (2008). Correlation of passivity symptoms and dysfunctional visuomotor action monitoring in psychosis. *Brain* 131: 2783-97

Schoffelen JM, Oostenveld R, Fries P. (2008). Imaging the human motor system's beta-band synchronization during isometric contraction. *Neuroimage* 41: 437-47

Schultz CC, Koch K, Wagner G, Roebel M, Nenadic I, Schachtzabel C, Reichenbach JR, Sauer H, Schlosser RG. (2010). Complex pattern of cortical thinning in schizophrenia: results from an automated surface based analysis of cortical thickness. *Psychiatry Res* 182: 134-40

Sei Y, Ren-Patterson R, Li Z, Tunbridge EM, Egan MF, Kolachana BS, Weinberger DR. (2007). Neuregulin1-induced cell migration is impaired in schizophrenia: association with neuregulin1 and catechol-o-methyltransferase gene polymorphisms. *Mol Psychiatry* 12: 946-57

Selemon LD, Rajkowska G, Goldman-Rakic PS. (1998). Elevated neuronal density in prefrontal area 46 in brains from schizophrenic patients: application of a three-dimensional, stereologic counting method. *J Comp Neurol* 392: 402-12

Selemon LD, Goldman-Rakic PS. (1999). The reduced neuropil hypothesis: a circuit based model of schizophrenia. *Biol Psychiatry* 45: 17-25

Shapleske J, Rossell SL, Woodruff PW, David AS. (1999). The planum temporale: a systematic, quantitative review of its structural, functional and clinical significance. *Brain Res Brain Res Rev* 29: 26-49

Sharma T, Lancaster E, Lee D, Lewis S, Sigmundsson T, Takei N, Gurling H, Barta P, Pearlson G, Murray R. (1998). Brain changes in schizophrenia. Volumetric MRI study of families multiply affected with schizophrenia--the Maudsley Family Study 5. *Br J Psychiatry* 173: 132-8

Shaw A, Brealy J, Richardson H, Muthukumaraswamy SD, Edden RA, John Evans C, Puts NA, Singh KD, Keedwell PA. (2013). Marked reductions in visual evoked responses but not gamma-aminobutyric acid concentrations or gamma-band measures in remitted depression. *Biol Psychiatry* 73: 691-8

Shenton ME, Dickey CC, Frumin M, McCarley RW. (2001). A review of MRI findings in schizophrenia. *Schizophr Res* 49: 1-52

Siapas AG, Lubenov EV, Wilson MA. (2005). Prefrontal phase locking to hippocampal theta oscillations. *Neuron* 46: 141-51

Sigurdsson T, Stark KL, Karayiorgou M, Gogos JA, Gordon JA. (2010). Impaired hippocampal-prefrontal synchrony in a genetic mouse model of schizophrenia. *Nature* 464: 763-7

Slater E, Shields J. (1953). *Psychotic and neurotic illnesses in Twins*. London: Her Majesty's Stationary Office.
Slonimsky A, Levy I, Kohn Y, Rigbi A, Ben-Asher E, Lancet D, Agam G, Lerer B. (2010). Lymphoblast and brain expression of AHI1 and the novel primate-specific gene, C6orf217, in schizophrenia and bipolar disorder. *Schizophr Res* 120: 159-66
Smiley JF, Rosoklija G, Mancevski B, Mann JJ, Dwork AJ, Javitt DC. (2009). Altered volume and hemispheric asymmetry of the superficial cortical layers in the schizophrenia planum temporale. *Eur J Neurosci* 30: 449-63
Smiley JF, Rosoklija G, Mancevski B, Pergolizzi D, Figarsky K, Bleiwas C, Duma A, Mann JJ, Javitt DC, Dwork AJ. (2011). Hemispheric comparisons of neuron density in the planum temporale of schizophrenia and nonpsychiatric brains. *Psychiatry Res* 192: 1-11
Smiley JF, Konnova K, Bleiwas C. (2012). Cortical thickness, neuron density and size in the inferior parietal lobe in schizophrenia. *Schizophr Res* 136: 43-50
Smith SM, Jenkinson M, Woolrich MW, Beckmann CF, Behrens TE, Johansen-Berg H, Bannister PR, De Luca M, Drobnjak I, Flitney DE, Niazy RK, Saunders J, Vickers J, Zhang Y, De Stefano N, Brady JM, Matthews PM. (2004). Advances in functional and structural MR image analysis and implementation as FSL. *Neuroimage* 23 Suppl 1: S208-19
Smith SM, Fox PT, Miller KL, Glahn DC, Fox PM, Mackay CE, Filippini N, Watkins KE, Toro R, Laird AR, Beckmann CF. (2009). Correspondence of the brain's functional architecture during activation and rest. *Proc Natl Acad Sci U S A* 106: 13040-5
Spence SA, Brooks DJ, Hirsch SR, Liddle PF, Meehan J, Grasby PM. (1997). A PET study of voluntary movement in schizophrenic patients experiencing passivity phenomena (delusions of alien control). *Brain* 120 (Pt 11): 1997-2011
Spencer KM, Nestor PG, Niznikiewicz MA, Salisbury DF, Shenton ME, McCarley RW. (2003). Abnormal neural synchrony in schizophrenia. *J Neurosci* 23: 7407-11
Spencer KM, Nestor PG, Perlmutter R, Niznikiewicz MA, Klump MC, Frumin M, Shenton ME, McCarley RW. (2004). Neural synchrony indexes disordered perception and cognition in schizophrenia. *Proc Natl Acad Sci U S A* 101: 17288-93
Spencer KM, Salisbury DF, Shenton ME, McCarley RW. (2008). Gamma-band auditory steady-state responses are impaired in first episode psychosis. *Biol Psychiatry* 64: 369-75
Sprooten E, McIntosh AM, Lawrie SM, Hall J, Sussmann JE, Dahmen N, Konrad A, Bastin ME, Winterer G. (2012). An investigation of a genomewide supported psychosis variant in ZNF804A and white matter integrity in the human brain. *Magn Reson Imaging* 30: 1373-80
Stagg CJ, Bachtiar V, Johansen-Berg H. (2011a). What are we measuring with GABA magnetic resonance spectroscopy? *Commun Integr Biol* 4: 573-5
Stagg CJ, Bestmann S, Constantinescu AO, Moreno LM, Allman C, Mekle R, Woolrich M, Near J, Johansen-Berg H, Rothwell JC. (2011b). Relationship between physiological measures of excitability and levels of glutamate and GABA in the human motor cortex. *J Physiol* 589: 5845-55
Stanley JA, Williamson PC, Drost DJ, Rylett RJ, Carr TJ, Malla A, Thompson RT. (1996). An in vivo proton magnetic resonance spectroscopy study of schizophrenia patients. *Schizophr Bull* 22: 597-609
Steen RG, Hamer RM, Lieberman JA. (2005). Measurement of brain metabolites by 1H magnetic resonance spectroscopy in patients with schizophrenia: a systematic review and meta-analysis. *Neuropsychopharmacology* 30: 1949-62

Stefansson H, Sigurdsson E, Steinthorsdottir V, Bjornsdottir S, Sigmundsson T, Ghosh S, Brynjolfsson J, Gunnarsdottir S, Ivarsson O, Chou TT, Hjaltason O, Birgisdottir B, Jonsson H, Gudnadottir VG, Gudmundsdottir E, Bjornsson A, Ingvarsson B, Ingason A, Sigfusson S, Hardardottir H, Harvey RP, Lai D, Zhou M, Brunner D, Mutel V, Gonzalo A, Lemke G, Sainz J, Johannesson G, Andresson T, Gudbjartsson D, Manolescu A, Frigge ML, Gurney ME, Kong A, Gulcher JR, Petursson H, Stefansson K. (2002). Neuregulin 1 and susceptibility to schizophrenia. *Am J Hum Genet* 71: 877-92

Steinberg S, Mors O, Borglum AD, Gustafsson O, Werge T, Mortensen PB, Andreassen OA, Sigurdsson E, Thorgeirsson TE, Bottcher Y, Olason P, Ophoff RA, Cichon S, Gudjonsdottir IH, Pietilainen OP, Nyegaard M, Tuulio-Henriksson A, Ingason A, Hansen T, Athanasiu L, Suvisaari J, Lonnqvist J, Paunio T, Hartmann A, Jurgens G, Nordentoft M, Hougaard D, Norgaard-Pedersen B, Breuer R, Moller HJ, Giegling I, Glenthoj B, Rasmussen HB, Mattheisen M, Bitter I, Rethelyi JM, Sigmundsson T, Fossdal R, Thorsteinsdottir U, Ruggeri M, Tosato S, Strengman E, Kiemeney LA, Melle I, Djurovic S, Abramova L, Kaleda V, Walshe M, Bramon E, Vassos E, Li T, Fraser G, Walker N, Toulopoulou T, Yoon J, Freimer NB, Cantor RM, Murray R, Kong A, Golimbet V, Jonsson EG, Terenius L, Agartz I, Petursson H, Nothen MM, Rietschel M, Peltonen L, Rujescu D, Collier DA, Stefansson H, St Clair D, Stefansson K. (2011). Expanding the range of ZNF804A variants conferring risk of psychosis. *Mol Psychiatry* 16: 59-66

Stern AJ, Savostyanova AA, Goldman A, Barnett AS, van der Veen JW, Callicott JH, Mattay VS, Weinberger DR, Marenco S. (2008). Impact of the brain-derived neurotrophic factor Val66Met polymorphism on levels of hippocampal N-acetyl-aspartate assessed by magnetic resonance spectroscopic imaging at 3 Tesla. *Biol Psychiatry* 64: 856-62

Stevens AA, Goldman-Rakic PS, Gore JC, Fulbright RK, Wexler BE. (1998). Cortical dysfunction in schizophrenia during auditory word and tone working memory demonstrated by functional magnetic resonance imaging. *Arch Gen Psychiatry* 55: 1097-103

Straub RE, Lipska BK, Egan MF, Goldberg TE, Callicott JH, Mayhew MB, Vakkalanka RK, Kolachana BS, Kleinman JE, Weinberger DR. (2007). Allelic variation in GAD1 (GAD67) is associated with schizophrenia and influences cortical function and gene expression. *Mol Psychiatry* 12: 854-69

Suddath RL, Christison GW, Torrey EF, Casanova MF, Weinberger DR. (1990). Anatomical abnormalities in the brains of monozygotic twins discordant for schizophrenia. *N Engl J Med* 322: 789-94

Sullivan PF, Kendler KS, Neale MC. (2003). Schizophrenia as a complex trait: evidence from a meta-analysis of twin studies. *Arch Gen Psychiatry* 60: 1187-92

Susser E, Hoek HW, Brown A. (1998). Neurodevelopmental disorders after prenatal famine: The story of the Dutch Famine Study. *Am J Epidemiol* 147: 213-6

Sweet RA, Pierri JN, Auh S, Sampson AR, Lewis DA. (2003). Reduced pyramidal cell somal volume in auditory association cortex of subjects with schizophrenia. *Neuropsychopharmacology* 28: 599-609

Swettenham JB, Muthukumaraswamy SD, Singh KD. (2009). Spectral properties of induced and evoked gamma oscillations in human early visual cortex to moving and stationary stimuli. *J Neurophysiol* 102: 1241-53

Swettenham JB, Muthukumaraswamy SD, Singh KD. (2013). BOLD Responses in Human Primary Visual Cortex are Insensitive to Substantial Changes in Neural Activity. *Front Hum Neurosci* 7: 76

Symond MP, Harris AW, Gordon E, Williams LM. (2005). "Gamma synchrony" in first-episode schizophrenia: a disorder of temporal connectivity? *Am J Psychiatry* 162: 459-65

Tadepally HD, Burger G, Aubry M. (2008). Evolution of C2H2-zinc finger genes and subfamilies in mammals: species-specific duplication and loss of clusters, genes and effector domains. *BMC Evol Biol* 8: 176

Tallon-Baudry C, Bertrand O, Peronnet F, Pernier J. (1998). Induced gamma-band activity during the delay of a visual short-term memory task in humans. *J Neurosci* 18: 4244-54

Tao R, Cousijn H, Jaffe A, Burnet PW, Edwards F, Eastwood SL, Shin JH, Lane TA, Walker M, Maher BJ, Weinberger DR, Harrison PJ, Hyde TM, Kleinman JE. (submitted). ZNF804A Expression in Human Brain: A Novel Transcript Fetally Regulated by the Psychosis Risk SNP rs1344706, and Alterations in Schizophrenia, Bipolar Disorder and Major Depression.

Taulu S, Kajola M, Simola J. (2004). Suppression of interference and artifacts by the Signal Space Separation Method. *Brain Topogr* 16: 269-75

Tek C, Gold J, Blaxton T, Wilk C, McMahon RP, Buchanan RW. (2002). Visual perceptual and working memory impairments in schizophrenia. *Arch Gen Psychiatry* 59: 146-53

Tesche CD. (1997). Non-invasive detection of ongoing neuronal population activity in normal human hippocampus. *Brain Res* 749: 53-60

Tesche CD, Karhu J. (2000). Theta oscillations index human hippocampal activation during a working memory task. *Proc Natl Acad Sci U S A* 97: 919-24

Thermenos HW, Seidman LJ, Breiter H, Goldstein JM, Goodman JM, Poldrack R, Faraone SV, Tsuang MT. (2004). Functional magnetic resonance imaging during auditory verbal working memory in nonpsychotic relatives of persons with schizophrenia: a pilot study. *Biol Psychiatry* 55: 490-500

Thimm M, Kircher T, Kellermann T, Markov V, Krach S, Jansen A, Zerres K, Eggermann T, Stocker T, Shah NJ, Nothen MM, Rietschel M, Witt SH, Mathiak K, Krug A. (2011). Effects of a CACNA1C genotype on attention networks in healthy individuals. *Psychol Med* 41: 1551-61

Thompson PM, Cannon TD, Narr KL, van Erp T, Poutanen VP, Huttunen M, Lonnqvist J, Standertskjold-Nordenstam CG, Kaprio J, Khaledy M, Dail R, Zoumalan CI, Toga AW. (2001). Genetic influences on brain structure. *Nat Neurosci* 4: 1253-8

Thompson PM, Ge T, Glahn DC, Jahanshad N, Nichols TE. (2013). Genetics of the connectome. *Neuroimage* 80: 475-88

Tienari P. (1991). Interaction between genetic vulnerability and family environment: the Finnish adoptive family study of schizophrenia. *Acta Psychiatr Scand* 84: 460-5

Tillmann C., Wibral M., Leweke F. M., Kohler A., Singer W., D. K, L. K, K. M, Uhlhaas PJ. (2008). High-frequency gamma-band oscillations during perceptual organisation in chronic and first-episode schizophrenia patients. *Soc. Neurosci. Abstr* 34:54.2

Torrey EF. (2007). Schizophrenia and the inferior parietal lobule. *Schizophr Res* 97: 215-25

Trachtenberg AJ, Filippini N, Ebmeier KP, Smith SM, Karpe F, Mackay CE. (2012). The effects of APOE on the functional architecture of the resting brain. *Neuroimage* 59: 565-72

Traub RD, Whittington MA, Stanford IM, Jefferys JG. (1996). A mechanism for generation of long-range synchronous fast oscillations in the cortex. *Nature* 383: 621-4

Tremblay S, Beaule V, Proulx S, de Beaumont L, Marjanska M, Doyon J, Pascual-Leone A, Lassonde M, Theoret H. (2013). Relationship between transcranial magnetic stimulation measures of intracortical inhibition and spectroscopy measures of GABA and glutamate+glutamine. *J Neurophysiol* 109: 1343-9

Tsuang M. (2000). Schizophrenia: genes and environment. *Biol Psychiatry* 47: 210-20

Tunbridge EM, Eastwood SL, Harrison PJ. (2011). Changed relative to what? Housekeeping genes and normalization strategies in human brain gene expression studies. *Biol Psychiatry* 69: 173-9

Tunbridge EM, Farrell SM, Harrison PJ, Mackay CE. (2013). Catechol-O-methyltransferase (COMT) influences the connectivity of the prefrontal cortex at rest. *Neuroimage* 68: 49-54

Tzourio-Mazoyer N, Landeau B, Papathanassiou D, Crivello F, Etard O, Delcroix N, Mazoyer B, Joliot M. (2002). Automated anatomical labeling of activations in SPM using a macroscopic anatomical parcellation of the MNI MRI single-subject brain. *Neuroimage* 15: 273-89

Uhlhaas PJ, Linden DE, Singer W, Haenschel C, Lindner M, Maurer K, Rodriguez E. (2006). Dysfunctional long-range coordination of neural activity during Gestalt perception in schizophrenia. *J Neurosci* 26: 8168-75

Uhlhaas PJ, Singer W. (2010). Abnormal neural oscillations and synchrony in schizophrenia. *Nat Rev Neurosci* 11: 100-13

Umeda-Yano S, Hashimoto R, Yamamori H, Okada T, Yasuda Y, Ohi K, Fukumoto M, Ito A, Takeda M. (2013). The regulation of gene expression involved in TGF-beta signaling by ZNF804A, a risk gene for schizophrenia. *Schizophr Res* 146: 273-8

Unschuld PG, Buchholz AS, Varvaris M, van Zijl PC, Ross CA, Pekar JJ, Hock C, Sweeney JA, Tamminga CA, Keshavan MS, Pearlson GD, Thaker GK, Schretlen DJ. (2013). Prefrontal Brain Network Connectivity Indicates Degree of Both Schizophrenia Risk and Cognitive Dysfunction. *Schizophr Bull*

van den Heuvel MP, van Soelen IL, Stam CJ, Kahn RS, Boomsma DI, Hulshoff Pol HE. (2013). Genetic control of functional brain network efficiency in children. *Eur Neuropsychopharmacol* 23: 19-23

van der Heijden CD, Rijpkema M, Arias-Vasquez A, Hakobjan M, Scheffer H, Fernandez G, Franke B, van de Warrenburg BP. (2013). Genetic variation in ataxia gene ATXN7 influences cerebellar grey matter volume in healthy adults. *Cerebellum* 12: 390-5

van Elst LT, Valerius G, Buchert M, Thiel T, Rusch N, Bubl E, Hennig J, Ebert D, Olbrich HM. (2005). Increased prefrontal and hippocampal glutamate concentration in schizophrenia: evidence from a magnetic resonance spectroscopy study. *Biol Psychiatry* 58: 724-30

van Pelt S, Boomsma DI, Fries P. (2012). Magnetoencephalography in twins reveals a strong genetic determination of the peak frequency of visually induced gamma-band synchronization. *J Neurosci* 32: 3388-92

van Pelt S, Fries P. (2013). Visual stimulus eccentricity affects human gamma peak frequency. *Neuroimage* 78: 439-47

Van Veen BD, van Drongelen W, Yuchtman M, Suzuki A. (1997). Localization of brain electrical activity via linearly constrained minimum variance spatial filtering. *IEEE Trans Biomed Eng* 44: 867-80

Vaquerizas JM, Kummerfeld SK, Teichmann SA, Luscombe NM. (2009). A census of human transcription factors: function, expression and evolution. *Nat Rev Genet* 10: 252-63

Venkataraman A, Whitford TJ, Westin CF, Golland P, Kubicki M. (2012). Whole brain resting state functional connectivity abnormalities in schizophrenia. *Schizophr Res* 139: 7-12

Venkatasubramanian G, Jayakumar PN, Keshavan MS, Gangadhar BN. (2011). Schneiderian first rank symptoms and inferior parietal lobule cortical thickness in antipsychotic-naive schizophrenia. *Prog Neuropsychopharmacol Biol Psychiatry* 35: 40-6

Voineskos AN, Lerch JP, Felsky D, Tiwari A, Rajji TK, Miranda D, Lobaugh NJ, Pollock BG, Mulsant BH, Kennedy JL. (2011). The ZNF804A gene: characterization of a novel neural risk mechanism for the major psychoses. *Neuropsychopharmacology* 36: 1871-8

Walsh T, McClellan JM, McCarthy SE, Addington AM, Pierce SB, Cooper GM, Nord AS, Kusenda M, Malhotra D, Bhandari A, Stray SM, Rippey CF, Roccanova P, Makarov V, Lakshmi B, Findling RL, Sikich L, Stromberg T, Merriman B, Gogtay N, Butler P, Eckstrand K, Noory L, Gochman P, Long R, Chen Z, Davis S, Baker C, Eichler EE, Meltzer PS, Nelson SF, Singleton AB, Lee MK, Rapoport JL, King MC, Sebat J. (2008). Rare structural variants disrupt multiple genes in neurodevelopmental pathways in schizophrenia. *Science* 320: 539-43

Walter H, Schnell K, Erk S, Arnold C, Kirsch P, Esslinger C, Mier D, Schmitgen MM, Rietschel M, Witt SH, Nothen MM, Cichon S, Meyer-Lindenberg A. (2011). Effects of a genome-wide supported psychosis risk variant on neural activation during a theory-of-mind task. *Mol Psychiatry* 16: 462-70

Walters JT, Corvin A, Owen MJ, Williams H, Dragovic M, Quinn EM, Judge R, Smith DJ, Norton N, Giegling I, Hartmann AM, Moller HJ, Muglia P, Moskvina V, Dwyer S, O'Donoghue T, Morar B, Cooper M, Chandler D, Jablensky A, Gill M, Kaladjieva L, Morris DW, O'Donovan MC, Rujescu D, Donohoe G. (2010). Psychosis susceptibility gene ZNF804A and cognitive performance in schizophrenia. *Arch Gen Psychiatry* 67: 692-700

Wang XJ, Buzsaki G. (1996). Gamma oscillation by synaptic inhibition in a hippocampal interneuronal network model. *J Neurosci* 16: 6402-13

Ward KE, Friedman L, Wise A, Schulz SC. (1996). Meta-analysis of brain and cranial size in schizophrenia. *Schizophr Res* 22: 197-213

Wassink TH, Epping EA, Rudd D, Axelsen M, Ziebell S, Fleming FW, Monson E, Ho BC, Andreasen NC. (2012). Influence of ZNF804a on brain structure volumes and symptom severity in individuals with schizophrenia. *Arch Gen Psychiatry* 69: 885-92

Wei Q, Kang Z, Diao F, Shan B, Li L, Zheng L, Guo X, Liu C, Zhang J, Zhao J. (2012). Association of the ZNF804A gene polymorphism rs1344706 with white matter density changes in Chinese schizophrenia. *Prog Neuropsychopharmacol Biol Psychiatry* 36: 122-7

Wei Q, Kang Z, Diao F, Guidon A, Wu X, Zheng L, Li L, Guo X, Hu M, Zhang J, Liu C, Zhao J. (2013). No association of ZNF804A rs1344706 with white matter integrity in schizophrenia: a tract-based spatial statistics study. *Neurosci Lett* 532: 64-9

Weickert CS, Sheedy D, Rothmond DA, Dedova I, Fung S, Garrick T, Wong J, Harding AJ, Sivagnanansundaram S, Hunt C, Duncan C, Sundqvist N, Tsai SY, Anand J, Draganic D, Harper C. (2010). Selection of reference gene expression in a schizophrenia brain cohort. *Aust N Z J Psychiatry* 44: 59-70

Weinberger DR, Wagner RL, Wyatt RJ. (1983). Neuropathological studies of schizophrenia: a selective review. *Schizophr Bull* 9: 193-212

Weinberger DR. (1987). Implications of normal brain development for the pathogenesis of schizophrenia. *Arch Gen Psychiatry* 44: 660-9

Weinberger DR, Berman KF, Suddath R, Torrey EF. (1992). Evidence of dysfunction of a prefrontal-limbic network in schizophrenia: a magnetic resonance imaging and regional cerebral blood flow study of discordant monozygotic twins. *Am J Psychiatry* 149: 890-7

Weinberger DR, Egan MF, Bertolino A, Callicott JH, Mattay VS, Lipska BK, Berman KF, Goldberg TE. (2001). Prefrontal neurons and the genetics of schizophrenia. *Biol Psychiatry* 50: 825-44

Weinberger DR, McClure RK. (2002). Neurotoxicity, neuroplasticity, and magnetic resonance imaging morphometry: what is happening in the schizophrenic brain? *Arch Gen Psychiatry* 59: 553-8

Wender PH, Rosenthal D, Kety SS, Schulsinger F, Welner J. (1974). Crossfostering. A research strategy for clarifying the role of genetic and experiential factors in the etiology of schizophrenia. *Arch Gen Psychiatry* 30: 121-8

Whiteside ST, Goodbourn S. (1993). Signal transduction and nuclear targeting: regulation of transcription factor activity by subcellular localisation. *J Cell Sci* 104 (Pt 4): 949-55

Williams HJ, Norton N, Dwyer S, Moskvina V, Nikolov I, Carroll L, Georgieva L, Williams NM, Morris DW, Quinn EM, Giegling I, Ikeda M, Wood J, Lencz T, Hultman C, Lichtenstein P, Thiselton D, Maher BS, Malhotra AK, Riley B, Kendler KS, Gill M, Sullivan P, Sklar P, Purcell S, Nimgaonkar VL, Kirov G, Holmans P, Corvin A, Rujescu D, Craddock N, Owen MJ, O'Donovan MC. (2011). Fine mapping of ZNF804A and genome-wide significant evidence for its involvement in schizophrenia and bipolar disorder. *Mol Psychiatry* 16: 429-41

Williamson PC, Allman JM. (2012). A framework for interpreting functional networks in schizophrenia. *Front Hum Neurosci* 6: 184

Winterer G, Ziller M, Dorn H, Frick K, Mulert C, Dahhan N, Herrmann WM, Coppola R. (1999). Cortical activation, signal-to-noise ratio and stochastic resonance during information processing in man. *Clin Neurophysiol* 110: 1193-203

Wirth C, Schubert F, Lautenschlager M, Bruhl R, Klar A, Majic T, Lang UE, Ehrlich A, Winterer G, Sander T, Schouler-Ocak M, Gallinat J. (2012). DTNBP1 (dysbindin) gene variants: in vivo evidence for effects on hippocampal glutamate status. *Curr Pharm Biotechnol* 13: 1513-21

Wolf RC, Vasic N, Sambataro F, Hose A, Frasch K, Schmid M, Walter H. (2009). Temporally anticorrelated brain networks during working memory performance reveal aberrant prefrontal and hippocampal connectivity in patients with schizophrenia. *Prog Neuropsychopharmacol Biol Psychiatry* 33: 1464-73

Woolrich M, Hunt L, Groves A, Barnes G. (2011). MEG beamforming using Bayesian PCA for adaptive data covariance matrix regularization. *Neuroimage* 57: 1466-79

Wright IC, Sharma T, Ellison ZR, McGuire PK, Friston KJ, Brammer MJ, Murray RM, Bullmore ET. (1999). Supra-regional brain systems and the neuropathology of schizophrenia. *Cereb Cortex* 9: 366-78

Wright IC, Rabe-Hesketh S, Woodruff PW, David AS, Murray RM, Bullmore ET. (2000). Meta-analysis of regional brain volumes in schizophrenia. *Am J Psychiatry* 157: 16-25

Yoo SY, Yeon S, Choi CH, Kang DH, Lee JM, Shin NY, Jung WH, Choi JS, Jang DP, Kwon JS. (2009). Proton magnetic resonance spectroscopy in subjects with high genetic risk of schizophrenia: investigation of anterior cingulate, dorsolateral prefrontal cortex and thalamus. *Schizophr Res* 111: 86-93

Yuan H, Liu T, Szarkowski R, Rios C, Ashe J, He B. (2010). Negative covariation between task-related responses in alpha/beta-band activity and BOLD in human sensorimotor cortex: an EEG and fMRI study of motor imagery and movements. *Neuroimage* 49: 2596-606

Zaehle T, Frund I, Schadow J, Tharig S, Schoenfeld MA, Herrmann CS. (2009). Inter- and intra-individual covariations of hemodynamic and oscillatory gamma responses in the human cortex. *Front Hum Neurosci* 3: 8

Zhang F, Chen Q, Ye T, Lipska BK, Straub RE, Vakkalanka R, Rujescu D, St Clair D, Hyde TM, Bigelow L, Kleinman JE, Weinberger DR. (2011a). Evidence of sex-modulated association of ZNF804A with schizophrenia. *Biol Psychiatry* 69: 914-7

Zhang R, Lu SM, Qiu C, Liu XG, Gao CG, Guo TW, Valenzuela RK, Deng HW, Ma J. (2011b). Population-based and family-based association studies of ZNF804A locus and schizophrenia. *Mol Psychiatry* 16: 360-1

Zumer JM, Brookes MJ, Stevenson CM, Francis ST, Morris PG. (2010). Relating BOLD fMRI and neural oscillations through convolution and optimal linear weighting. *Neuroimage* 49: 1479-89